organized by

UNIVERSITY OF OSTRAVA
FACULTY OF SCIENCE

Porous Materials for Environmental Applications 2026

Conference Scope

- Materials Design and Functional Systems
- Characterization, Modeling and Stability
- Environmental and Catalytic applications
- Energy and Functional conversion
- Biomedical and Future perspectives

15 - 19.03.2026

Hotel Bania

Białka Tatrzańska • Poland

POROUS MATERIALS FOR ENVIRONMENTAL APPLICATIONS 2026

BOOK OF ABSTRACTS

Institute of Chemistry,
Pavol Jozef Šafárik University in Košice
Moyzesova 11, 040 04 Košice
Slovakia
&
Department of Chemistry,
University of Ostrava
30. dubna 22, 701 03 Ostrava
Czech Republic
&
Slovak Chemical Society
Radlinského 9
812 15 Bratislava
Slovakia

Dr. Nikolas Király & Assoc. Prof. Miroslav Almáši (ed.)

THIS EVENT WAS SUPPORTED BY

ANAMET
ANALYTICAL & MEASURING & TESTING

Anton Paar

HERMES
LabSystems

NETZSCH

Porous Materials for Environmental Applications 15. - 19.03.2026 • Poland

Edited by:

Dr. Nikolas Király, Department of Inorganic Chemistry, Institute of Chemistry, Faculty of Science, Pavol Jozef Šafárik University in Košice, Košice, Slovakia
nikolas.kiraly@upjs.sk

Assoc. Prof. Miroslav Almáši, Department of Inorganic Chemistry, Institute of Chemistry, Faculty of Science, Pavol Jozef Šafárik University in Košice, Košice, Slovakia
miroslav.almasi@upjs.sk

Reviewed by:

Prof. Adrian Bonilla Petriciolet, Technological Institute in Aguascalientes, Aguascalientes, Mexico
petriciolet@hotmail.com

Prof. Ankur Jain, Centre for Renewable Energy & Storage, Suresh Gyan Vihar University, Jaipur, India; Natural Science Centre for Basic Research & Development, Hiroshima University, Higashi-Hiroshima, Japan
ankur.jain@mygyanvihar.com; ankur@hiroshima-u.ac.jp

Assoc. Prof. Weijun Gui, Jiangxi University of Water Resources and Electric Power, Nanchang, China
wjgui668@163.com

Assoc. Prof. Satya Pal-Nehra, Deenbandhu Chhotu Ram University of Science and Technology, Sonipat, India
spnehra.energy@dcrustm.org

Dr. Laura Gabriela Elvir Padilla, Reynosa-Aztlán Multidisciplinary Academic Unit, Autonomous University of Tamaulipas, Reynosa, Tamaulipas, Mexico
gelvir@uat.edu.mx

Organisation Committee:

Assoc. Prof. Miroslav Almáši, Department of Inorganic Chemistry, Institute of Chemistry, Faculty of Science, Pavol Jozef Šafárik University in Košice, Košice, Slovakia
miroslav.almasi@upjs.sk

Dr. Tomáš Zelenka, Department of Chemistry, Faculty of Science, University of Ostrava, Ostrava, Czech Republic
tomas.zelenka@osu.cz

Dr. Nikolas Király, Department of Inorganic Chemistry, Institute of Chemistry, Faculty of Science, Pavol Jozef Šafárik University in Košice, Košice, Slovakia
nikolas.kiraly@upjs.sk

Dr. Milica Želinská, Department of Inorganic Chemistry, Institute of Chemistry, Faculty of Science, Pavol Jozef Šafárik University in Košice, Košice, Slovakia
milica.zelinska@gmail.com

Eng. Michaela Halinkovičová, Slovak Chemical Society, Bratislava, Slovakia
hospodarka@schems.sk

Availabe at: www.unibook.upjs.sk
Publication date: 04. 03. 2026

ISBN 978-80-574-0507-8 (e-publication)

DOI: https://doi.org/10.33542/PMEA-0507-8

TABLE OF CONTENTS

PREFACE

On behalf of the Organizing Committee of the Porous Materials for Environmental Applications Conference (PMEA 2026), we are pleased to present these proceedings. PMEA 2026 was held on 15–19 March 2026 in Białka Tatrzańska, Poland, in the High Tatras region. The event was organized by the Institute of Chemistry, Pavol Jozef Šafárik University in Košice (Slovakia); the Department of Chemistry, University of Ostrava (Czech Republic); and the Slovak Chemical Society (Slovakia).

PMEA 2026 provided an international forum for scientists working in the fields of porous materials, heterogeneous catalysis, adsorption processes, energy storage, green chemistry, and related areas to present their most recent results, exchange ideas, and discuss current scientific challenges. The primary aim of the meeting was to strengthen interdisciplinary communication and encourage collaboration across chemistry, materials science, environmental science, and chemical engineering.

These proceedings contain contributions presented during the conference in both oral and poster sessions. We believe that this collection reflects current developments in the design, characterization, and application of porous materials and highlights their importance for sustainable technologies and industrial processes.

We sincerely thank all participants for their active engagement, inspiring discussions, and valuable contributions to the scientific atmosphere of the conference. We are especially grateful to the authors for their high-quality submissions, which ensured the scientific standard of the meeting, and to the reviewers for their careful evaluation of the manuscripts. Our gratitude also extends to the members of the organizing committee for their dedicated efforts in preparing this event.

Finally, we acknowledge the national and international funding schemes and research projects that supported the work presented here. We hope that PMEA 2026 provided a stimulating environment for scientific exchange and contributed to the establishment of new collaborations within the international research community. We look forward to the continued development of the PMEA conference series and to welcoming the scientific community again in 2028 in Slovakia.

Nikolas Király
Miroslav Almáši

Tailoring Titania Material Properties for Sustainable Chemistry Applications: Opportunities and Challenges

N. Gys[a,b], R. An[a,c], B. Mysore Ramesha[a], A. Fanourgiakis[a], C. Chandran[a,b], L. Van den Bergh[a,d], S. Van Doorslaer[d], P. Adriaensens[e], E. Derveaux[e], V. Meynen[a,f]*

[a]Laboratory of Adsorption and Catalysis (LADCA), University of Antwerp, Groenenborgerlaan 171, 2020 Antwerp, Belgium
[b]Research group Sustainable Materials Engineering (SUME), lab of Electrochemical and Surface Engineering (SURF), Vrije Universiteit Brussel, Pleinlaan 2, 1050 Brussel, Belgium
[c]Organic Synthesis (ORSY), University of Antwerp, Groenenborgerlaan 171, 2020 Antwerp, Belgium
[d]Theory and Spectroscopy of Materials and Molecules (TSM^2), Department of Chemistry, University of Antwerp, Universiteitsplein 1, 2610 Wilrijk, Belgium
[e]Institute for Materials Research (IMO-IMOMEC), NMR group, UHasselt, Agoralaan 1, 3590 Diepenbeek, Belgium
[f]Flemisch institute for technological research (VITO N.V.), Boeretang 200, 2400 Mol, Belgium

*vera.meynen@uantwerpen.be

Titania materials are applied in a variety of applications, including separation and (photo)catalysis, in which their performance depends on their structural, physico-chemical and surface properties. Although material properties can be varied, controlling surface interactions is challenging, certainly in the case of metal oxides. To enhance surface interaction and/or to introduce specific active sites, multiple approaches can be followed. In this presentation, two approaches will be discussed: introducing defect sites in titania and synthesizing hybrid organic-inorganic titania.

Hybrid organic-inorganic materials allow to introduce a wide diversity of chemical interactions not only through the choice in the type of organic functional group but also via the methodology in which the organic functional group is attached to the inorganic matrix [1]. Moreover, synthetic conditions and the choice of anchoring group, as well as differences in the support properties in case of surface modification, create a large matrix of control, adjustable to the specific requirements of the application. Although this provides significant opportunities to enhance material's functionalities for certain applications, it also holds challenges and pitfalls [2]. An overview of synthesis approaches for hybrid organic-inorganic titania and its opportunities for separation and catalysis will be provided but also lessons learned when developing and applying hybrid organic-inorganic titania based materials.

A second example that will be discussed is the reduction of titania to black titania, introducing defect sites that are claimed to improve photocatalytic performance in literature [3]. In our work, we produce black titania through a solid-state $NaBH_4$ thermal reduction of (white/pristine) titania, a method that is widely described in literature. Nevertheless, there is still controverse on the obtained properties after reduction, the reduction mechanism and its impact on photocatalysis [4]. Our work shows several unexpected and titania-dependent features that might be at the origin of these controversial observations in literature. Moreover, it highlights the need for extended characterisation, safety precautions, detailed description of the method and titania materials applied as well as the need for additional fundamental research on the reduction mechanism and the correlation between properties and photocatalytic performance.

Acknowledgements

FWO, F.R.S.-FNRS, VITO, VLAIO and UAntwerp are acknowledged for their financial support through projects including FWO project G.0121.17 N, PHOSPORE (Excellence of Science (EOS) program reference number: 40007504), VLAIO Moonshot cSBO (SYN-CAT) (HBC.2020.2614), BOF GOA colours of titania. This work is also supported by Hasselt University and FWO Vlaanderen via the Hercules projects AUHL/15/2-GOH3816N and I001324N.

References

[1] A. Fanourgiakis, C. Chandran, R. Tomer, S. Hermans, V. Meynen, Chapter 16 in Phosphonate Chemistry, Technology and Applications: Industrial, Environmental, and Energy Applications, Eds. K. D. Demadis, Elsevier (2026)
[2] N. Gys, et al., ChemPlusChem **88** (2023) e20220044.
[3] X. Chen, L. Liu, P. Y. Yu, S. S. Mao, Science **331**(2011) 746–750.
[4] T. S. Rajaraman, S. P. Parikh, V. G. Gandhi, Chem. Eng. J. **389** (2020).

Structural Flexibility in Porous Materials upon Adsorption

O. I. Tovar-Arredondo[a], A. Missyul[b], C. Carrillo-Carrión[c], J. Silvestre-Albero[a]*

[a]Advanced Materials Laboratory, Inorganic Chemistry Department, University of Alicante, Spain
[b]Cells – ALBA synchrotron, Cerdanyola del Vallés, Spain
[c]Institute of Chemical Research (IIQ), CSIC-University of Seville, Spain

*joaquin.silvestre@ua.es

The removal of emerging and persistent contaminants (e.g., PFOAS, solvents, etc.) in industrial effluents require the design of porous materials combining a highly developed porous structure, and a dedicated surface chemistry to promote specific interactions with the target molecules. Among porous materials, metal-organic frameworks (MOFs) represent promising candidates due to their tailorable structure, engineered porosity and designed surface chemistry. Zeolitic-imidazolate frameworks (ZIFs) are a subclass of MOFs characterized by fascinating reversible structural transformations upon an external stimulus (heat, adsorption, pressure, etc.) [1]. The high degree of framework flexibility identified to date, allows to design crystalline networks with molecular-induced selectivity, depending on the nature of the organic ligands, the functional groups associated, the porous structure, among others. Overall, it depends on the competition between strong non-bonding interactions, that promote the formation of highly dense structure, and bonding interactions, that favour the formation of high symmetry, low-density crystal structures [2,3]. Furthermore, these intracrystalline interactions can be altered/modified, depending on the nature of the adsorbate molecules, thus opening the gate to unexplored adsorption phenomena in gas and liquid-phase processes. In this communication, we will summarize some examples of structural changes in ZIFs (Figure 1), their sensitivity to the nature of the probe, and how the knowledge of the associated mechanism can be used to design porous materials with an enhanced performance in a wide range of application from gas storage/separation, to mechanical energy storage, and liquid-phase selective separation processes [4,5]. Special attention will be given to liquid-phase adsorption processes to emphasize the crucial role of the solvent, and how the associated solvent-adsorbate and solvent-framework interactions will determine the appearance of structural changes in ZIFs (e.g., breathing phenomena) [6].

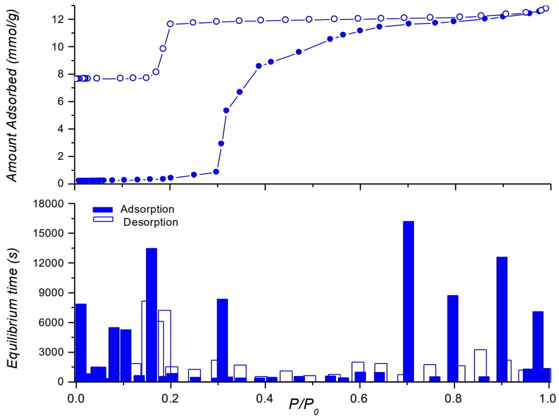

Figure 1 N_2 adsorption/desorption isotherm for ZIF-7 at 77K (upper panel). Time required to reach equilibrium for each of the adsorption and desorption points (lower panel).

Acknowledgements

The authors acknowledge financial support from the MINECO (Project PID2022-142960OB-C21), Conselleria de Innovación, Ciencia y Sociedad Digital (Project CIPROM/2021/022), and European Union: Horizon Europe (Project MOST-H2; Grant agreement nº 101058547).

References

[1] R. P. Lively, M. E. Dose, J. A. Thompson et al., Chem. Commun. **47** (2011) 8667.
[2] M. E. Casco, Y. Q. Cheng, L. L. Daemen, D. Fairen-Jimenez, E. V. Ramos-Fernandez, A. J. Ramirez-Cuesta, J. Silvestre-Albero, Chem. Commun. **52** (2016) 3639.
[3] J. Gandara-Loe, A. Missyul, F. Fauth, L. L. Daemen, Y. Q. Cheng, A. Ramirez-Cuesta, P. I. Ravikovitch, J. Silvestre-Albero, J. Mater. Chem. A **7** (2019) 14552.
[4] J. Gandara-Loe, R. Bueno-Perez, A. Missyul, D. Fairen-Jimenez, J. Silvestre-Albero, ACS Appl. Nano Mater. **4** (2021) 3519.
[5] E. Amayuelas, J. Farrando-Perez, A. Missyul, Y. Grosu, J. Silvestre-Albero, C. Carrillo-Carrión, ACS Appl. Mater. Interf. **16** (2024) 46374.
[6] J. Farrando-Perez, A. Missyul, A. Martín-Calvo, et al., J. Mater. Chem. A **12** (2024) 28975.

Using Porous Materials in the Medical and Health-Related Fields of Applications

V. Hornebecq[a]*, D. Bergé-Lefranc[b], T. N. T Phan[b], P. Prinderre[b], F. Chaspoul[b], C. Pardanaud[c], M. Almasi[d], E. Benova[d], V. Zelenak[d]

[a]Aix-Marseille University, MADIREL Laboratory, Marseille, France
[b]Aix-Marseille University, ICR, Marseille, France
[c]Aix-Marseille University, PIIM Laboratory, Marseille, France
[d]Department of Inorganic Chemistry, Institute of Chemistry, Faculty of Science, Pavol Jozef Šafárik University Košice, Slovak Republic

*virginie.hornebecq@univ-amu.fr

Porous materials are highly adaptable, allowing new materials to be optimized or designed in terms of functionality. They are characterized by a three-dimensional structure, cavities or pores and an internal surface. These three elements open important prospects in terms of properties and, therefore, potential applications. The internal surface is responsible for the many catalytic and adsorption properties of porous solids. These properties are even more interesting when the internal surface is large and/or modified. The pores or cavities can be used in several ways. The available pore volume allows molecules to be trapped. This ability to trap compounds is used in several applications such as storage and controlled release. These pores can also be used as chemical nanoreactors to prepare composite materials or for the confinement of unstable compound. In this presentation, four examples will be developed to illustrate the high adaptability of porous materials in medical and health-related fields.

The two first examples concern the sensitive detection of small molecules at low concentrations, this detection being is of great importance especially for the drug intoxication and the disease diagnosis. Firstly, an example concerning the detection of biomarkers of exposure will be presented. These biomarkers are chemical compounds (or their metabolites) measured in human fluids and whose presence can attest an exposure to toxic substances. The detection of biomarkers is thus a powerful tool in the health risk assessment and the clinical diagnosis since the impact of toxic compounds is associated to a high probability of pathology outcome, even after decades. An important challenge lies in the improvement of both threshold detection and facility of biomarkers separation. In this context the solution we propose, consist in the design of advanced functional porous materials presenting on their surface specific functions able to realize "lock/key" type interaction with the biomarker. For that purpose, hybrid mesoporous silicas were prepared using as templates, original laboratory-made block copolymers containing densely polypeptides functions. They were then studied for the detection of a specific biomarker. Secondly, we will focus on the detection of drugs in case of intoxication. In the area of analytical toxicology, the presence of drugs and their metabolites in biologic fluids is mainly performed using either immunochemical or chromatographic methods. Efforts are devoted to develop methods combining advantages of these two techniques without their disadvantages. In this context, porous nanocomposites composed of mesoporous silicas and noble metal Au nanoparticles were studied as SERS substrates for the detection at low concentration of oxazepam, a benzodiazepine metabolite. [1, 2]

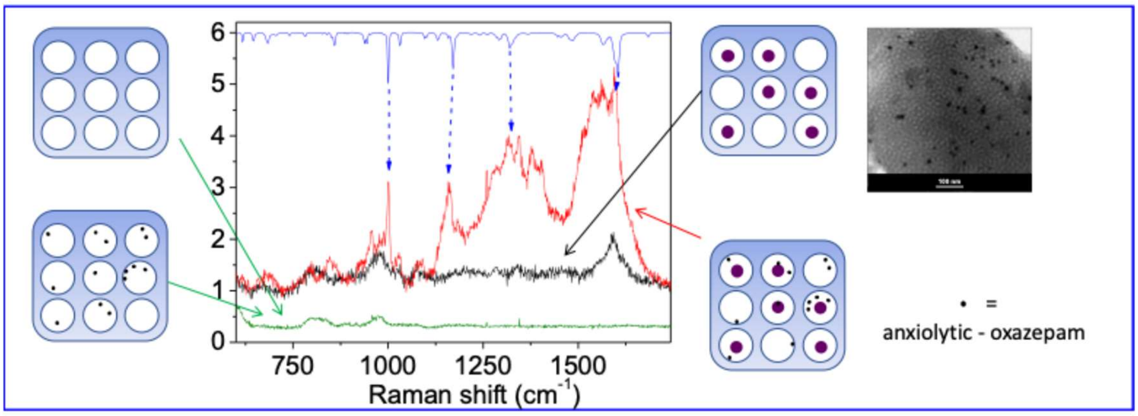

Figure 1 SERS detection of oxazepam using porous substrates containing gold nanoparticles.

The third example concerns the design of drug delivery systems (DDS). Indeed, the growing interest for finding more efficient drug administration has induced huge research efforts devoted to the design of new functional materials as controlled drug delivery systems (DDS) to maximize therapeutic efficacy and minimize side effects. Among the various drug nanocarriers explored, stimuli-responsive mesoporous silicas are excellent candidates for which the drug release can be triggered by the exogenous or the endogenous stimuli. In this context, pH-sensitive and light-sentitive mesoporous silicas were synthesized and used, both *in vitro* and *in vivo*, as DDS. [3, 5]

In the fourth example, the pores were used to stabilize amorphous compounds. Indeed, the poor solubility of numerous pharmaceutical compounds significantly impede their bioavailability, thereby diminishing therapeutic efficacy. To overcome this issue and to increase the solubility of a BCS Class II active pharmaceutical ingredient (API), we propose to confine it in its amorphous form within the pores of a porous material, thereby enhancing its bioavailability. Indeed, compared to its crystalline counterpart, the dissolution of an API in its thermodynamically unstable amorphous state allows for transient increase in the apparent solubility (C_{eq}). Vaterite was chosen as the porous material and curcumin as the model molecules for poorly soluble API.

Acknowledgements

This work was supported by ANR (1147/DOM TOM), AMIDEX and AMUTECH.

References

[1] Patent WO/2021/245255, ‘Process for forming a nanoparticles-containing porous material’, 2021

[2] A. Merlen, C. Pardanaud, K. Gratzer, S. Coussan, D. Machon, A. Forestier, D. Berge-Lefranc, T. N. T. Phan, V. Hornebecq, J. Raman Spectr. **51** (2020) 2192-2198.

[3] E. Benova, V. Hornebecq, V. Zelenak, V. Huntosova, M. Almasi, M. Macajova, D. Berge-Lefranc, Appl. Surf. Sci. **561** (2021).

[4] E. Benova, D. Berge-Lefranc, V. Zelenak, M. Almasi, V. Huntosova, V. Hornebecq, Appl. Surf. Sci. **504** (2020) 144028.

[5] V. Zelenak, E. Benova, M. Almasi, D. Halamova, V. Hornebecq, V. Hronsky, New J. Chem. **42** (2018) 13263-13271.

Tuning Porosity in Nanoporous Carbons via Controllable Sulfur Insertion for Various Applications

M. Bytniewska[a], M. Barczak[a]*

[a]Institute of Chemical Sciences, Faculty of Chemistry, Maria Curie-Sklodowska University, 20-031 Lublin, Poland

*mariusz.barczak@mail.umcs.pl

Sulfur doping of carbon materials has attracted considerable attention due to the growing interest in applications of the resulting composites, predominantly as electrode materials for lithium-sulfur batteries [1], as well as photoactive materials [2]. Sulfur can be incorporated into the structure of nanoporous carbons by various methods; however, these approaches are often energy-intensive, rely on harmful solvents, or offer poor control over the amount and spatial distribution of sulfur [3-6].

Sulfur can be introduced into porous carbons by a variety of methods; however, these approaches are often energy-intensive, rely on toxic solvents, and suffer from limited scalability as well as poor synthetic control over both the sulfur content and its spatial distribution. Importantly, none of the existing strategies enables precise control over the amount of sulfur and its pore-size-dependent allocation, nor do they broadly address potential applications beyond batteries, e.g. separation science and, potentially, biomedicine, considering the unique properties of sulfur [7].

Recently, we proposed a new method of the controlled insertion of sulfur into nanoporous carbon matrices (called SASI: Steam-Assisted Sulfur Insertion) intrinsically combined with the possibility of porosity tuning and regulation of pore accessibility [7]. This opens a pathway to carbon-sulfur composites exhibiting a wide spectrum of unique and tunable physicochemical properties. Precise control over both the sulfur loading and its pore-size-dependent allocation enabled the rational design of carbon-sulfur interfaces; the schematic idea is shown in Figure 1.

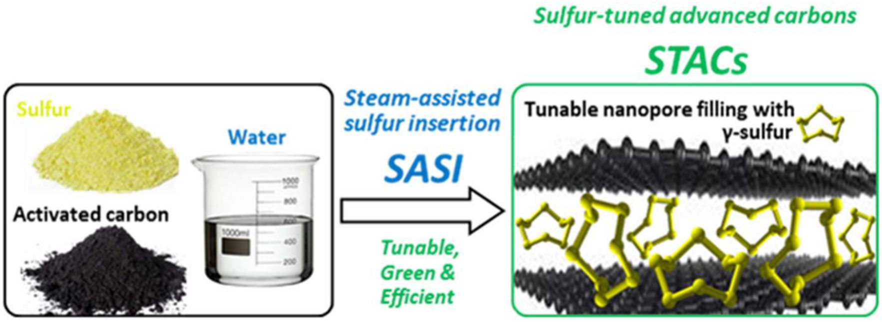

Figure 1 Schematic presentation of the sulfur insertion scheme.

In this presentation, a range of applications explored to date for these sulfur-tuned carbon materials will be discussed, highlighting how precise control over porosity and sulfur loading translates into functional performance. The range of possible applications spans from electrode materials, through efficient adsorbents for environmental remediation and separation processes to biomedical applications. In each of these applications, a key role is played by the interdependence between the accessible porosity and the amount of sulfur allocated within the pores.

Acknowledgements

This research was funded by the National Science Centre (Poland), grant no. 2023/51/B/ST5/01911 titled *Novel sulfur-tuned advanced carbons: synthesis, characterization and applications*.

References

[1] D. Lv, J. Zheng et al., Adv. Energy Mater. **5** (2015) 1402290.
[2] T. J. Bandosz et al., Carbon **156** (2020) 10–23.
[3] R. Pay et al., Nature Commun. **5** (2022) 17.
[4] M. Helen et al., ACS Omega **3** (2018) 11290-11299.
[5] M. V. Coulet et al., ChemPhysChem **23** (2022) e202200416.
[6] Y. Chen et al., RSC Adv. **6** (2016) 81950-81957.
[7] M. Barczak et al., Adv. Funct. Mater. **34** (2023) 2310398.

Bimetallic MOF Composites Decorated on Porous Carbon Textiles for Multifunctional Air and Water Purification via Catalysis–Adsorption Synergy

F. Florides[a], K. Ioannou[a,b], M. Bytniewska[a], N. Kostoglou[c], A. Michalicha[d], C. Rebholz[b], M. Barczak[a], D. A. Giannakoudakis[a]*

[a]Institute of Chemical Sciences, Faculty of Chemistry, Maria Curie-Sklodowska University, 20-031 Lublin, Poland
[b]Department of Mechanical and Manufacturing Engineering, University of Cyprus, 2109 Nicosia, Cyprus
[c]Institute of Geoenergy, Foundation for Research and Technology – Hellas, 73100, Chania, Greece
[d]Chair and Department of Biochemistry and Biotechnology, Medical University of Lublin, Chodźki 1, 20-093 Lublin, Poland

*dagchem@gmail.com / dimitrios.giannakoudakis@mail.umcs.pl

The development of next-generation materials for air and water purification, ranging from household filtration systems to personal protective equipment for emergency or crisis situations, such as gas masks and garments, requires multifunctional remediation media capable of capturing, degrading, and neutralizing diverse hazardous species. In this context, the synthesis of reactive nanomaterials plays a key role [1].

Metal-Organic Frameworks (MOFs) possess unique physicochemical characteristics, including high and hierarchical porosity, accessible reactive centers within their pores/cages, and the ability to exist as nanostructured particles. However, their practical deployment is limited by several drawbacks, such as insufficient thermal and chemical stability, particularly poor resistance to humidity, high cost, and challenges associated with large-scale synthesis. To overcome these limitations, it is essential to design MOF-based materials/composites that mitigate these inherent weaknesses [2-4]. In this work, two main strategies are followed: (i) the development of defect-rich bimetallic frameworks and (ii) the formation of composites with carbon-based nanostructures, including reduced graphene oxide, graphitic carbon nitride, and carbon quantum dots. Toward real-life applications, our goal is to employ the greenest possible synthesis protocols, achieving high yields using water as the sole solvent and mechanochemical driven approaches, while minimizing the required amount of MOF material by homogeneously decorating selected substrates [2,5].

Within this content, we demonstrate the optimization of the synthesis of bimetallic MOFs, specifically Zeolitic Imidazolate Frameworks (ZIFs) based on Co- and Zn (**ZIF-678**), using water as the only solvent (Figure 1). Systematic variation of the metal ratios enabled compositional optimization to maximize porosity, structural stability, and active-site availability. Subsequently, we examine how composite formation using minimal carbon-based filler loadings (~1 wt.%) effectively enhances key physicochemical properties and, consequently, the remediation efficiency of ZIF-678 toward organic contaminants in both water and air. Pharmaceuticals were employed as model water contaminants, while chemical warfare agent (CWA) vapors, including blister and nerve agents, served as representative airborne threats. In addition, the chemical and hydrothermal stability, H_2 storage and CO_2 capture capacity, as well as antibacterial activity of the ZIF-678 composites were evaluated. The bimetallic ZIF-678 nanocomposites exhibited significantly enhanced porosity, gas-storage performance, and antibacterial efficiency compared to their monometallic counterparts.

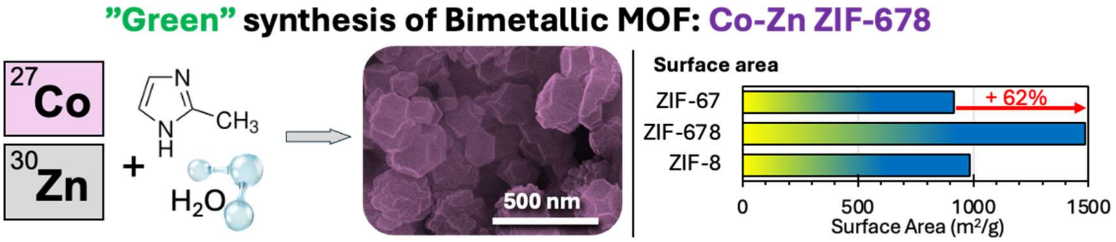

Figure 1 Schematic illustration of the green, water-based synthesis of defect-rich bimetallic Co–Zn ZIF-678 nanocrystals. A relative enhancement in textural properties of up to +62% is observed for the bimetallic ZIF-678 compared to monometallic analogues.

Nanoporous carbon textiles (C-Texts) are highly attractive candidates, either as standalone materials or as substrates, for air and water purification applications due to their high surface area, tunable surface chemistry, low density, flexibility, and cost-effectiveness [6-8]. Nevertheless, their rational optimization remains challenging and relies on two complementary strategies: (i) fine-tuning key physicochemical properties, particularly surface-chemistry heterogeneity, and (ii) nanoengineering through the incorporation of catalytically active nanophases [2,8]. Based on our experience, it was determined that, for C-Texts to be effectively utilized as substrates, surface-chemistry heterogeneity must be enhanced, especially through the introduction of oxygen-containing functional groups [2]. In addition, we demonstrated that the detoxification efficiency of C-Texts is not affected by the presence of humidity, which may originate from environmental conditions or from perspiration and breathing during use [9].

Building on these materials-design principles, this work highlights also strategies to enhance the multifunctional performance of C-Texts for air and water decontamination toward large-scale protective media. Initially, the adsorption efficiency of commercial and chemically modified C-Texts was evaluated, identifying the physicochemical parameters most critical to performance, while systematically investigating the influence of humidity under realistic conditions. Further improvements were achieved by developing scalable and cost-effective methods to decorate C-Texts with minimal loadings of mono- and bimetallic MOFs, specifically ZIF-based active phases. The resulting hybrid textiles (Figure 2) exhibited superior removal of diclofenac from water, as well as catalytic detoxification of CWA vapors and droplets, accompanied by exceptionally high antibacterial efficiency. These enhancements are attributed to homogeneous nanoparticle dispersion and synergistic adsorption–catalysis interfacial effects, with oxygen-containing surface functional groups on the C-Texts playing a key role by enabling efficient catalytic detoxification, strong and stable retention of hazardous molecules, and successful crystallization and anchoring of the ZIF nanoparticles.

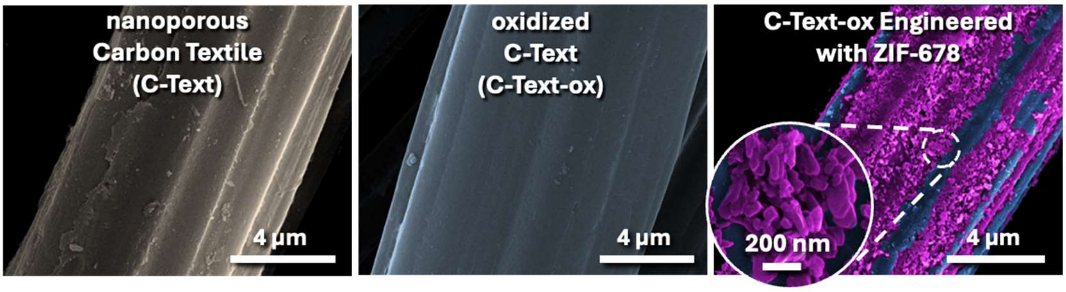

Figure 2 Scanning electron microscopy (SEM) images illustrating the surface morphology evolution of nanoporous carbon textiles (C-Texts): pristine C-Text on the left, oxidized C-Text (C-Text-ox) at the center, and C-Text-ox homogeneously engineered with Co–Zn ZIF-678 nanoparticles on the right. Oxidation induces surface cleaning/roughening and enhanced surface chemical heterogeneity, enabling uniform anchoring of ZIF-678 nanocrystals, as highlighted in the magnified inset.

Acknowledgements

The work is financially supported by the National Science Centre (NCN) of Poland via the SONATA-19 grant 2023/51/D/ST5/01915 (PI: D. Giannakoudakis).

References

[1] D. A. Giannakoudakis, T. J. Bandosz, Springer International Publishing **1** (2017).
[2] D. A. Giannakoudakis, P. S. Pauletto, M. Florent, T. J. Bandosz, RSC Adv. Interfaces **2** (2025) 1275-1287.
[3] D. A. Giannakoudakis, T. J. Bandosz, Molecules **24** (2019**)** 4529.
[4] D. A. Giannakoudakis, T. J. Bandosz, ACS Appl. Mater. Interf. **12** (2020) 14678-14689.
[5] D. A. Giannakoudakis, Y. Hu, M. Florent, T. J. Bandosz, Nanoscale Hor. **2** (2017) 356-364.
[6] D. A. Giannakoudakis, M. Barczak, M. Florent, T. J. Bandosz, Chem. Eng. J. **362** (2019) 758-766.
[7] D. A. Giannakoudakis et al., Chem. Eng. J. **524** (2025) 169457.
[8] P. S. Pauletto, D. A. Giannakoudakis, M. Florent, T. J. Bandosz, Carbon **230** (2024) 119673.
[9] D. A. Giannakoudakis, P. S. Pauletto, M. Florent, T. J. Bandosz, J. Hazard. Mater. **487** (2025) 137155.

Porous Framework Materials for Proton Conduction

D. Matoga[a]*

[a]Faculty of Chemistry, Jagiellonian University, Gronostajowa 2, 30-387 Kraków, Poland

*dariusz.matoga@uj.edu.pl

Porous framework materials (PFMs), including metal-organic frameworks (MOFs), covalent organic frameworks (COFs), and hydrogen-bonded organic frameworks (HOFs), represent a broad class of materials characterized by modularity, crystallinity and porosity [1]. These features enable the design and exploration of PFMs in a wide range of applications, such as catalysis, drug delivery, sensing, gas storage, mixture separations, and energy storage and conversion. Notably, proton-conductive PFMs (PC-PFMs) hold significant promise as solid electrolytes in proton-exchange membrane fuel cells. Several strategies have been developed for synthesizing PC-PFMs, with the most effective approaches involving the incorporation of Brønsted acid groups into the organic framework and the filling of cavities with acidic ions or molecules [2]. In this presentation, our original synthetic strategies for creating PC-PFMs will be presented [3,4].

One approach involves chlorosulfonation of selected organic building blocks, which, upon assembly into MOFs, results in the incorporation of terminal sulfonic groups into the MOF backbones. Another strategy involves the conversion of non-conductive MOFs with open metal sites into proton conductive MOFs or metalo-HOFs through a solvent-free mechanochemical process, utilizing thiocyanate salts with protic cations. Lastly, we employ an inverse electron-demand Diels-Alder reaction as a covalent post-synthetic modification of MOFs containing a tetrazine entity. This reaction is carried out under mild conditions using functionalized dienophiles, further enhancing the functionality of the material.

Acknowledgements
National Science Center in Poland is acknowledged for financial support (Grant no. 2025/57/B/ST5/04899).

References

[1] G. Gong, B. Yang, Y. Chen, N. Xia, Y. Xiong, D. A. Asamannaba, X. Chen, Chem. Commun. **61** (2025) 12885-12903.
[2] D. - W. Lim, H. Kitagawa, Chem. Soc. Rev. **50** (2021) 6349-6368.
[3] M. Szufla, J. A. R. Navarro, K. Góra-Marek, D. Matoga, ACS. Appl. Mater. Interfaces **15** (2023) 28184-28192; M. Lupa-Myszkowska, M. Oszajca, D. Matoga, Chem. Sci. **14** (2023) 14176-14181
[3] D. Jędrzejowski, M. Pander, E. Stachura, K. Matlak, W. Bury, D. Matoga, J. Mater. Chem. A **13** (2025) 23671-23679.

BIOLOGICAL AND BIOMEDICAL APPLICATIONS

Environmentally Friendly Preservation Approaches for Stone Substrates in Cultural Heritage Structures and Collections

R. Pericleanu[a], A. Ș. Dumbravă[a], I. C. Marinaș[b], P. Badică[c], N. D. Batalu[d*], A. Târșoaga[e], A. Spatariu[e], M. C. Chifiriuc[a,b,f], V. Lazăr[a,b], I. Gheorghe-Barbu[a,b]

[a]Faculty of Biology, University of Bucharest, Intrarea Portocalelor no. 1-3, 060101 Bucharest, Romania (RO);
[b]The Research Institute of the University of Bucharest (ICUB), 050095 Bucharest, RO;
[c]National Institute of Materials Physics, Măgurele, Atomistilor no. 405A, 077125, Măgurele, RO;
[d]National University of Science and Technology Politehnica Bucharest, Splaiul Independentei no. 313, 060042 Bucharest, RO;
[e]Credo Design S.R.L., Valea lui Mihai no. 9, 061752, Bucharest, RO
[f]Academy of Romanian Scientist, Ilfov no. 3, 050094, Bucharest, RO

*dan_batalu@yahoo.com

In Romania, *in vitro* investigations on the antimicrobial activity of plant extracts against biodeteriogenic microorganisms remain limited [1, 2]. The present study aims to address this gap by evaluating the antimicrobial efficacy of eco-friendly strategies that combine plant-derived bioactive compounds with magnesium diboride (MgB_2) (nano)powders. These innovative approaches represent potential solutions for controlling a broad spectrum of biodeteriogenic microorganisms relevant to the Romanian geographical, historical, and architectural context.

Hydro-alcoholic extracts from *Allium sativum* (cloves), *Rosmarinus officinalis, Equisetum arvense, Polygonum hydropiper,* and *Ononis spinosa* (leaves) were obtained by dynamic maceration. Oxidative protection was assessed using DPPH, CUPRAC, FRAP, ABTS, and NO scavenging methods to investigate antioxidant mechanisms that may contribute to the neutralization of oxidative atmospheric pollutants. The antimicrobial and anti-biofilm effects of these extracts, alongside three MgB_2 nanopowders manufactured by LTS Research Laboratories in 2019 and 2021, respectively, and by Alfa Aesar in 2023 and characterized through scanning electron microscopy (SEM) were tested against bacteria, yeast and filamentous fungi isolated in 2025 from class A stone churches in Romania. Microbial identification was performed via culture-dependent and metagenomic sequencing. Antimicrobial assessment included adapted diffusion assays, minimum inhibitory concentration (MIC) determination, *slime* assays, synergy analysis via the Fractional Inhibitory Concentration Index (FICI) and anti-enzymatic activity using sub-inhibitory concentrations (MIC/2 and MIC/4).

The results obtained demonstrated that in the three Class A churches in Vâlcea County (Cozia, Bolnița, and Măldărăști), modern diagnostic methods revealed areas with high deterioration potential, which were correlated with local climatic fluctuations. A significant antioxidant effect was observed only in the presence of vegetal extracts, while MgB_2 alone exhibited minimal activity, demonstrating the critical importance of vegetal extracts in the formulation aimed at mitigating oxidative damage to cultural heritage assets. Using both culture-dependent (MALDI-TOF) and culture-independent approaches (16S and ITS sequencing), dominant genera such as *Cladosporium*, *Aspergillus*, *Alternaria*, and *Bacillus* were identified, with high diversity in zones exposed to elevated humidity and temperature variability. The isolated bacterial and microfungi strains exhibited the capacity to produce degradative enzymes (cellulases, esterases, amylases) and organic acids, and were subsequently used to investigate conservation and restoration strategies. *R. officinalis* extract exhibited the highest antioxidant and antibacterial activities, particularly against *Bacillus megaterium* (MIC values: 7.81–62.5 µL/mL) and significant inhibition of bacterial adherence. *A. sativum* extract demonstrated superior effeciency against fungi, including *Aspergillus niger*, *Cladosporium* spp., and *Rhodotorula mucilaginosa*. MgB_2 nanopowders exhibited broad-spectrum antimicrobial activity (MIC: 0.07–0.62 mg/mL). Synergy with *R. officinalis* extract was observed in 57% of tested strains. The investigated solutions showed strain-dependent effects, including enzymatic inhibition and modulation of organic acid activity at sub-inhibitory concentrations, influenced by the biochemical environment.

These findings highlight the potential of integrating natural plant extracts with MgB_2 nanopowders as effective, low-impact alternatives for microbial control in cultural heritage conservation.

Acknowledgements
This research was supported by PN-IV-P7-7.1-PED-2024-2249 (9PED/2025), funded by UEFISCDI.

References

[1] V. M. Corbu, I. Gheorghe-Barbu, I. C. Marinas, S. M. Avramescu, I. Pecete, E. I. Geană, M. C. Chifiriuc, Inter. J. Molec. Sci. **23** (2022) 11463.
[2] V. M. Corbu, I. Gheorghe, I. C. Marinaş, E. I. Geană, M. I. Moza, O. Csutak, M. C. Chifiriuc, Molecules **26** (2021) 7195.

Conductive Nanocellulose: Towards the Green Electronics Applications

E. Bencurova[a]*, T. Dandekar[b]

[a]University of Würzburg, Würzburg, Germany
[b]EMBL Heidelberg, BioComputing Unit, Heidelberg, Germany

*elena.bencurova@uni-wuerzburg.de

Over the last two decades, the global production of electronic devices has risen enormously, and with it, the amount of electronic waste. For this reason, the development of green electronics is a priority to decrease environmental pollution from heavy metals, toxic components, and plastic particles. Nanocellulose is a natural polymer with excellent properties—it is biodegradable, lightweight, mechanically strong, inexpensive to produce, and sustainable. It can be derived from various sources, such as organic waste, bacteria, microalgae, or plants. The structure of nanocellulose depends on its type: nanocrystals are 2-5 nm wide and approximately 100 nm long particles, while nanofibrillated nanocellulose contains ribbon-like fibers, 2-3 nm wide, which form a network with pores ranging from a few nm to µm, depending on the cultivation and treatment conditions [1]. Nanocellulose itself is an insulator, so for use in green electronics it must be combined with conductive materials, such as metal particles, carbon materials, or other conductive polymers, using techniques like in-situ polymerization, doping, oxidative graft copolymerization, or vapor deposition polymerization [2].

In the present study, we prepared bacterial nanocellulose from a SCOBY membrane (kombucha), which was incubated for 24 hours in 1M NaOH to remove impurities and microorganisms. The nanocellulose was blended, filtered through a 0.45 micrometer filter under vacuum, and rinsed to reach a neutral pH. For the conductive nanocellulose composite, graphene oxide (0.5 - 2 mg/ml) and iodine (0.01 - 0.025 M) were added to the bacterial nanocellulose and mixed using a magnetic stirrer at room temperature for 24 hours. The nanocellulose was then filtered to remove excess water and dried at 60°C for 12 hours. Conductivity measurements were performed using a Laqua Twin meter (Horiba, Japan) according to the manufacturer's instructions in triplicate. The samples were imaged in a JSM-7500F field emission scanning electron microscope (SEM; JEOL, Tokyo, Japan) with an acceleration voltage of 5 kV, a probe current of 0.3 nA, and a working distance of 6.0 mm. SEM images of untreated nanocellulose and iodine-doped nanocellulose are depicted in panels A and B. The results (panels C, D) reveal that untreated nanocellulose exhibits relatively low conductivity, whereas GO-treated nanocellulose displays a marked increase in conductivity at lower concentrations compared to treatments with iodine. Specifically, untreated nanocellulose shows a conductivity of approximately 0.1 S/m, while GO-treated nanocellulose achieves up to 200 S/m, demonstrating its transition towards conductive and semiconductive properties (Figure 1) [3].

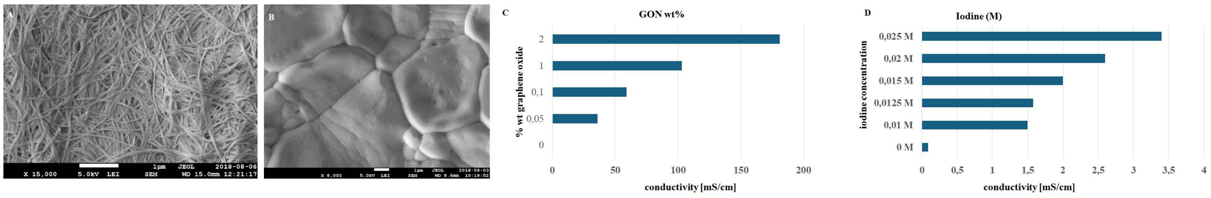

Figure 1 Exploration of nanocellulose properties. A. SEM analysis of SCOBY membrane (symbiotic culture of bacteria and yeasts) after alkaline treatment and blending. B. Nanocellulose with 0,02M iodine dopping. C. Conductivity of nanocellulose dopped with graphene oxide and D. iodine treatment.

References

[1] A. Kumar, R. Moolemane, T. Rajendran, S. B. N. Krishna, J. Renew. Mater. **13** (2025).
[2] W. Gao, Q. Tu, P. Wang, J. Zeng, J. Li, B. Wang,J. Xu, K. Chen, Z. Zhang, N. Abidi, L. A. Lucia, Polymer Rev. **64** (2024)162-191.
[3] E. Bencurova, S. Shityakov, D. Schaack, M. Kaltdorf, E. Sarukhanyan, A. Hilgarth, C. Rath, S. Montenegro, G. Roth, D. Lopez, T. Dandekar, Front. Bioeng. Biotech. **10** (2022) 869111.

Silver(I) Complexes as Potential Antibacterial and Anticancer Agents

K. Harbuľáková[a]*, Z. Vargová[a]

[a]Department of Inorganic Chemistry, Institute of Chemistry, Faculty of Science, Pavol Jozef Šafárik University in Košice, Moyzesova 11, 040 01 Košice, Slovak Republic

*kristina.harbulakova@student.upjs.sk

Microbial infections and cancer represent major global health challenges today, primarily managed through antibiotics and anticancer drugs like cisplatin. However, overuse of these treatments has rapidly fueled resistance development, while adverse effects such as nausea, dysbiosis of the gut microbiome and hearing loss are frequently reported with their administration. Therefore, the development of novel, potent antimicrobial and anticancer therapeutics is urgently required [1, 2].

Silver(I) compounds represent a promising alternative in combating rising bacterial resistance in the treatment of infections caused by pathogenic microorganisms. Their toxicity toward bacterial cells has long been known, while their toxicity to human cells remains relatively low, which is a significant advantage over other medically relevant metals. The choice of ligand is crucial; es it directly influences the biological activity of silver(I) complexes. The efficacy of these complexes is closely linked to their water solubility and stability, lipophilicity, and rate of release of the silver(I) ions [3]. Moreover, in recent decades, silver(I) complexes with various ligands have emerged as selective anticancer agents effective against different types of cancer cells [4].

Metal-organic frameworks (MOFs) have recently garnered substantial attention for encapsulating and storing various active agents. They stand out as adaptable crystalline structures featuring customizable pore sizes, exceptionally large surface areas, and diverse functional attributes, rendering them highly suitable for diverse uses. [5].

Within our experimental study, we prepare stable complexes of silver(I) ions with selected ligands. We selected ligands that naturally occur in the human body and fulfill physiological roles, such as the amino acid glutamic acid, malonic acid and α-ketoglutaric acid. The synthesized complexes underwent comprehensive physicochemical characterization using techniques such as elemental analysis, IR spectroscopy, X-ray crystallography and thermal analysis. As a next step in our research, we will focus on evaluating the biological activity, with emphasis on their potential antibacterial and anticancer effects. Also, the synthesized silver(I) complexes can be encapsulated into MOFs through post-synthetic modification, such as post-synthetic metalation (PSMet).

Acknowledgements

This work was supported by**:** VEGA 1/0268/24, KEGA 007UPJŠ-4/2024 and VVGS vvgs-2023-2543.

References

[1] S. K. Raju, et al., German J. Pharm. Biomaterials **2** (2022) 6–28.
[2] M. M. Aljeldah, Antibiotics **11** (2022) 1082.
[3] S. Medici et al.: Coord. Chem. Rev **327** (2016) 349-359.
[4] M. Rendošová et al.: J. Inorg. Biochem. **168** (2017) 1-12.
[5] S. A. A. Razavi, A. Morsali, Coord. Chem. Rev. **399** (2019) 213023.

BIOLOGICAL AND BIOMEDICAL APPLICATIONS

Modular Particles for Advanced Bioimaging and Photodynamic Therapy

V. Huntošová[a]*, M. Almáši[b]

[a]Center for Interdisciplinary Biosciences, Technology and Innovation Park, Pavol Jozef Šafárik University in Košice, Jesenná 5, 041 54 Košice, Slovak Republic
[b]Department of Inorganic Chemistry, Institute of Chemistry, Pavol Jozef Šafárik University in Košice, Moyzesova 11, 040 04 Košice, Slovak Republic

*veronika.huntosova@upjs.sk

The expansion of advanced imaging techniques in biology and medicine is pushing the boundaries of innovative applications and the development of contrast agents. Advanced imaging utilizes sophisticated detection techniques that integrate multiple complementary imaging modalities along with state-of-the-art image analysis. This multimodality results in considerable enhancement in data analysis and opens avenues for real-time applications in medicine and biology.

Metal-organic frameworks (MOFs) offer new possibilities for bioimaging and enhance multimodality in nano- and microparticle bioapplications [1]. These porous materials can entrap both hydrophobic and hydrophilic molecules and can be tailored to deliver specific combinations dedicated to detection and treatment conditions. Combination therapies captured by chemotherapeutics can be supplemented with contrast agents conjugated within the particles or on functional layers attached to the surface of the MOFs [2].

In our study, we employed microparticles based on MIL-101 and nanoparticles based on UiO-66 archetypal structures, known for their large surface area, defined mesopores, and excellent thermal and chemical stability. These structures were investigated using fluorescence microscopy, Raman spectroscopy, and optical coherence tomography in 2D and 3D cellular models to describe the morpho-molecular responses of cells to selected treatments [3]. Photosensitive molecules active in photodynamic therapy were loaded into the pores to introduce a bi-modal function for photodiagnostics (emitting fluorescence) and light-activated treatment by generating reactive oxygen species (singlet oxygen, superoxide, and hydrogen peroxide) to destroy targeted biological structures [4, 5]. The surface of the MOFs was functionalized for targeted drug delivery (folic acid, histidine, SARS-CoV-2 spike RBD protein, and ligands highly recognized by breast cancer cells) [5, 6].

Overall, the hierarchical structure of the developed transport systems demonstrated broad applicability and potential for bioimaging, photodiagnostics, anticancer treatment, bacterial inhibition, photodynamic antibacterial treatment, and viral inactivation through interaction with MOFs.

Acknowledgements

This research was funded by the EU NextGenerationEU through the Recovery and Resilience Plan for Slovakia under the project BCOrgFluorIDA No. 09I03-03-V04-00007.

References

[1] Y. Liu, T. Jiang, Z. Liu, Nanotheranostics **6** (2022) 143-160.
[2] Z. Lafi, S. Matalqah, E. Abu-Saleem, N. Asha, H. Mhaidat, S. Asha, L. Al-Nashash, H.S. Janabi, Med. Oncol. **42** (2024) 26.
[3] X. Li, A. Krause, G. Giardina, Z. Jiang, M. Andreana, V. Huntosova, A. Unterhuber, Optical Biopsy XXII: Toward real-time spectroscopic imaging and diagnosis **12836** (2024) 128360D.
[4] M. Macajova, L. Ambro, M. Meta, L. Zauska, T. Gulyasova, B. Bilcik, I. Cavarga, G. Zelenkova, E. Sedlak, M. Almasi, Int. J. Mol. Sci. **26** (2025) 11681.

[5] V. Huntosova, A. Benziane, L. Zauska, L. Ambro, S. Olejarova, J. Joniova, N. Hlavkova, G. Wagnieres, G. Zelenkova, P. Diko, J. Bednarcik, F. Zakany, T. Kovacs, E. Sedlak, G. Vamosi, M. Almasi, J. Colloid Interface Sci. **691** (2025) 137454.
[6] A. Migasova, L. Zauska, T. Zelenka, D. Volavka, M. Ferova, T. Gulyasova, S. Tomkova, M. Salakova, V. Kucharova, T. Samuely, J. Bednarcik, C. Slaby, M. Macajova, B. Bilcik, T. Schubert, A. Walter, V. Hornebecq, V. Huntosova, M. Almasi, Chem. Eng. J. **522** (2025) 167857.

Design and Evaluation of Functionalized SiO_2 Nanoparticles for Sustained Apixaban Release

E. Liptáková[a], E. Beňová[a], M. Šuleková[b], V. Zeleňák[a], N. Király[a]*

[a]Department of Inorganic Chemistry, Institute of chemistryJozef Šafárik University in Košice, Moyzesova 11,
041 54 Kosice, Slovak Republic
[b]Department of Chemistry, Biochemistry and Biophysics, Institute of Pharmaceutical Chemistry, The University
of Veterinary Medicine and Pharmacy, Komenského 73, 041 81, Kosice, Slovak Republic

*nikolas.kiraly@upjs.sk

Despite substantial progress in the development of stable and controlled drug delivery systems, the clinical translation of many newly developed pharmaceutical formulations remains limited, primarily due to insufficient bioavailability. In this context, silica-based nanomaterials have emerged as promising drug carriers owing to their excellent biocompatibility and porous architecture, which enable efficient loading and controlled release of therapeutic agents. Porous SiO_2 nanoparticles are characterized by high specific surface area, adjustable pore dimensions, and the presence of reactive surface functionalities such as –OH, $–NH_2$, –SH, and –Cl groups, which significantly broaden their applicability and enhance performance in biomedical systems. In addition, their chemical robustness and physiological compatibility make them particularly suitable for drug delivery applications [1].

Apixaban (APX) is an orally administered anticoagulant that acts as a selective and reversible inhibitor of coagulation factor Xa. It is widely prescribed for the prevention and treatment of thromboembolic conditions, including atrial fibrillation, pulmonary embolism, and deep vein thrombosis. Pharmacokinetic studies indicate that APX exhibits approximately 50% oral bioavailability, reaches maximum plasma concentration within 4 hours, and possesses an elimination half-life of around 12 hours, allowing for twice-daily dosing regimens [2].
The experimental strategy consisted of three consecutive synthesis stages, each designed with specific objectives and reaction conditions to systematically enhance the encapsulation efficiency and release behavior of APX from silica-based nanocarriers. In the initial stage, the primary aim was to identify suitable experimental conditions. SMS-APX samples containing 5, 25, and 50 mg of APX per 250 mg of silica carrier were prepared, compressed into tablets, and subjected to release studies. The tablets were immersed in 50 mL of physiological saline solutions at pH 2, simulating gastric conditions, and pH 7, representing the bloodstream. Aliquots were collected at predetermined time intervals over a period of 0–120 hours to evaluate the release kinetics of the active pharmaceutical ingredient.

The second stage focused on optimizing critical parameters, particularly the volume of the release medium and the mode of drug administration. Selected impregnated samples (SMS-APX, SMS-SH-APX, SMS-NH_2-APX, and SMS-Cl-APX; 50 mg each) were introduced directly into the release medium without tablet formation. Release experiments were conducted in two parallel series using 400 mL of physiological saline solutions at pH 2 and pH 7 to assess the influence of surface functionalization and experimental conditions on drug release behavior.
In the final stage, after establishing optimal parameters, attention was directed toward evaluating release dynamics under repeated dosing conditions and assessing potential toxicity-related risks. This phase aimed to estimate safe and effective dosage levels and to examine the possibility of cumulative drug release under simulated physiological environments. A defined amount of SMS-APX (50 mg) was dispersed in 400 mL of distilled water adjusted to pH 2 and pH 7. Fractional samples were collected at fixed time intervals following the same protocol as in previous experiments. Unlike earlier stages, an additional 50 mg of SMS-APX was introduced after 72 hours, and the sampling procedure was repeated. After a further 72 hours (approximately 145 hours from the start of the experiment), a third dose of 50 mg SMS-APX was added, allowing the cumulative release profile to be monitored over extended time periods.

Acknowledgements

This work was supported by the EU NextGenerationEU through the Recovery and Resilience Plan for Slovakia, project No. 09I03-03-V04-00722.

References

[1] R. Khoz, F. Yazdian, M. Pourmadad, A. Rahdar, S. Fathi-Karkan, S. Pandey, Chem. Eur. J. **12** (2024) 100206.

[2] W. Byon, S. Garonzik, R. A. Boyd, C. E. Frost, Clin. Pharmacokinet. **58** (2019) 1265–1279.

BIOLOGICAL AND BIOMEDICAL APPLICATIONS

In vivo Study of Enriched Iron Implants for Bone Substitution in a Critical Tibial Bone Defect (Rat Model)

M. Kožár[a]*, B. Šišková[a], E. Tomovčíková[a], R. Oriňaková[b]

[a]Small Animal Clinic, The University of Veterinary Medicine and Pharmacy in Košice, 040 01 Košice, Slovak Republic
[b]Department of Physical Chemistry, Pavol Jozef Šafárik University in Košice, Moyzesova 11, 040 01, Košice, Slovak Republic

*martin.kozar@uvlf.sk

Bone defect healing is a complex process influenced by biological and mechanical factors [1] which may impede normal biomechanics and the structural stability of bone as an organ. In many cases, the correction of bone defects requires extensive surgical intervention involving bone-grafting techniques and other procedures in which healing is slow, the risk of infection is high, and considerable pain is provoked - with no guarantee of complete correction of the defect [2]. Traditional orthopaedics techniques use metal implants made of stainless steel or titanium have long been the standard for fracture fixation. Despite their advantages, these materials still carry risks for patients, such as infection, the need for a secondary surgery to remove the implant, and potential biological complications related to corrosion or ion release. Also, biomechanical compatibility of the traditional metallic implants, presents a risk of unstable adhesion between the hard tissues and the implant [3]. These limitations have resulted in extensive research into biodegradable materials that provide adequate mechanical support during healing and later degrade gradually without the need for reoperation. Autografts remain the gold standard, but their use is limited by donor site morbidity and restricted availability [4]. Allografts and synthetic substitutes carry risks of immune rejection or infection [5]. Biodegradable implants offer an attractive alternative as they are gradually resorbed and replaced by new bone, thus avoiding secondary removal surgery [6]. Polymers offer good biocompatibility but lack sufficient strength for hard tissue applications [7]. On the other hand, biodegradable metals, such as magnesium- and iron-based alloys, offer superior mechanical integrity, though they require better control over degradation rates [8]. Ceramics, especially hydroxyapatite, are valuable as bioactive coatings that enhance implant integration [9]. Current research focuses on the development of iron-based porous implants with tailored corrosion and mechanical properties. Porous structure has been recognized as an effective way to eliminate this mismatch of elastic modulus [10]. The presence of material voids permits the infiltration of cells, mechanical compliance, and outward diffusion of pharmaceutical agents. Various studies have confirmed that porosity indeed promotes favourable tissue responses, including minimal fibrous encapsulation during the foreign body reaction (FBR) [11]. The porous structure also provides high interfacial bond area for vascularization and bone ingrowth [12], promoting the biological fixation of implants and bones. The present study describes the design and in vivo evaluation of a novel sponge-like iron-based biodegradable implant intended for bone replacement, demonstrating promising potential for orthopaedic applications [13].

The experimental study focused on establishing a standardized critical 5 mm full-thickness bone defect in the tibia in a rat model (Rattus norvegicus, Wistar strain), and the use of iron implants for bone substitution with monitoring period of one year.

In animals three implants and one control group were used:

1. Pure iron implant,
2. Iron implant enriched with hydroxyapatite,
3. Iron implant enriched with gentamicin,
4. Control group without internal bridging of the bone stumps.

The methodology was focused on evaluating inflammatory markers during the first 21 days after defect creation and implantation of the biodegradable material. Monitoring and evaluation of metallic material incorporation into bone tissue and its degradation were carried out over a 365-day period following surgery. Another part of the evaluation of bone tissue formation was the gene expression analysis for: Collagen type I alpha 1 (COL1A1), Osteocalcin, Osteopontin, Osteonectin in predetermined intervals on 28, 90, 180, and 365-day after the surgical application. Macroscopic assessment of bone expression was focused on: The bone fragments status, Osteointegration and degradation of the iron implants, Bridging - overgrowing of the bone defect and Reaction of the surrounding structures. In the results of macroscopic evaluation, the greatest reactivity of the soft tissue like surrounding structures at the defect site was observed in the group with gentamicin-enriched iron implants, manifested as a strong inflammatory reaction, poor incorporation into the bone stump, and increased postoperative complications.

The most notable ingrowth of new tissue through the iron implant was observed from day 180 in the group with hydroxyapatite-enriched implants. The limitations of pure iron implants emerged: Formation of cartilaginous pseudo-tissue as the initial stage of callus formation, Loss of stability of the pure implant, Delayed osteointegration due to the reactivity of surrounding structures during degradation and increased inflammatory response after implantation.

The results of an experimental study of critical bone defects in Rats as an animal model using enriched iron implants pointed to limitations and the need for further research. Further research should be focused on developing a porous structural matrix made from multiple materials with different stiffness and resorption times, aimed at creating bio composites for bone tissue replacement.

Acknowledgements

This work was supported by the projects APVV-20-0278 and APVV-24-0033 of the Slovak Research and Development Agency.

References

[1] C. R. Perry, Clin. Orthop. Relat. Res. **360** (1999) 71–86.

[2] E. Guerado, E. Caso, World J. Orthop. **8** (2017) 87–98.

[3] Z. Chen, Mater. Sci. Eng. C **106 (**2020) 110289.

[4] G. Liu, L. Zhao, W. Zhang, L. Cui, W. Liu, Y. Cao, J. Mater. Sci. Mater. Med. **19** (2008) 2367–2376.

[5] R. W. Lindsey, Z. Gugala, E. Milne, M. Sun, F. H. Gannon, L. L. Latta, J. Orthop. Res. **24** (2006) 1438–1453.

[6] A. M. S. Ibrahim, P. G. L. Koolen, K. Kim, G. S. Perrone, D. L. Kaplan, S. J. Lin, Clin. Podiatr. Med. Surg. **32** (2015) 61–72.

[7] A. Prasad, Mater. Today Proc. **44** (2021) 2447–2453.

[8] G. Gąsior, J. Szczepański, A. Radtke, Materials (Basel). **14** (2021) 1-8.

[9] A. M. Parizi, A. Oryan, Z. Shafiei-Sarvestani, A. Bigham-Sadegh, J. Orthop. Traumatol. **14** (2013) 259–268.

[10] D. K. Pattanayak, Acta Biomater. **7** (2011) 1398–1406.

[11] J. L. Hernandez, K. A. Woodrow, Adv. Healthc. Mater. **11** (2022) 1–50.

[12] Y. Li, C. Yang, H. Zhao, S. Qu, X. Li, Y. Li, Materials (Basel). **7** (2014) 1709–1800.

[13] B. Wegener, Sci. Rep. **10** (2020) 1–10.

Cysteine-Functionalized UiO-66(Zr)-NH_2: Synthesis, Characterization and Potential for Improved Bioconjugation and Targeted Delivery

A. Migasová[a]*, G. Zelenková[b], T. Zelenka[b], V. Huntošová[c], M. Almáši[a]

[a]Department of Inorganic Chemistry, Institute of Chemistry, Faculty of Science, P. J. Šafárik University
in Košice, Moyzesova 11, 040 01 Košice, Slovak Republic
[b]Department of Chemistry, Faculty of Science, University of Ostrava, 30. dubna 22, 702 00 Ostrava,
Czech Republic
[c]Center for Interdisciplinary Biosciences, Technology and Innovation Park, P. J. Šafárik University in Košice,
Jesenná 5, 041 54 Košice, Slovak Republic

*alexandra.migasova@student.upjs.sk

Infectious diseases are increasing each year and posing growing challenges to scientific readiness. It is therefore essential to be prepared for these threats from the very onset of an outbreak. For example, the coronavirus disease pandemic that emerged in 2019 affected more than one hundred million people worldwide and had profound consequences for society, public health, and the global economy [1]. In emergency responses, three key principles are particularly important: prevention, early diagnosis, and targeted therapy.

Among the developing promising strategies to address these challenges are modular nanoparticles, which offer a combination of versatility, multifunctionality, and the potential for real-time monitoring of therapeutic outcomes. This class of nanoparticles also includes a metal-organic framework (MOF) material, specifically UiO-66(Zr)-NH_2 — a highly stable, biocompatible, and porous material composed of zirconium clusters connected by 2-aminoterephthalate linkers. UiO-66(Zr)-NH_2 is outstanding by its small particle size, chemical robustness, catalytic activity, and high drug-loading capacity. Its large surface area and accessible amine functional groups enable efficient surface modification, making it particularly suitable for targeted drug delivery and subcellular transport [2]. Previous studies have demonstrated its potential in anti-inflammatory therapy and wound healing applications. More recently, the MOF MIL-101(Al)-NH_2 has been shown to be effective for antiviral drug delivery, spike protein immobilisation, as well as applications in bioimaging and antibacterial photodynamic therapy [3].

This study focuses on the synthesis, characterization and properties study of a novel nanosystem based on UiO-66(Zr)-NH_2 modified with cysteine molecules for future functionalization of the SARS-CoV-2 receptor binding domain (RBD) protein. This modification strategy aimed to interact between the material and biological molecules or cells to enhance the selective targeting of ACE2 receptors, mimicking the virus's entry mechanisms.

UiO-66(Zr)-NH_2 was synthesized via a solvothermal method using zirconium chloride and 2-aminoterephthalic acid as precursors. Surface modification with cysteine was achieved through amide bond formation between the amine groups of the MOF and the carboxyl groups of cysteine. The resulting materials were characterized by available physicochemical techniques, specifically using infrared spectroscopy, powder X-ray diffraction, argon adsorption/desorption analysis, thermogravimetric analysis, Raman spectroscopy and fluorescence spectroscopy. Infrared and Raman spectroscopy with argon adsorption/desorption measurements confirmed the successful synthesis and cysteine modification of the UiO-66(Zr)-NH_2 material. An example of confirmation of this conclusion can be the descending surface area (S_{BET}) and pore volume values obtained from the argon adsorption/desorption measurements. For pristine material UiO-66(Zr)-NH_2 S_{BET} was 625 $m^2\ g^{-1}$ and pore volume was 0.314 $cm^3\ g^{-1}$. For modified material UiO-66(Zr)-Cys these values were 564 $m^2\ g^{-1}$ and 0.275 $cm^3\ g^{-1}$. Also, thermogravimetric analysis revealed that the materials remained thermally stable up to 400 °C, corresponding to decomposition of the organic linker, and quantified the amount of bound cysteine as 22.6 $mg\ g^{-1}$. At the same time, according to powder X-ray diffraction analysis, the crystallinity and structural integrity of the material were preserved after modification. These materials can also be used in fluorescence bioimaging to monitor the distribution of nanoparticles in biological samples, as they showed fluorescence emission maxima between 400-475 nm after 280 and 405 nm excitation.

In the field of biological activity, the biocompatibility of UiO-66(Zr)-NH_2 and UiO-66(Zr)-Cys nanoparticles was studied with HEK293T cells at concentration range from 0.02 to 0.07 mg mL^{-1} over a 48 h incubation period and the results are shown in Figure 1. The metabolic activity of mitochondria, reflected by the production of formazan, showed no significant differences between untreated control cells and those exposed to nanoparticles below 0.017 mg mL^{-1} for UiO-66(Zr)-NH_2 or UiO-66(Zr)-Cys. However, at higher particle concentrations (0.035 and 0.07 mg mL^{-1}), a significant increase in formazan production was observed. It was also observed that UiO-66(Zr)-NH_2 nanoparticles simultaneously provide catalytic support for NADH regeneration and thus detect metabolic markers. This catalytic behaviour may account for the increase in formazan levels detected at higher concentrations of UiO-66(Zr)-NH_2 and UiO-66(Zr)-Cys, likely through their influence on cellular redox processes.

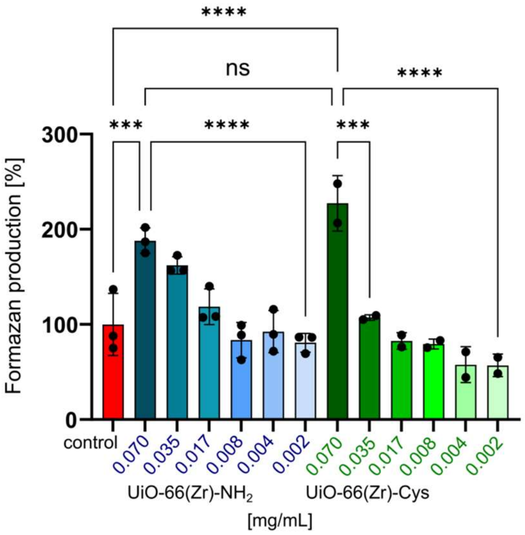

Figure 1 Display of metabolic activity of HEK293T cells determined by MTT assay after 48 hours of incubation with different concentrations of UiO-66(Zr)-NH_2 nanoparticles (blue bars) and UiO-66(Zr)-Cys (green bars).

Acknowledgements

This work was supported by the EU NextGenerationEU through the Recovery and Resilience Plan for Slovakia under the project No. 09I03-03-V04-00007.

References

[1] M. Nicola, Z. Alsafi, C. Sohrabi et. al. Int. J. Surg. **78** (2020) 185-193.
[2] K. L. Timofeev, S. A. Kulinich, T. S. Kharlamova, Molecules **28** (2023) 3916.
[3] V. Huntošová, A. Benziane, Ľ. Zauška et. al. J. Colloid Interface Sci. **691** (2025) 137454.

Insulin Determination in Blood Serum via Screen-printed Carbon Electrodes Modified by Laser-Synthesized Nickel Nanoparticles

I. Šišoláková[a]*, M. Cvek[b], J. Shepa[a], M. Kožár[b], R. Oriňaková[a]

[a]Department of Physical Chemistry, Pavol Jozef Šafárik University in Košice, Moyzesova 11, 040 01 Košice, Slovak Republic
[b]Small Animal Clinic, University of Veterinary Medicine and Pharmacy in Košice, Komenského 73, Košice, 040 01, Slovak Republic

*ivana.sisolakova@upjs.sk

Diabetes mellitus represents a long-term metabolic disease associated with persistent hyperglycemia resulting from inadequate insulin secretion, reduced insulin sensitivity, or a combination of both [1]. Reliable and timely diagnosis is essential for appropriate disease management and for minimizing the risk of secondary complications. Currently, diabetes is commonly diagnosed using established clinical assays, including the Fasting Plasma Glucose (FPG), Oral Glucose Tolerance Test (OGTT), Glycated Hemoglobin (HbA1c), and Random Plasma Glucose tests [2]. Despite their widespread use, many of these diagnostic approaches rely on enzymatic electrochemical principles, which are often limited by enzyme instability, elevated production costs, and sensitivity to external conditions such as temperature, pH, and humidity. Consequently, increasing attention has been directed toward non-enzymatic electrochemical sensing strategies, which provide improved operational stability, reproducibility, and economic advantages for the determination of insulin levels [3].

In this work non-enzymatic insulin sensor based on screen-printed carbon electrodes (SPCEs) modified with LAL-produced Ni NPs (LAL-NiNPs-SPCE) for insulin determination in blood serum was developed.

Electrochemical determination of insulin in blood serum samples

Electrochemical measurements of insulin in blood serum were conducted by cyclic voltammetry within a potential window ranging from 0 to +1.0 V, applying a scan rate of 100 mV/s. The obtained voltammetric profiles (Figure 1) reflect the analytical performance of the LAL-NiNPs-SPCE sensor toward insulin over a concentration range of 0.5–5 µM. Notably, all analyses were performed directly in blood serum, demonstrating the sensor's ability to function effectively in a complex biological environment.

In the presence of serum, the cyclic voltammograms revealed a pronounced increase in anodic current associated with insulin oxidation (Figure 1A), while the overall shape of the voltammetric response remained unaffected by matrix components. A strong linear dependence between the oxidation peak current and insulin concentration was observed ($R^2 = 0.99$), with the oxidation peak potential showing negligible variation across the examined concentration range (Figure 1B). These observations indicate that typical serum constituents, including glucose, ascorbic acid, uric acid, and albumin, did not produce measurable interference under the applied experimental conditions.

The lack of peak deformation, signal attenuation, or background distortion highlights the high selectivity of the proposed sensor, which can be attributed to the combined effects of the nickel nanoparticle-modified electrode surface and the inherent electrochemical selectivity of insulin oxidation. Collectively, these results confirm the robustness of the LAL-NiNPs-SPCE in real biological matrices and underscore its promising applicability for clinical insulin monitoring.

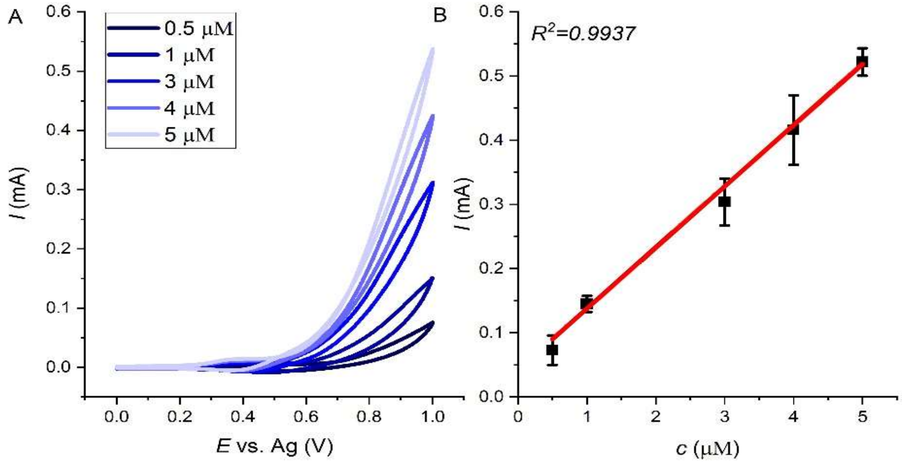

Figure 1 A) Cyclic voltammograms for different concentrations of insulin in human blood serum and 0.1 M NaOH solution (0.5, 1, 2, 3, 4, and 5 µM) at 100 mV/s. B) Dependence of current response to concentration of insulin fitted by a linear function.

Taken together, the findings demonstrate that the LAL-NiNPs-SPCE provides an effective platform for the quantitative determination of insulin. The successful establishment of a robust linear calibration relationship within a complex blood serum environment highlights the sensor's excellent selectivity, sensitivity, and resistance to matrix-related interferences, confirming its strong potential for application in clinical diagnostics as well as pharmacological evaluation of insulin.

Acknowledgements

This work was funded by the NATO Science for Peace and Security Programme under grant id G6106.

References

[1] M. J. Hossain, M. Al-Mamun, M. R. Islam, Heal. Sci. Reports. **7** (2024) 5–9.
[2] A. Bascones-Martínez, J. González-Febles, J. Sanz-Esporrín, Am. J. Dent. **27** (2014) 63–67.
[3] I. Šišoláková, J. Hovancová, R. Oriňaková, A. Oriňak, D. R. Garcia, O. Shylenko, J. Radoňak, Electroanalysis **31** (2019) 103–112.

Carbon Paste Electrode as a Sustainable Tool for Electrochemical Determination of Insulin in Blood Serum Samples

I. Šišoláková[a]*, J. Shepa[a], S. Vanchak[a], R. Filip[a], M. Kožár[b], R. Oriňaková[a]

[a]Department of Physical Chemistry, Pavol Jozef Šafárik University in Košice, Moyzesova 11, 040 01 Košice, Slovak Republic
[b]Small Animal Clinic, University of Veterinary Medicine and Pharmacy in Košice, Komenského 73, Košice, 040 01, Slovak Republic

*ivana.sisolakova@upjs.sk

The accurate determination of insulin is essential for diabetes diagnostics, biomedical research, and pharmaceutical quality control [1]. However, conventional analytical techniques are often associated with high costs, complex sample preparation, and significant environmental burden [2]. In response to the growing demand for sustainable and accessible analytical tools, this work presents a novel, environmentally friendly carbon paste electrode (CPE) designed for non-enzymatic electrochemical determination of insulin in real blood serum samples.

The proposed sensor was fabricated exclusively from eco-friendly and waste-derived materials, incorporating carbon powder obtained from waste processing, coconut oil as a natural binder, and a pencil lead as the working electrode substrate. To enhance the electrochemical performance toward insulin oxidation, the CPE surface was modified with copper using cyclic voltammetry method via following steps.

CPE modification

5g of carbon powder (L-274-A) was mixed with appropriate 1.5 g of melted coconut oil. Thereafter, 10 mL of ethanol was added to the mixture and homogenised by ultra sonification during 10 min. Then samples were stored at 60 °C to evaporate ethanol from the samples. Prepared paste was applied on the bottom of pencil CPE, and the surface of carbon paste was polished. Cu particles were electrodeposited on the surface of the CPE via cyclic voltammetry within the potential window from 0 to -1 V, at scan rate 100 mV/s from the solution of 12 g $CuSO_4$, 2.6 mL H_2SO_4, and 6 mL ethanol in 1 litter of distilled water. For all electrochemical measurements was used three electrodes system where Pt electrode, Ag/AgCl/KCl, and carbon paste electrode were used as auxiliary, reference, and working electrode, respectively.

Electrochemical determination of insulin in blood serum samples

The determination of insulin in blood serum was performed using cyclic voltammetry in the potential range from −1.0 to +1.0 V at a scan rate of 100 mV s^{-1}. The recorded cyclic voltammograms (Figure 1) illustrate the analytical response of the copper-modified carbon paste electrode (Cu/CPE) toward insulin within the concentration interval of 0.66 µM to 3.3 µM. Importantly, all experiments were carried out directly in a blood serum matrix, confirming the capability of the electrode to operate reliably in a complex biological medium.

The voltammetric curves display a distinct and irreversible anodic peak, which can be attributed to the electrochemical oxidation of insulin, primarily involving tyrosine residues. The oxidation peak potential remains essentially unchanged across the studied concentration range, indicating a stable and reproducible reaction pathway. Quantitative evaluation is provided in the inset, where the calibration relationship was obtained by correlating the anodic peak current (I) with insulin concentration (c). A strong linear dependence was observed within the examined range of 0.66–3.3 µM, demonstrating a linear dynamic response, with a limit of detection of 0.7 µM and a sensitivity of 170 µA μM^{-1}.

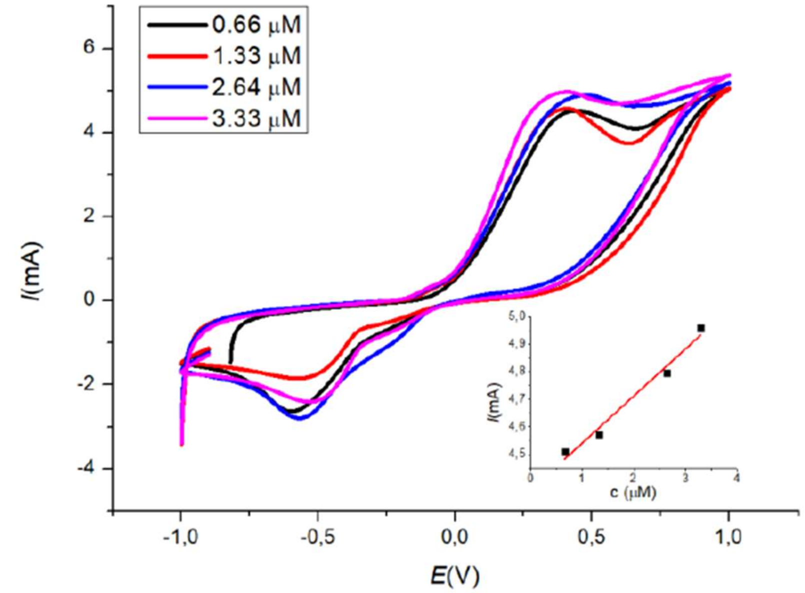

Figure 1 Cyclic voltammograms for Cu/CPE with various concentrations of insulin in bovine blood serum. Inset: Calibration curve.

Overall, the obtained results confirm the high efficiency of the Cu/CPE for quantitative insulin analysis. The formation of a reliable linear calibration model in the presence of a complex blood serum matrix underscores the sensor's high selectivity, sensitivity, and tolerance toward matrix effects, highlighting its considerable potential for use in clinical diagnostics and pharmacological insulin analysis.

Acknowledgements

Funded by the EU NextGenerationEU through the Recovery and Resilience Plan for Slovakia under the project No. 09I03-03-V04-00180.

References

[1] M. Zhang, C. Mullens, W. Gorski, Anal. Chem. **77** (2005) 6396–6401.
[2] I. Šišoláková, J. Hovancová, R. Oriňaková, A. Oriňak, D. R. Garcia, O. Shylenko, J. Radoňak, Electroanalysis **31** (2019) 103–112.

Nanoparticles Designed for Targeted Therapy of Cancer

S. Tomková[a]*, A. Migasová[b], M. Almáši[b], V. Huntošová[a]

[a]Center for Interdisciplinary Biosciences, Technology and Innovation Park, Pavol Jozef Šafárik University in
Košice, Jesenná 5, 041 54 Košice, Slovak Republic
[b]Department of Inorganic Chemistry, Institute of Chemistry, Pavol Jozef Šafárik University in Košice,
Moyzesova 11, 040 04 Košice, Slovak Republic

*silvia.tomkova@upjs.sk

Although UiO-66 is a classic metal-organic framework (MOF), its advantages are its large surface area and thermal stability. Its porosity allows the incorporation of small molecules at high loading capacity, and surface modifications of UiO-66 enable the development of targeted delivery systems for various diseases. Moreover, functionalisation can control the premature release of drugs from the delivery system. On the other hand, its acidic sensitivity makes this system highly suitable for targeted drug release in tumour tissue, which is characterised by low pH. Different metals doped into UiO-66 can be used to create nanostructures, but the zirconium modification is the most biocompatible and therefore suitable for biological applications. It has been reported that UiO-66(Zr) has high stability in water, flexibility, compatibility, and, most importantly, low toxicity [1].

In the present study, histidine (His) modification of UiO-66(Zr)-NH_2 was investigated for the delivery of methylene blue (MB) and 5-fluorouracil (5-FU) into breast cancer cells. This delivery can target L-type amino acid transporter 1 (LAT1), which can be overexpressed in certain types of cancer cells [2]. The delivery system developed in this study was designed to combine chemotherapy and photodynamic therapy, which was activated with orange light.

UiO-66(Zr)-His modification facilitated the transport of nanoparticles into cancer cells, as observed by both fluorescence microscopy and flow cytometry. Fluorescence microscopy revealed that MB release was inhibited by His modification in solution and in cells. Nevertheless, photodynamic action triggered by irradiation of breast cancer cells with 590 nm light resulted in inhibition of cell proliferation. The cells studied had either overexpressed or down-expressed HER2 receptors, which was influenced by the treatment. The expression of HER2 receptors in cells was confirmed by highly specific binding of a bioluminescent DARPin-Luciferase fusion protein that recognises HER2 receptors in living cells. Cell proliferation was even more affected when a combination treatment of MB and 5-FU was used. This treatment significantly influenced cell signalling, leading to apoptosis and autophagy.

In summary, the developed transport system with targeted delivery and combination therapy demonstrated strong potential for cancer treatment.

Acknowledgements

This research was funded by university project VVGS 2025-3747, and by the EU NextGenerationEU through the Recovery and Resilience Plan for Slovakia under the project BCOrgFluorIDA No. 09I03-03-V04-00007.

References

[1] M. Pormadadi, Z. Omrani, Z. Forootan, M. S. Ebadi, F. Yazdian, J Drug Deliv. Sci. Technol. **86** (2023) 104690.
[2] A. Migasova, L. Zauska, T. Zelenka, D. Volavka, M. Ferova, T. Gulyasova, S. Tomkova, M. Salakova, V. Kucharova, T. Samuely, J. Bednarcik, C. Slaby, M. Macajova, B. Bilcik, T. Schubert, A. Walter, V. Hornebecq, V. Huntosova, M. Almasi, Chem. Eng. J. **522** (2025) 167857.

BIOLOGICAL AND BIOMEDICAL APPLICATIONS

Porous Innovations: Materials Designing the Future of Precision Medicine

A. Trabolsi[a]*

[a]New York University Abu Dhabi, Abu Dhabi, United Arab Emirates

*at105@nyu.edu

The development of multifunctional drug delivery systems (MDDS) targeting diseased areas arose from the need to overcome drug limitations such as cytotoxicity, immunogenicity, short circulation times, uncontrolled bio-distribution, and the inability to target specific tissues. Significant advances in nanobiotechnology have led to the development of MDDS to serve diagnostic and therapeutic purposes through a single medical device capable of performing bioimaging tasks while improving the therapeutic efficacy of marketed drugs. Stimuli-responsive nanostructures can take advantage of changes in the biological microenvironment of the disease in question and respond to changes in temperature, pH, redox conditions, reactive oxygen species (ROS), and enzyme concentration, with combinations of stimuli increasing the therapeutic versatility of MDDS. This approach, defined as a new paradigm in nanomedicine, has applications in several fields, including cancer therapy, drug delivery, tissue engineering, and even bionics. In this scenario, the intrinsic properties of nanoparticles are used to develop active devices with diagnostic, therapeutic, or even theranostic functions. Our group has developed several theranostic covalent organic frameworks (COFs) as smart trigger-responsive MDDSs that cover a wide range of applications from cancer therapy to bioimaging to diabetes control. Nanoscale COFs have shown tremendous potential as new candidates for nanomedicine due to their unique properties-large surface area, tunable pore geometry, crystallinity, versatility, as well as responsiveness to physiological environments. COFs exhibit a long-range ordered structure that results in regular pores with diameters that facilitate the loading and controlled release of prominent drugs and proteins/enzymes. Moreover, their high flexibility in molecular design makes them versatile and uniquely responsive to their environment. Recently, we published the formation of imine-linked nanoscale COFs linked for cancer therapy. The resulting COFs were stable under physiological conditions but disintegrated in an acidic medium, an essential property of the microenvironment of most solid tumors, and facilitated site-specific drug release.[1] On the other hand, we reported a triazine-based COF with high stability under harsh acidic environmental conditions for oral insulin delivery to diabetic rats.[2] The insulin-loaded COF crossed the intestinal barrier and sustainably lowered blood glucose levels in vivo in diabetic rats (T1D), and blood glucose levels completely returned to normal without causing systemic toxicity compared with the control group of nondiabetic rats. In my talk, I hope to offer some key elements to answer the question, "Can COF nanoparticles serve as effective therapeutics for various disease treatments?"

Acknowledgements

This work was supported by NYUAD.

References

[1] F. Benyettou, G. Das, A. Ramdas Nair, T. Prakasam, D. Shinde, S. K. Sharma, J. Whelan, Y. Lalatonne, H. Traboulsi, R. Pasricha, O. Abdullah, R. Jagannathan, Z. Lai, L. Motte, F. Gándara, K. C. Sadler, A. Trabolsi, J. Am. Chem. Soc. **142** (2020) 18782–18794.

[2] F. Benyettou, N. Kaddour, T. Prakasam, G. Das, S. K. Sharma, S. A. Thomas, F. Bekhti-Sari, J. Whelan, M. A. Alkhalifah, M. Khair, H. Traboulsi, R. Pasricha, R. Jagannathan, N. Mokhtari-Soulimane, F. Gándara, A. Trabolsi, Chem. Sci. **12** (2021) 6037–6047.

BIOLOGICAL AND BIOMEDICAL APPLICATIONS

Hierarchically Porous MIL-101-Cr/Carbon Monoliths as Carriers for Anticancer Drugs

L. Zelená[a,b]*, Ľ. Zauška[a], M. Almáši[a], T. Zelenka[b], P. Diko[c]

[a]Department of Inorganic Chemistry, Faculty of Science, P. J. Šafárik University, Moyzesova 11, SK-041 01 Košice, Slovak Republic
[b]Department of Chemistry, Faculty of Science, University of Ostrava, 30. dubna 22, Ostrava, CZ-702 00 Czech Republic
[c]Institute of Experimental Physics, Slovak Academy of Sciences, Watsonova 47, SK-040 01 Košice, Slovak Republic

*lucie.zelena@student.upjs.sk

The integration of metal–organic frameworks into carbon-based architectures represents an effective strategy for the design of multifunctional porous materials with potential biomedical relevance. In particular, hybrid systems combining the high surface area and tunable porosity of MOFs with the structural robustness of hierarchically porous carbon supports offer promising opportunities for the development of advanced drug carrier platforms [1]. Among these materials, the chromium-based MIL-101-Cr framework stands out due to its exceptional textural properties and chemical stability, which have been widely demonstrated in drug delivery studies [2].

In this contribution, a hybrid composite material based on MIL-101-Cr was prepared and incorporated into a hierarchically porous carbon monolith (MMM) using an in situ growth method. This synthetic strategy enabled the direct formation of the MOF phase inside the carbon matrix, resulting in a structurally integrated composite while maintaining the hierarchical pore system of the carrier. The successful incorporation and distribution of MIL-101-Cr within the carbon monolith was verified by X-ray diffraction, nitrogen adsorption–desorption measurements, and scanning electron microscopy, which together confirmed the coexistence of both components without structural degradation.

The resulting MIL-101(Cr)@HPCM composites are envisaged as advanced carriers for anticancer agents, with particular emphasis on 5-fluorouracil and pemetrexed. Owing to their combined porous structure and enhanced stability, these materials are expected to provide high drug-loading capacity and enable controlled drug release, potentially influenced by environmental conditions such as pH [2,3]. Further investigations are currently focused on drug encapsulation efficiency and release behavior under conditions relevant to biomedical applications.

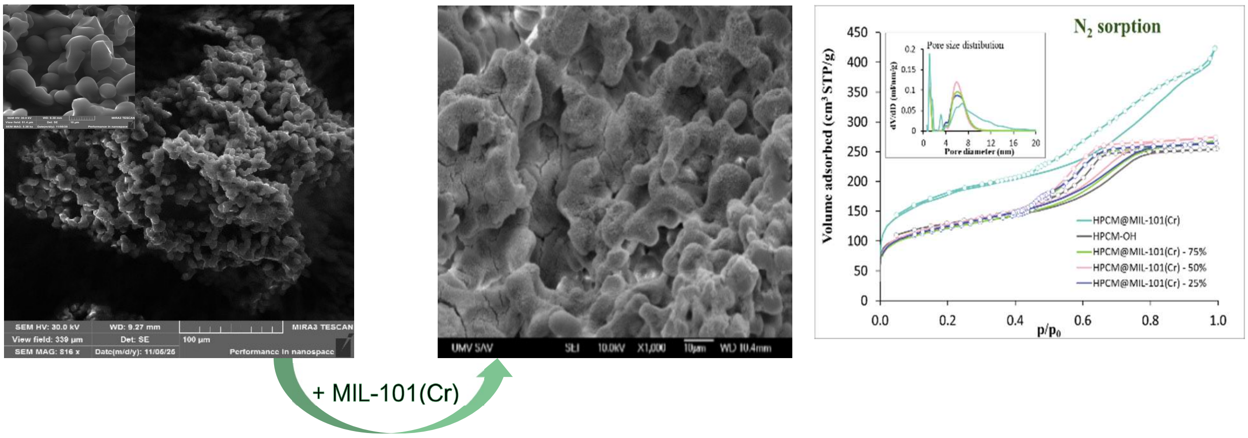

Figure 1 A) SEM analysis of HPCM and B) composite MMM@MIL-101-Cr, C) N_2 (77K) sorption results.

Acknowledgements

Funded by the EU NextGenerationEU through the Recovery and Resilience Plan for Slovakia under the project No. 09I03-03-V02-00021.

References

[1] P. Horcajada, R. Gref, T. Baati, G. Maurin, P. Couvreur, G. Férey, R. E. Morris, C. Serre, Chem. Rev. **112** (2012) 1232–1268.
[2] P. Horcajada, T. Chalati, C. Serre, B. Gillet, T. Baati, J. F. Eubank, J. - S. Chang, Y. K. Hwang, V. Marsaud, G. Férey, R. Gref, J. Am. Chem. Soc. **132** (2010) 1107–1116.
[3] S. Rojas, A. Arenas-Vivo, P. Horcajada, Coord. Chem. Rev. **388** (2019) 202–226.

Hierarchically Porous MOF–Carbon Composites for Efficient Amoxicillin Delivery

L. Zelená[a,b*], Ľ. Zauška[a], T. Zelenka[b], E. Kinnertová[b], P. Diko[c], Ľ. Ambro[d], V. Huntošová[d], M. Almáši[a]

[a]Department of Inorganic Chemistry, Faculty of Science, P. J. Šafárik University, Moyzesova 11, SK-041 01 Košice, Slovak Republic
[b]Department of Chemistry, Faculty of Science, University of Ostrava, 30. dubna 22, Ostrava, CZ-702 00 Czech Republic
[c]Institute of Experimental Physics, Slovak Academy of Sciences, Watsonova 47, SK-040 01 Košice, Slovak Republic
[d]Center for Interdisciplinary Biosciences, Technology and Innovation Park, Pavol Jozef Šafárik University, Jesenná 5, SK-041 54 Košice, Slovak Republic

*lucie.zelena@student.upjs.sk

Porous composite materials based on metal–organic frameworks (MOFs) and hierarchically porous carbon materials (HPCM) represent promising platforms for controlled drug delivery [1,2]. In this work, composite systems containing UiO-66 and UiO-66-NH_2 integrated with HPCM were prepared via an *in situ* approach and evaluated as carriers for the antibacterial drug amoxicillin. The materials were comprehensively characterized to assess their structural integrity, porosity, and drug loading capacity.

Drug release studies revealed sustained *pH*-responsive release (Figure 1a), with more intense release in physiologically relevant media. Importantly, the composites demonstrated the ability to retain the drug under acidic conditions, suggesting their potential suitability for environments where it is necessary to minimize early drug loss. The antibacterial efficacy of composites containing amoxicillin was evaluated against Staphylococcus aureus (CCM 4223, ATCC 29213, Figure1b). The tested systems showed significant antibacterial activity, confirming that the drug retained its biological activity after incorporation into and release from the composite matrices. The results highlight the synergistic potential of MOF–carbon composites as advanced drug delivery systems with effective antibacterial activity [2,3].

Overall, the prepared composites show high potential as carriers for controlled antibiotic delivery and represent promising materials for future biomedical applications.

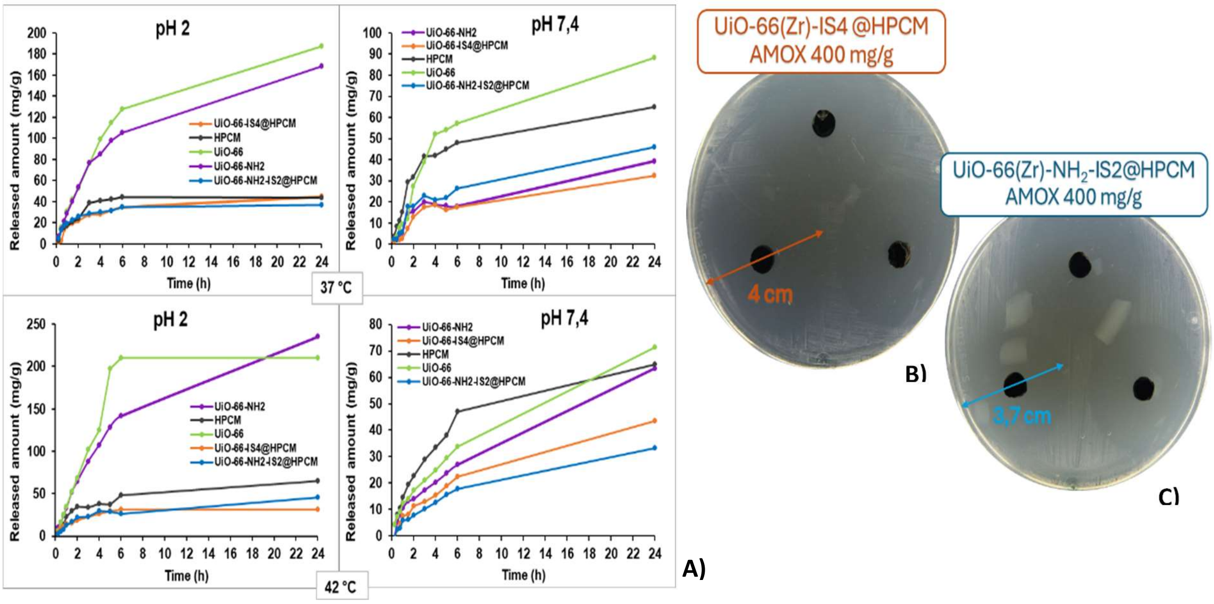

Figure 1a) Release of amoxicillin, b) antibacterial efficacy of UiO-66(Zr)-IS4@HPCM and c) UiO-66(Zr)-NH$_2$-IS2@HPCM with amoxicillin.

Acknowledgements

Funded by the EU NextGenerationEU through the Recovery and Resilience Plan for Slovakia under the project No. 09I03-03-V02-00021

References

[1] P. Horcajada, R. Gref, T. Baati, et al., Chem. Rev. **112** (2012) 1232–1268.
[2] S. Rojas, A. Arenas-Vivo, P. Horcajada, Coord. Chem. Rev. **388** (2019) 202–226.
[3] K. M. L. Taylor-Pashow, J. Della Rocca, Z. Xie, et al., J. Am. Chem. Soc. **131** (2009) 14261–14263.

CATALYSIS AND PHOTOCATALYSIS

Functionalised Metallic Foams for Catalytic and Photocatalytic Applications

N. Eißmann[a]*, F. Neupert[a], T. Büttner[a], A. Salomon[a], A. Tillmann[b], G. M. Lange[c], P. Falat[c], M. Al Aiti[c], I. Lindemann[a], T. Weißgärber[a,d]

[a]Fraunhofer Institute for Manufacturing Technology and Advanced Materials IFAM Dresden Branch, Winterbergstraße 28, 01277 Dresden, Germany
[b]Alantum Europe GmbH, Balanstraße 73, 81541 Munich, Germany
[c]TUD Dresden University of Technology, Faculty Mechanical Engineering, Institute of Materials Science, Chair Materials Science and Nanotechnology, Hallwachsstraße 3, 01062 Dresden, Germany
[d]TUD Dresden University of Technology, Faculty Mechanical Engineering, Institute of Materials Science, Chair Powder Metallurgy, Helmholtzstraße 7, 01062 Dresden, Germany

*nadine.eissmann@ifam-dd.fraunhofer.de

Open-cell metallic foams combine a unique set of structural and functional properties that make them highly attractive as substrates for catalytic and photocatalytic applications. Their three-dimensional, interconnected strut network provides a large accessible surface area while maintaining high permeability and low pressure drop. In addition, metallic foams exhibit excellent thermal and electrical conductivity as well as mechanical robustness, enabling operation under demanding reaction conditions.

Building on these intrinsic properties, the functional performance of metallic foams can be further tailored through suitable coating technologies. By selecting appropriate deposition methods, both the chemical composition and the structural characteristics of the foam can be adjusted in a controlled manner. Depending on the application, coatings can be designed to form homogeneous layers across the entire strut network or to introduce graded structures that locally modify surface area, activity or transport behaviour. In this way, the open-cell metallic foam serves as a flexible scaffold whose properties can be specifically adapted to the requirements of catalytic and photocatalytic processes.

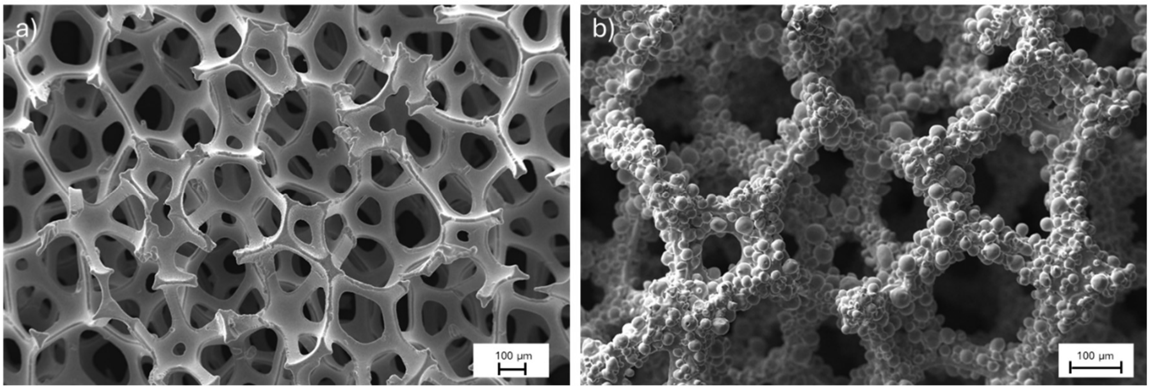

Figure 1 SEM analysis of open-cell metallic foam: a) uncoated Nickel foam and b) coated foam.

For both catalysis and photocatalysis, the high accessible surface area of metallic foams represents a key enabling factor, complementing their favourable transport, thermal and mechanical properties. In catalytic applications, metallic foams can either act as the catalytically active material themselves or serve as structured catalyst supports onto which active phases are deposited. This dual role allows the foam architecture to be exploited for different catalytic concepts, ranging from fully functionalised catalytic bodies to coated supports with tailored activity.

In photocatalytic systems, metallic foams primarily function as substrates for photoactive materials. Here, the three-dimensional porous structure provides a mechanically stable backbone for immobilising light-responsive coatings while maintaining permeability for flow-through operation. The integration of photoactive layers onto open-cell foams offers opportunities to combine large reactive surface area with efficient mass transport and, depending on the system, enhanced light accessibility.

The choice of coating method is therefore a critical design step. Suitable processes must ensure uniform coverage of the three-dimensional foam structure while providing sufficient adhesion, mechanical integrity and long-term stability under operating conditions. In some cases, additional post-deposition treatments, such as thermal processing, may be required to stabilise the coating or to achieve the desired phase composition and functionality.

To demonstrate these concepts, two representative applications are presented: one example from heterogeneous catalysis and one from photocatalysis. Together, they illustrate how metallic foams can be systematically functionalised to meet application-specific requirements and how coating strategies govern the interplay between structure, surface reactivity and transport in foam-based catalytic systems.

Acknowledgements

Freistaat Sachsen

This measure is co-financed with tax revenue based on the budget approved by the Saxon State Parliament.

CATALYSIS AND PHOTOCATALYSIS

Synthesis of Titanium Phosphonates in Water: Toward Efficient Heterogenous Catalysts for 5-HMF Synthesis

A. Fanourgiakis[a], R. Tomer[a,b], C. Chandran[a,c], N. Ghanemnia[e], N. Gys[a,c], A. Morena[d], M. Deiteren[a], C. Aprile[d], S. Hermans[b], T. Hauffman[c], W. Marchal[e], V. Meynen[a]*

[a]Laboratory of Adsorption and Catalysis (LADCA), University of Antwerp,
Groenenborgerlaan 171, 2020 Antwerp, Belgium
[b]Institute of Condensed Matter and Nanosciences (IMCN), Université Catholique de Louvain (UCLouvain),
Place Louis Pasteur 1, L4.01.03, Louvain-la-Neuve, Belgium
[c]Electrochemical and Surface Engineering (SURF), Department of Materials and Chemistry, Vrije Universiteit
Brussel, Pleinlaan 2, 1050 Brussels, Belgium
[d]Unit of Nanomaterials Chemistry (CNano) - Namur Institute of Structured Matter (NISM), UNamur, 5000
Namur, Belgium
[e]UHasselt, Institute for Materials Research (IMO-IMOMEC), Analytical and circular Chemistry (ACC),
Agoralaan, 3590 Diepenbeek, Belgium

*vera.meynen@uantwerpen.be

Porous metal phosphonates (PMPs) are a class of hybrid materials formed from the reaction of metal precursors with organophosphonic acids or esters and are characterized by high BET surface areas, often exceeding 300 m^2 g^{-1}, together with notable chemical stability across wide pH ranges and thermal stability typically above 200 °C [1–3]. Moreover, the hybrid combination of metal oxide and phosphonic acid moieties provides metal phosphonates with both Brønsted and Lewis acidity. PMPs can be categorized into phosphonate MOFs, layered metal phosphonates and (meso)porous metal phosphonates. This projects aims at the formation of the latter and its application in biomass conversion reactions.

Despite their potential, the controlled synthesis and isolation of (meso)porous PMPs remain a significant challenge, particularly in understanding the relationship between synthetic conditions, material properties, and catalytic performance. The strong and fast interactions between phosphonic acid groups and metal oxide units, which are in our case Ti(IV) centers, require precise control over reaction parameters. In this study, we introduce phosphonic acid moieties via in-situ hydrolysis of tetraethylpropylene-1,3-diphosphonate (TEPD) [4], aiming to prevent rapid precipitation and enabling a controlled assembly of the hybrid (meso)porous network.

A greener synthetic route was explored by shifting from conventional titanium phosphonate syntheses using organic solvents (or their mixtures with water) to a fully aqueous system. Titanium(IV) bis(ammonium lactato)dihydroxide (TiBALDH), a water-soluble and stable titanium precursor, was employed. However, this approach presents additional complexity, as the hydrolysis of phosphonic esters proceeds much faster in aqueous media.

Our goal is to adapt (meso)porous titanium phosphonates properties in a controlled way by tuning the synthesis conditions and to evaluate their performance in the catalytic production of 5-hydroxymethylfurfural (5-HMF), a key platform molecule in biorefinery processes [5]. 5-HMF can be directly sourced from the cellulose fraction of lignocellulosic biomass, following a three-step catalytic conversion process: (1) hydrolysis of cellulose to glucose, (2) isomerization of glucose to fructose, and (3) dehydration of fructose to 5-HMF. These steps require a combination of Brønsted and Lewis acid sites (Figure 1). Traditionally used homogeneous mineral acids (e.g., HCl, H_2SO_4) pose issues like equipment corrosion and difficult waste management, while heterogeneous catalysts (e.g. sulfonated carbonaceous materials, metal oxides and zeolites) often suffer from deactivation, leaching, or limited tunability [6]. Therefore, robust and tunable catalysts with co-existing Brønsted and Lewis acid sites are crucial for high selectivity and efficiency.

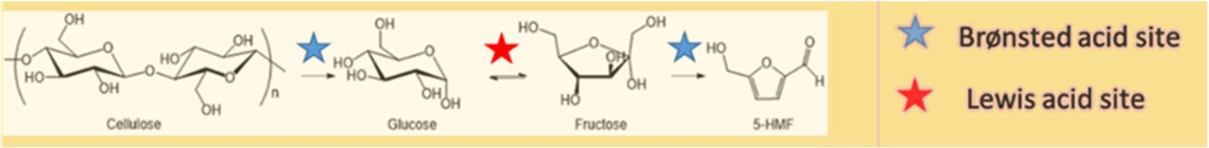

Figure 1 Overview of the catalytic pathway for 5-HMF production.

Acknowledgements

This work is part of the PHOSPORE consortium and was supported by the Excellence of Science (EOS) programme, project number 40007504.

References

[1] Y. Wang, J. G. Alauzun, P. H. Mutin, Chem. Mater. **32** (2020), 2910-2918.
[2] B. Pawlak, W. Marchal, B. M. Ramesha, B. Joos, L. Calvi, J. D'Haen, B. Ruttens, A. Hardy, V. Meynen, P. Adriaensens, R. Carleer, Microp. Mesop. Mater. **341** (2022) 112080.
[3] M. V. Vasylyev, E. J. Wachtel, R. Popovitz-Biro, R. Neumann, Chemistry **12** (2006) 3507-14.
[4] B. M. Ramesha, B. Pawlak, E. D. Arenas, G. Reekmans, S. Bals, W. Marchal, R. Carleer, P. Adriaensens, V. Meynen, Chemphyschem. **24** (2023) e202300437.
[5] R. J. van Putten, J. C. van der Waal, E. de Jong, C. B. Rasrendra, H. J. Heeres, J. G. de Vries, Chem. Rev. **113** (2013) 1499-597.
[6] R. Tomer, A. Tonelli, A. Morena, L. Fusaro, V. Meynen, C. April, S. Hermans, Biomass and Bioenergy **202** (2025) 108320.

Multifunctional Bimetallic MOFs/ZIFs for Air and Water Purification: Optimization of Water-Based Mechanochemical-Assisted Green Synthesis

F. Florides[a]*, K. Ioannou[a,b], M. Bytniewska[a], A. Michalicha[c], N. Kostoglou[d], C. Rebholz[b], M. Barczak[a], D. A. Giannakoudakis[a]

[a]Institute of Chemical Sciences, Faculty of Chemistry, Maria Curie-Sklodowska University, 20-031 Lublin, Poland
[b]Department of Mechanical and Manufacturing Engineering, University of Cyprus, 2109 Nicosia, Cyprus
[c]Chair and Department of Biochemistry and Biotechnology, Medical University of Lublin, Chodźki 1, 20-093 Lublin, Poland
[d]Institute of Geoenergy, Foundation for Research and Technology-Hellas, 73100, Chania, Greece

*fivos.florides@mail.umcs.pl

The escalating challenges of environmental pollution necessitate multifunctional processes that synergistically combine adsorption and catalytic activity for efficient air and water remediation. Advanced nanomaterials play a central role in delivering high performance while maintaining sustainability. Over the last two decades, Metal-Organic Frameworks (MOFs) have attracted significant attention due to their exceptionally high surface area, tunable pore structure, and versatile chemical functionality, facts that establish them as prosperous candidates for air and water purification. However, issues such as structural instability, especially upon exposure to humid conditions, high synthesis costs, and limited regeneration efficiency continue to challenge their practical real-life applications of MOFs [1].

Introduced during World War I, Chemical Warfare Agents (CWAs) remain among the most hazardous classes of chemicals used as weapons, necessitating the development of advanced materials for their effective capture and catalytic detoxification. Mustard gas or bis(2-chloroethyl) sulfide (HD), a blister agent, was the most widely deployed CWA and hence is referred to as the “King of Battle Gases”. The main critical aspect upon exposure is its ability to penetrate through regular textiles, causing skin burns, blindness, nervous system failure, and even death [2]. Since, HD is highly toxic and banned for any use, 2-chloroethyl ethyl sulfide (CEES) was used for lab purposes as a surrogate. In parallel, diclofenac (DICL) is regarded as a contaminant of significant concern in water purification, as it is widely prescribed as an analgesic and anti-inflammatory drug and is among the most frequently detected pharmaceuticals in wastewater treatment plant effluents [3].

In this work, we present the optimization of an established ultrasound-assisted green, water-based synthesis of bimetallic Co/Zn zeolitic imidazolate framework (ZIF-678) nanoparticles. The influence of ultrasound-assisted synthesis compared to conventional magnetic stirring was systematically evaluated to identify the most effective synthesis strategy and to elucidate the impact of mechanochemical energy input on the physicochemical properties of the resulting materials. Both monometallic and bimetallic ZIF powders were assessed against representative organic contaminant simulants in aqueous and airborne environments, using diclofenac sodium (DICL) as a model water pollutant and CEES as a simulant of airborne chemical threats. The ZIF powders exhibited high multifunctional detoxification efficiency, integrating adsorption with catalytic degradation to effectively neutralize CEES, with Co-Zn co-presence significantly enhancing catalytic activity. Notably, the bimetallic ZIF synthesized with an equimolar Co:Zn ratio (1:1) displayed the highest overall performance, indicating an optimal synergistic interaction between the two metal centers. In parallel, efficient removal of diclofenac (DICL) from water was achieved, confirming the suitability of the materials for aqueous micropollutant remediation. Additionally, the antibacterial activity of the ZIF powders was evaluated, revealing that Co incorporation substantially improved the inactivation of E. coli cells, further highlighting the multifunctional character of the optimized bimetallic system.

Acknowledgements

The work is financially supported by the National Science Centre (NCN) of Poland via the SONATA-19 grant 2023/51/D/ST5/01915 (PI: D. Giannakoudakis).

References

[1] D. A. Giannakoudakis, P. S. Pauletto, M. Florent, and T. J. Bandosz, RSC Appl. Interf. **2** (2025) 1275.

[2] D. A. Giannakoudakis, P. S. Pauletto, M. Florent, and T. J. Bandosz, J. Hazard. Mater. **487** (2025) 137155.

[3] P. Schröder et al., Envir. Sci. Poll. Res. **23** (2016) 12835–12866.

Catalyst Integration Strategies in 3D-Printed Porous Inorganic Polymer Scaffolds for Water Remediation

N. P. F. Gonçalves[a]*, J. G. Cuadra[b], R. M. Silva[b], T. Trindade[a], R. M. Novais[b]

[a]Department of Chemistry/CICECO-Aveiro Institute of Materials, University of Aveiro, Campus Universitário de Santiago, 3810-193 Aveiro, Portugal
[b]Department of Materials and Ceramic Engineering/CICECO-Aveiro Institute of Materials, University of Aveiro, Campus Universitário de Santiago, 3810-193 Aveiro, Portugal

*nunopfgoncalves@ua.pt

The transition from powder-based photocatalysts to structured, porous systems is essential for overcoming the recovery and mass transfer limitations of traditional water treatment processes. This study explores the use of Direct Ink Writing (DIW) to fabricate ceramic-like inorganic polymer (IPs) scaffolds, providing a modular and mechanically robust platform for supported photocatalysis [1]. By leveraging the geometric freedom of additive manufacturing, we designed porous lattice structures optimized for flow-through applications and evaluated three distinct catalyst integration strategies for the degradation of antibiotics (Ciprofloxacin, Sulfamethoxazole) and complex mixtures of emerging pollutants.

Two independent catalyst integration strategies were investigated. In the first study, multi-walled carbon nanotube (MWCNT) functionalization of the scaffold surface was followed by conformal TiO_2 deposition via Atomic Layer Deposition (ALD), yielding a well-controlled photocatalytic interface. In a second, separate study, g-C_3N_4 was deposited onto the printed scaffolds by drop-casting to promote visible-light-driven activity [2]. In addition, a bulk approach based on the direct incorporation of Nb_2O_5 into the printable inorganic polymer ink was explored to enable one-pot fabrication of photocatalytic active structures.

The results demonstrate the high chemical and mechanical resilience of the inorganic polymer matrix in aqueous environments. While bulk incorporation offers manufacturing simplicity, the surface-localized engineering strategies (ALD and drop-casting) significantly enhanced the accessibility of active sites and light utilization. Notably, all fabricated scaffolds exhibited exceptional stability and consistent reusability across multiple cycles, confirming the potential of 3D-printed inorganic polymers as a scalable technology for modular water treatment applications.

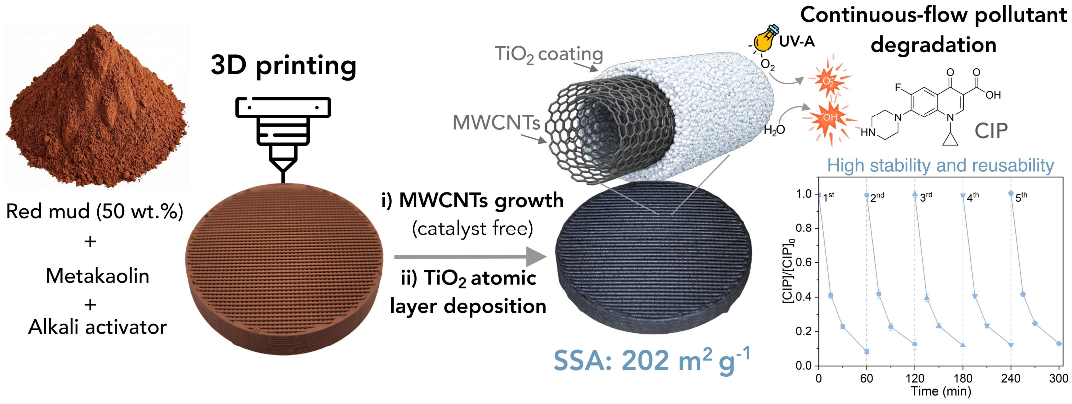

Figure 1 Schematic illustration of 3D-printing of IPs followed by MWCNTs growth via thermal-CVD and TiO_2 deposition via ALD.

Acknowledgements

This work was developed within the scope of the project CICECO Aveiro Institute of Materials, UID/50011/2025 (DOI 10.54499/UID/50011/2025) & LA/P/0006/2020 (DOI 10.54499/LA/P/0006/2020), financed by national funds through the FCT/MCTES (PIDDAC). NG acknowledge the funding from the European Union's Horizon Europe research and innovation programme under the Marie Skłodowska-Curie Actions PF grant agreement No 101065059 and from FCT 2022.06593.CEECIND/CP1720/CT0024 (DOI 10.54499/2022.06593.CEECIND/CP1720/CT0024) and FEDER - Fundo Europeu de Desenvolvimento Regional funds through the COMPETE 2030 in the framework of the project COMPETE2030-FEDER-00767900 (FCT: 16508).

References

[1] N. P. F. Gonçalves, S. M. Olhero, J. A. Labrincha, R. M. Novais, J. Clean. Prod. (2023) 135315.

[2] J. G. Cuadra, N. P .F. Gonçalves, K. Ben Tayeb, C. Venancio, S. Costa, I. Lopes, T. Trindade, J. Labrincha, R. M. Novais, Chem. Eng. J. (2025) 172457.

CATALYSIS AND PHOTOCATALYSIS

Acidity Tuned Templated Synthesis of Mesoporous TiO_2 Diphosphonate from Preformed Partially Hydrolyzed TiO_2 Sol for 5-HMF Production: From Sol – Gel Nanoparticles to Mesoporous Catalyst

C. Chandran[a,b]*, R. Tomer[a,c], N. Gys[a,b], A. Fanourgiakis[a], A. Morena[d], L. Fusaro[d], A. Tonelli[c], S. Hermans[c], C. April[d], T. Hauffman[b], V. Meynen[a]

[a]Laboratory of adsorption and catalysis, Department of Chemistry, University of Antwerp, Groenenborgerlaan 171, 2020 Antwerp, Belgium.
[b]Electrochemical and Surface Engineering (SURF), Department of Materials and Chemistry, Vrije Universiteit Brussel, Pleinlaan 2, 1050 Brussels, Belgium.
[c]IMCN Institute, MOST division, Université catholique de Louvain (UCLouvain), Place L. Pasteur 1, 1348 Louvain-la-Neuve, Belgium
[d]University of Namur, NISM, Department of Chemistry, Unit of Nanomaterials Chemistry, 5000 Namur, Belgium

*chandana.chandran@uantwerpen.be

Mesoporous metal phosphonates (PMPs) are a class of hybrid organic-inorganic materials made from the interaction between metals oxide precursors and organophosphonic acids or esters. They provide the ability to integrate both Lewis and brønsted acidity together with porosity in the catalyst. Establishing controlled synthesis approaches to make these materials mesoporous and with a controlled surface chemistry is however challenging. Specific reaction conditions are needed to control the molecular interactions of phosphonic acid moieties to the metal oxide units that determine surface chemistry and porosity to a large extent [1]. Bharadwaj et.al in 2022, prepared tetraethyl propane 1,3-diylbis(phosphonate) (TEPD) capped TiO_2 nanoparticle solution via a sol method [2]. By adapting the acid concentration, the TEPD (ester) hydrolysis degree and properties of the stable sol could be regulated.

In this presentation we report the synthesis of a novel mesoporous titania - diphosphonates (PMP), derived from these partially hydrolyzed TiO_2 diphosphonate sols, via a hydrothermal method using F127 as the structure directing agent (Figure 1a). The obtained mesoporous materials exhibit surface areas of 484-510 m^2/g , pore sizes of 5.3-5.6 nm and pore volumes of 0.65-0.68 cm^3/g (Figure 1b). The differences in synthesis approaches of these mesoporous titanium diphosphonates resulted in altered material properties, which we characterized via advanced surface analytical techniques like XPS and ^{31}P NMR to determine the coordination of the phosphorous to the titania and surface acidity. Our aim was to examine whether we can adapt the difference in the acidity of the sols, arising from the varying degree of hydrolysis of the diphosphonate ester, into the corresponding PMP. Although the sol particles exhibited distinct differences in acidity, FT-IR and XPS characterization of the porous materials derived from these sols revealed similar surface acidity.

To evaluate the impact of Brønsted and Lewis acidity of the sols and the corresponding porous Ti- diphosphonates, both were evaluated catalytically for the conversion of cellobiose to 5-HMF, a reaction requiring both Brønsted and Lewis acid sites. The study confirmed that the acidity differentiation present in the sols was not preserved during the mesostructure formation and all the PMPs showed similar activity whereas the sols activity varied depending on the acid equivalents used during synthesis. Nevertheless, the sol and PMP achieve conversions of 75% and 55%, respectively, which are comparable to literature benchmarks [3].Our study highlights the novel synthesis of mesoporous bisphosphonate ester based TiO_2 and shows how its porosity and surface properties complement with other hybrid materials like MOFs and its potential and first time use as heterogeneous acid catalyst for 5-HMF synthesis.

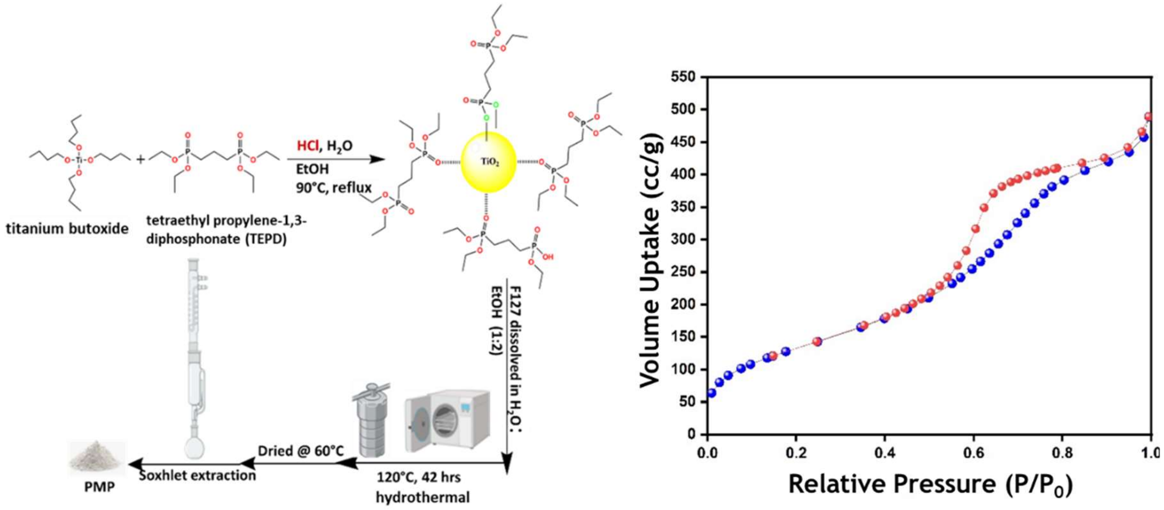

Figure 1 a) Schematic representation of the PMP synthesis, b) N_2 sorption isotherm of PMP prepared from sol made from 3 eq HCl.

Acknowledgements

This project and the majority of the authors are fully supported by funding from the FWO and F.R.S.-FNRS (Belgium) under the Excellence of Science (EOS) program (“PHOSPORE” – EOS reference number: 40007504).

References

[1] B. M. Ramesha and V. Meynen. Materials **13** (2020) 5366.

[2] B. M. Ramesha, B. Pawlak, D. A. Esteban, G. Reekmans, S. Bals, W. Marchal, R. Carleer, P. Adriaensens and V. Meynen. ChemPhysChem **24** (2023) e2023004.

[3] N. Hui, S. JinLiang, H. MinQiang, Y. DeZhong, F. HongLei and HAN BuXing. Sci. China Chem. **56** (2013).

CATALYSIS AND PHOTOCATALYSIS

Synthesis of Micro/Mesoporous HKUST-1 and Its Structure–Activity Relationship in Knoevenagel Condensation

N. Király[a]*, N. Vargová[a], R. Serbin[b], G. Zelenková[c], T. Zelenka[c], M. Almáši[a]

[a]Department of Inorganic Chemistry, Institute of Chemistry, Faculty of Science, University of Pavol Jozef Safarik in Kosice, Moyzesova 11, 041 54 Kosice, Slovak Republic
[b]Department of Analytical Chemistry, Institute of Chemistry, Faculty of Science, University of Pavol Jozef Safarik in Kosice, Moyzesova 11, 041 54 Kosice, Slovak Republic
[c]Department of Chemistry, Faculty of Science, University of Ostrava, 30. Dubna 22, CZ-702 00 Ostrava, Czech Republic

*nikolas.kiraly@upjs.sk

Metal–organic frameworks (MOFs) constitute a versatile group of crystalline porous materials formed by the coordination of metal ions or metal clusters with multitopic organic ligands, giving rise to well-ordered three-dimensional networks. Owing to their exceptionally high internal surface areas, adjustable pore structures, and notable thermal and chemical robustness, MOFs have attracted considerable interest for applications in gas storage and separation, heterogeneous catalysis, drug delivery, and chemical sensing [1]. In catalytic processes, MOFs are particularly advantageous because their modular architectures enable deliberate modification of both metal nodes and organic linkers, allowing precise control over the nature and distribution of active sites. Such tunability facilitates enhanced catalytic activity and selectivity in reactions including oxidation, hydrogenation, and carbon–carbon bond-forming condensations [2].

In the present work, two copper-based MOFs with distinct micro- and mesoporous features, designated HKUST-1(A) and HKUST-1(B), were synthesized and evaluated with respect to their catalytic behavior. Both materials were prepared via a solvothermal method using trimesic acid (H_3BTC) and copper(II) nitrate trihydrate [$Cu(NO_3)_2 \cdot 3H_2O$] dissolved in *N,N'*-dimethylformamide (DMF). Hierarchical porosity was introduced by adding cetyltrimethylammonium bromide (CTAB) and citric acid in varying concentrations as structure-directing agents. Following sonication for 10 minutes, the reaction mixtures were heated at 75 °C for 24 hours. The resulting blue crystalline products were recovered by filtration and thoroughly washed with DMF.

Template removal was achieved through a multistep post-synthetic treatment. Initially, the materials were exposed to a 1 M ammonium nitrate solution in an ethanol–water mixture (1:2, v/v) at 60 °C for 24 hours. After decantation, the solids were further washed with fresh ethanol–water (1:2, v/v) at ambient temperature for an additional 24 hours. Final activation was accomplished by Soxhlet extraction with methanol over a three-day period. Fourier-transform infrared (FTIR) spectroscopy confirmed both the integrity of the MOF structures and the efficient removal of the templating agents (Figure 1).

Textural properties were investigated using nitrogen adsorption–desorption measurements. HKUST-1(A) displayed a hierarchical pore system combining microporous and mesoporous domains, whereas HKUST-1(B) was dominated by mesoporosity. The Brunauer–Emmett–Teller (BET) specific surface areas were determined to be 1534 $m^2 \cdot g^{-1}$ for HKUST-1(A) and 1709 $m^2 \cdot g^{-1}$ for HKUST-1(B), demonstrating the effectiveness of the cooperative templating approach in generating mesostructured MOFs while preserving microporous framework walls.

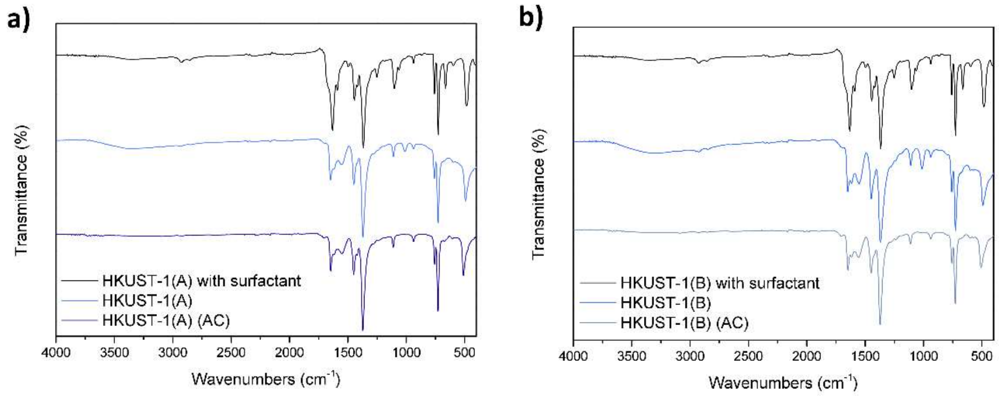

Figure 1 FTIR spectra of the as-synthesized, surfactant-removed, and fully activated samples of (a) HKUST-1(A) and (b) HKUST-1(B).

The catalytic performance of the activated MOFs was assessed using the Knoevenagel condensation between benzaldehyde (PhCHO) and malononitrile as a model reaction. Key reaction parameters, including solvent type (toluene, acetonitrile, and xylene), reaction temperature (60 °C, 80 °C, and 100 °C), and catalyst loading (25 mg and 50 mg), were systematically optimized. The most favorable conditions were identified as toluene as the solvent, a reaction temperature of 80 °C, and a catalyst amount of 50 mg.

Under optimized conditions, a series of benzaldehyde derivatives bearing electron-withdrawing substituents at the ortho (2-F, 2-Cl, 2-Br, 2-NO_2) and para (4-F, 4-Cl, 4-Br, 4-NO_2) positions were examined. In all cases, HKUST-1(B) demonstrated superior catalytic efficiency compared to HKUST-1(A). Among the ortho-substituted substrates, 2-nitrobenzaldehyde achieved the highest conversion (96%), while 4-chlorobenzaldehyde afforded the highest conversion (97%) within the para-substituted series. By comparison, HKUST-1(A) reached maximum conversions of 84% for 2-fluorobenzaldehyde and 91% for 4-chlorobenzaldehyde.

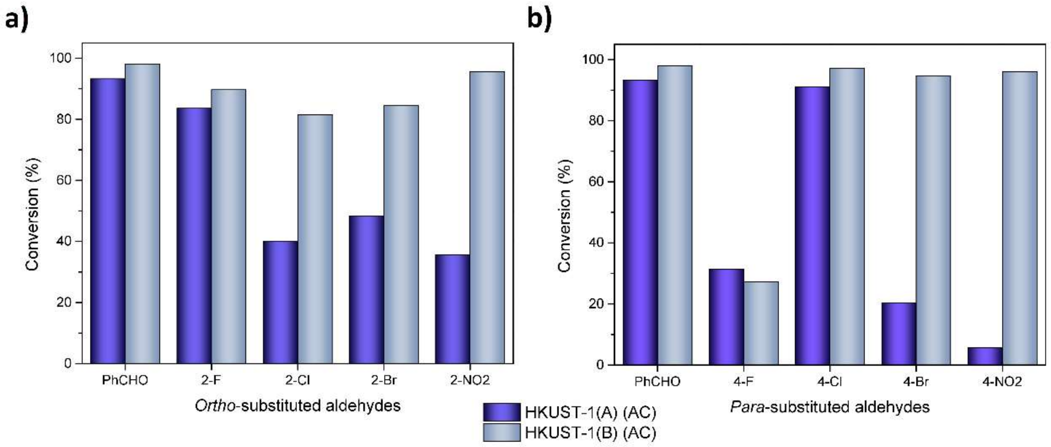

Figure 2 Comparison of the catalytic activities of (a) HKUST-1(A) and (b) HKUST-1(B) in the Knoevenagel condensation of ortho- and para-substituted aromatic aldehydes.

Acknowledgements

This research was created with the support of EU NextGenerationEU through the Recovery and Resilience Plan for Slovakia under the project No. 09I03-03-V05-00008 (VVGS-ESGV-2923).

References
[1] D. Yang, B. C. Gates, ACS Catal. **9** (2019) 1779-1798.
[2] Y. - S. Wei, M. Zhang, R. Zou, Q. Wu, Chem. Rev. **120** (2020) 12089-12174.

Mixed-Linker UiO-67 Frameworks for Photocatalytic Hydrogen Generation

P. Kopčan[a,b]*, K. Kočí[a,c]

[a]Institute of Environmental Technology, CEET, VŠB-Technical University of Ostrava, 17. listopadu 2172/15, 708 00 Ostrava-Poruba, Czech Republic
[b]Faculty of Materials Science and Technology, VŠB-Technical University of Ostrava, 17. listopadu 2172/15, 708 00 Ostrava-Poruba, Czech Republic
[c]Department of Physics and Materials Engineering, Faculty of Technology, Tomáš Baťa University in Zlín, Vavrečkova 275, Czech Republic

*patrik.kopcan@vsb.cz

The global transition toward clean and sustainable energy has intensified interest in photocatalysis as a strategy for both energy conversion and environmental remediation. Photocatalysis, a light-driven redox process enabling water splitting, alcohol reforming, and degradation of organic pollutants, offers carbon-neutral fuel production and pollutant removal under mild conditions [1,2]. However, conventional semiconductor photocatalysts are limited by narrow light absorption, rapid charge recombination, and poor chemical stability [1,2]. These challenges have stimulated growing attention toward metal–organic frameworks (MOFs) as a new class of photocatalysts that combine structural tunability, well-defined porosity, and high stability [3–6]. Among them, Zr-based UiO frameworks are particularly attractive due to their exceptional robustness, high surface area, and versatile post-synthetic modifiability.

In this study, we examine how incorporation of nitrogen-containing linkers influences the photocatalytic behavior of UiO-67. A series of mixed-linker UiO-67 materials was prepared using 2,2′-bipyridine (bpy) as a co-linker. The prepared photocatalysts were investigated for photocatalytic hydrogen generation from an aqueous methanol solution under UV-C irradiation (254 nm), enabling simultaneous hydrogen evolution and conversion of organics in water. XRD confirms retention of the UiO-67 framework across the series, while FTIR, SEM, and zeta-potential measurements reveal composition-dependent changes in surface chemistry, morphology, and interfacial charge. Photocatalytic testing shows that bpy-containing samples exhibit enhanced hydrogen production relative to pristine UiO-67. The observed trend indicates that the presence of N-containing linkers modifies the local framework/surface environment in a manner that impacts the photocatalytic reaction pathway. These results highlight mixed-linker engineering as an effective handle to tune UiO-type MOFs toward coupled hydrogen generation and water purification.

Acknowledgements

This work was supported by the Large Research Infrastructure ENREGAT (projects No. LM2023056 and LM2018098), European Union under the REFRESH—Research Excellence For REgion Sustainability High-tech Industries project (No. CZ.10.03.01/00/22_003/0000048) via the Operational Program Just Transition and COST Action EU4MOFs (COST Action CA22147).

References

[1] S. B. Beil, S. Bonnet, C. Casadevall, R. J. Detz, F. Eisenreich, S. D. Glover, C. Kerzig, L. Næsborg, S. Pullen, G. Storch, N. Wei, C. Zeymer, JACS Au **4** (2024) 2746–2766.
[2] H. H. Mohamed, G. Wazan, D. H. A. Besisa, Mater. Sci. Eng. B **286** (2022) 116077.
[3] M. Guo, M. Zhang, R. Liu, X. Zhang, G. Li, Adv. Sci. **9** (2022) 2103361.
[4] M. Khan, Z. Akmal, M. Tayyab, S. Mansoor, A. Zeb, Z. Ye, J. Zhang, S. Wu, L. Wang, Carbon Capture Sci. Technol. **11** (2024) 100191.
[5] X. Wang, L. Zhu, Z. Lv, Z. Qi, Y. Xu, T. Miao, X. Fu, L. Li, Chem. Eng. J. **442** (2022) 136186.
[6] S. Navalón, A. Dhakshinamoorthy, M. Álvaro, B. Ferrer, H. García, Chem. Rev. **123** (2023) 445–490.

CATALYSIS AND PHOTOCATALYSIS

HKUST-1-Based Metal–Organic Frameworks as Efficient Heterogeneous Catalysts for A^3-Coupling Reactions

N. Vargová[a*], N. Király[a], M. Želinská[a], R. Serbin[b], T. Zelenka[c], M. Almáši[a]

[a]Department of Inorganic Chemistry, Faculty of Science, Pavol Jozef Safarik University in Kosice, Moyzesova 11, 041 54 Kosice, Slovak Republic
[b]Department of Analytical Chemistry, Faculty of Science, Pavol Jozef Safarik University in Kosice, Moyzesova 11, 041 54 Kosice, Slovak Republic
[c]Department of Chemistry, Faculty of Science, University of Ostrava, 30. dubna 22, 071 03, Ostrava, Czech Republic

*nikola.vargova2@student.upjs.sk

The A^3-coupling reaction is a three-component condensation of an aldehyde, an amine, and a terminal alkyne that affords propargylamines with high atom economy, generating water as the only by-product. Owing to its mild reaction conditions, potential solvent-free operation, and compatibility with recyclable heterogeneous catalysts, this transformation aligns well with the principles of green chemistry. Metal–organic frameworks (MOFs), composed of metal nodes coordinated to organic linkers to form porous crystalline networks, have emerged as promising catalysts for A^3-coupling reactions due to their high surface areas, tunable pore structures, and structural stability, enabling efficient and sustainable catalytic performance [1, 2].

In this study, three porous materials, HKUST-1, HKUST-1(A), and HKUST-1(B), were synthesized via a solvothermal approach. While HKUST-1 is purely microporous, HKUST-1(A) and HKUST-1(B) exhibit hierarchical micro-/mesoporosity. Infrared spectroscopy confirmed the successful formation and activation of the frameworks, whereas nitrogen and argon adsorption–desorption analyses provided detailed insight into their textural properties. The templated synthesis route led to a pronounced enlargement of pore dimensions compared to parent HKUST-1 (BET surface area: 1787 $m^2 \cdot g^{-1}$), with pore diameters increasing from 0.9 to 8.5 nm (Figure 1a and Figure 1b). Both HKUST-1(A) and HKUST-1(B) display combined micro- and mesoporous character, with BET surface areas of 1687 and 1554 $m^2 \cdot g^{-1}$, respectively (Figure 1c).

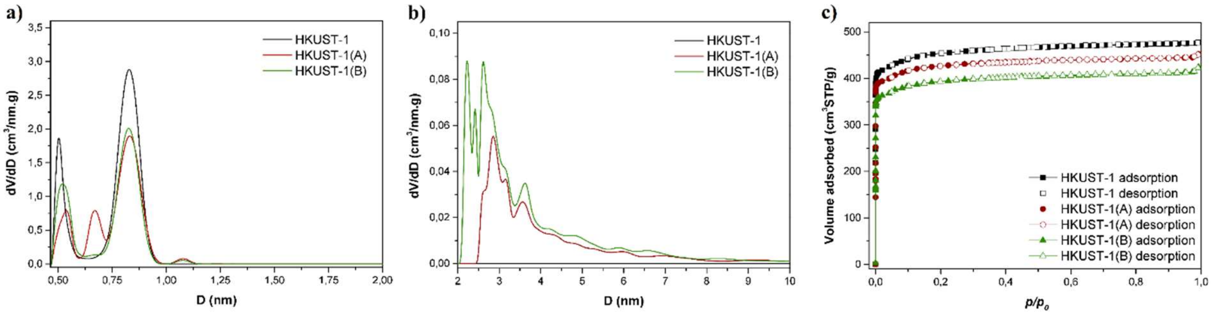

Figure 1 Comparison of a) microporosity, b) mesoporosity, and c) nitrogen adsorption and desorption isotherms of HKUST-1, HKUST-1(A) and HKUST-1(B).

The catalytic performance of the prepared materials was evaluated in the A^3-coupling reaction involving an aldehyde (paraformaldehyde or benzaldehyde), phenylacetylene, and an amine. In a typical experiment, 10 cm^3 of toluene, an internal standard (200 µl), aldehyde (1.8 mmol), phenylacetylene (1.8 mmol), amine (1.8 mmol), and 50 mg of the catalyst were introduced into a reaction flask and heated to 120 °C. Upon completion, the catalyst was separated by centrifugation, and the resulting products were analyzed by gas chromatography compared to internal standard (1-bromonaphtalene).

Besides the influence of catalyst pore size, the effect of aldehydes and amines was also investigated in this study. Two aldehydes, paraformaldehyde and benzaldehyde, were employed, with paraformaldehyde exhibiting higher catalytic activity as a result of its smaller molecular size. In the case of amines, both primary and secondary amines were examined; however, primary amines (ethylenediamine, aniline) showed no catalytic activity, whereas secondary amines exhibited good catalytic performance (showed bellow at Figure 2). As secondary amines as diethylamine, piperidine, and pyrrolidine were selected. For all three catalysts, the highest catalytic activity was observed for diethylamine; in the case of HKUST-1(B), the conversion of diethylamine reached 91 %, followed by pyrrolidine (85 %), while piperidine exhibited the lowest activity (71 %), which can again be attributed to differences in amine size. Investigation of the impact of catalyst pore size revealed that larger pore dimensions positively influence catalytic activity, resulting in the highest conversion for the coupling of diethylamine, paraformaldehyde, and phenylacetylene, where HKUST-1(B) achieved the highest conversion of 91 %, while HKUST-1(A) and HKUST-1 reached conversions of 84 % and 51 %, respectively, demonstrating that the efficiency of reactant and product transport to and from the catalytic sites is a key factor governing the overall catalytic performance.

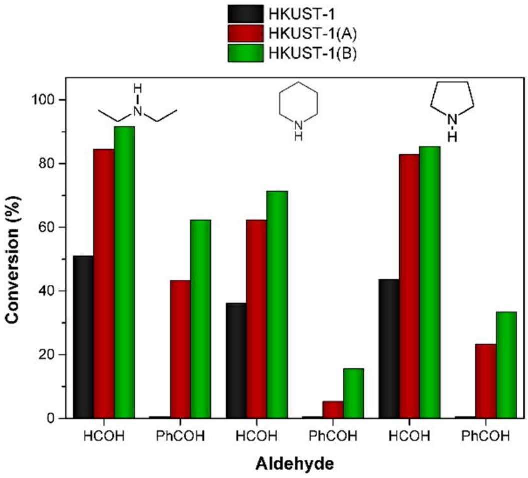

Figure 2 Comparison of conversions for reactions of various substrates catalyzed by HKUST-1, HKUST-1(A), and HKUST-1(B) in toluene at 120 °C.

Acknowledgements

This research was created with the support of grants VEGA 1/0058/25, VEGA 1/0442/25 and EU NextGenerationEU through the Recovery and Resilience Plan for Slovakia under project No. 09I03-03-V05-00008 (VVGS-ESGV-2923).

References

[1] M. A. Ghasemzadeh, B. Mirhosseini-Eshkevari, M. Tavakoli, F. Zamani, Green Chem. **22** (2020) 7265-7300.
[2] K. Van Beurden, S. de Koning, D. Molendijk, J. van Schijndel, Green Chem. Lett. Rev. **13** (2020) 349–364.

Reinventing HKUST-1 Synthesis: A Systematic Comparison of Advanced Synthetic Routes

K. Andrejev[a]*, M. Almáši[a]

[a]Department of Inorganic Chemistry, Institute of Chemistry, Faculty of Science, P. J. Šafárik University in Košice, Moyzesova 11, 041 54 Košice, Slovak Republic

*kiril.andrejev@student.upjs.sk

HKUST-1 (also known as MOF-199 or CuBTC) is a metal-organic framework, that was first synthesized by Williams and co-workers in 1999 [1]. This material is well-known for its microporous structure containing Cu(II) paddle-wheel cluster, trimesate H_3BTC linkers and a large specific surface area. It is commonly used for CO_2 capture, hydrogen storage, water purification and so on [2-4]. A wide variety of synthetic routes for HKUST-1 have been developed. The solvothermal method remains the standard and most widely used approach. However, some methods are more energy-efficient, less time-consuming, and still deliver quality results. To illustrate, the mechanochemical method minimizes solvent usage, while the sonochemical method reduces energy consumption compared to its solvothermal counterpart.

In this study, the synthesis of HKUST-1 is carried out using different methods while maintaining the same reaction mixture, reactants and the temperature settings. The purpose is to compare the obtained materials in terms of their structural and textural properties and to evaluate their adsorption performance in the following experiments. In all HKUST-1 syntheses, the same reaction mixture was used. Specifically, 0.444 g of H_3BTC was dissolved in 13.333 mL of a 1:1 DMF/ethanol mixture and added to 6.667 mL of an aqueous solution of 0.924 g of copper (II) nitrate trihydrate in a 30 mL glass vial. Depending on the type of synthesis, the resulting mixture in the vial was then processed under different conditions.

Three different syntheses of HKUST-1 were carried out, namely solvothermal (ST), sonochemical (SC) and microwave-assisted (MW) preparation and the methods yielded crystalline HKUST-1 materials. The solvothermal route produced a higher amount of material. Although the solvothermal synthesis typically requires about 8 hours and a temperature of 80°C, shortening the reaction time to 160 minutes resulted in a significantly lower yield compared to the sonochemical method performed for the same duration. Notably, microwave-assisted synthesis enabled the formation of comparable amounts of HKUST-1 within a substantially shorter reaction time, highlighting its superior time efficiency (see Figure 1a).

Further extension of the sonochemical synthesis to 240 minutes resulted in a substantial increase in yield, exceeding 80%, while still reducing the reaction time by half compared to the conventional 8-hour solvothermal protocol. This highlights the strong potential of sonochemical activation for achieving both high efficiency and significant process acceleration (see Figure 1b).

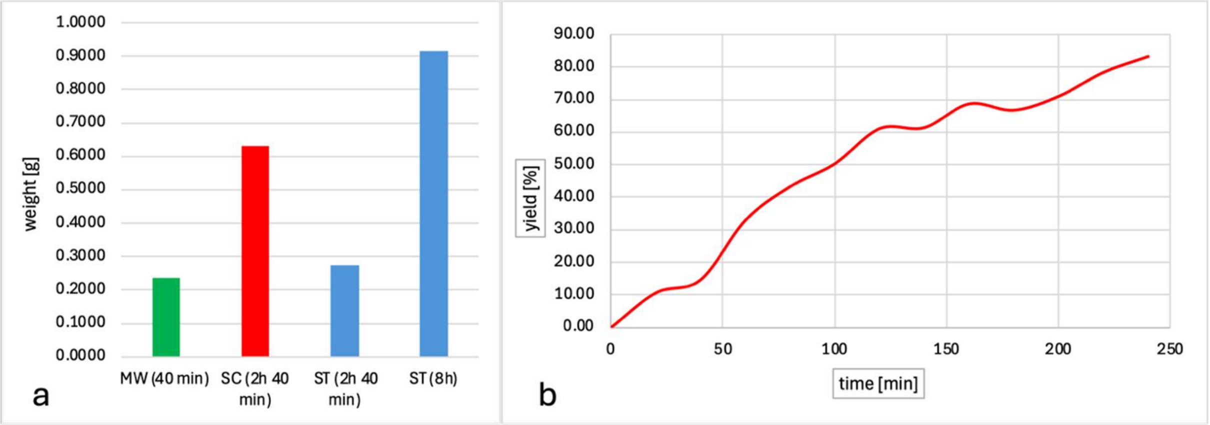

Figure 1 a) Comparison of HKUST-1 microwave-assisted (MW), sonochemical (SC) and solvothermal (ST) synthesis performance. b) Time-dependent evolution of HKUST-1 yield during sonochemical synthesis.

In the future work, the synthesized materials will be subjected to adsorption experiments to evaluate their sorption performance toward selected organic adsorbates, with particular emphasis on toxic volatile organic compounds (VOCs). Measurements will be carried out in a static system at 25 °C, with mass changes monitored to determine adsorption capacity and adsorption kinetics.

Acknowledgements

This work was supported by: VEGA 1/0058/25, VEGA 1/0442/25, EU NextGenerationEU through the Recovery and Resilience Plan for Slovakia under the Project No. 09I02-03-V01-00022 (SUNFLOWERS), No. 09I03-03-V03-00034 (MASS-PRAM) and No. 09I03-03-V05-00008 (VVGS-ESGV-2923).

References

[1] S. S. - Y. Chui, S. M. - F. Lo, J. P. H. Charmant, A. G. Orpen, I. D. Williams, Science **283** (1999) 1148–1150.
[2] Y. Cao, et al., J. Energy Chem. **23** (2014) 468–474.
[3] S. P. Shet, et al., Int. J. Hydrogen Energy **46** (2021) 11782–11803.
[4] Q. Salamat, et al., Sep. Purif. Technol. **379** (2025) 135031.

DESIGN AND SYNTHESIS OF MATERIALS

Mesoporous Silica Platforms for Controlled and Magnetically Guided Delivery of Apixaban

E. Beňová[a]*, N. Király[a], M. Šuleková[b], L. Váhovská[b], V. Zeleňák[a]

[a]Department of Inorganic Chemistry, Institute of Chemistry, Faculty of Science, Pavol Jozef Šafárik University in Košice, Moyzesova 11, 040 01 Košice, Slovak Republic
[b]Department of Chemistry, Biochemistry and Biophysics, University of Veterinary Medicine and Pharmacy in Košice, Komenského 73, 041 81, Košice, Slovak Republic

*eva.benova@upjs.sk

Mesoporous silica materials offer highly tunable pore architectures and large internal surface areas, making them attractive platforms for controlled guest molecule delivery. In the presented study, two mesoporous silica platforms were developed to demonstrate how different material architectures can address complementary delivery concepts using apixaban (APX) as a model compound. Apixaban was selected as a representative small-molecule drug compatible with mesoporous silica pore sizes and its limited aqueous solubility, which makes controlled release from porous carriers particularly relevant. A non-magnetic mesoporous silica carrier enables controlled, diffusion-driven release, while magnetic mesoporous core-shell nanoparticles enable externally guided delivery via magnetic field application [1].

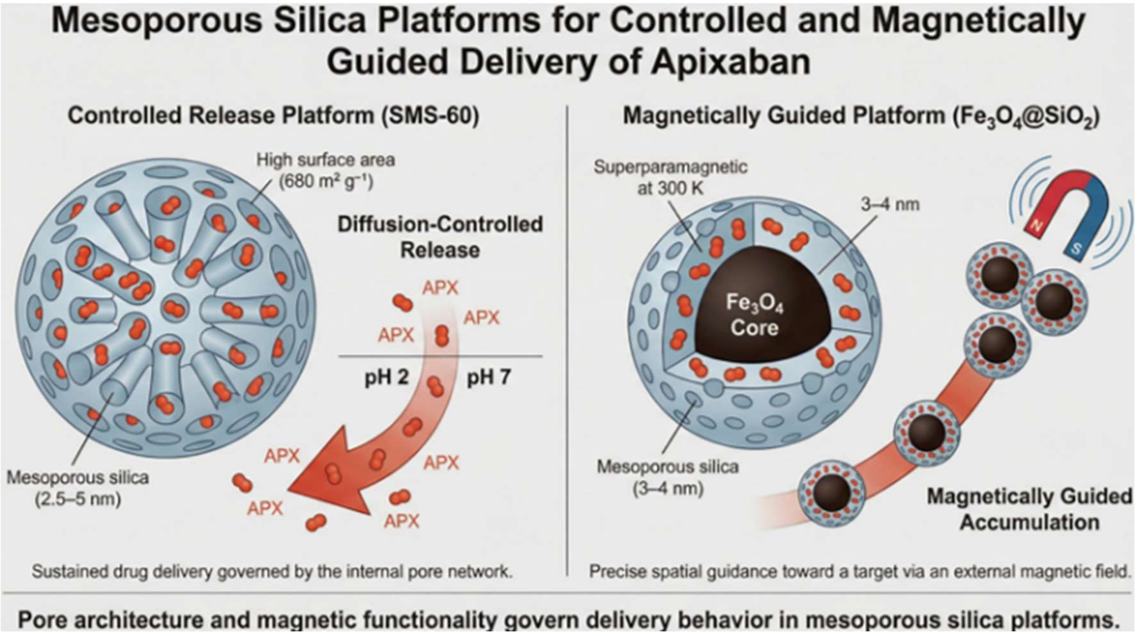

Figure 1 Schematic overview of mesoporous silica platforms for apixaban (APX) delivery, illustrating diffusion-controlled release from non-magnetic SMS-60 (left) and magnetically guided accumulation using $Fe_3O_4@SiO_2$ core–shell nanoparticles (right).

The first approach focuses on non-magnetic mesoporous silica (SMS-60) as a carrier for controlled release relevant to oral administration. SMS-60 exhibited a high specific surface area of 680 m^2 g^{-1} with a pore size distribution of 2.5–5 nm, enabling efficient APX loading via impregnation from methanol, reaching 170 $mg.g^{-1}$. After loading, the surface area decreased to 430 $m^2.g^{-1}$ with a narrowed pore size around 2.5 nm, confirming incorporation of APX within the mesoporous structure. Release studies performed in physiological solution at pH 7 and pH 2 over 72 h demonstrated sustained, diffusion-controlled release governed by the mesoporous pore network.

The second strategy employs magnetic core–shell nanoparticles composed of a superparamagnetic iron oxide core and a mesoporous silica shell to achieve spatially controlled delivery under an external magnetic field. These nanoparticles exhibited an average particle size of approximately 50 nm, a specific surface area of 480 $m^2.g^{-1}$, and pore sizes in the 3–4 nm range suitable for APX incorporation. Magnetic measurements revealed blocking temperatures below 300 K, confirming superparamagnetic behaviour at physiological temperature and suitability for magnetic guidance. Together, these results demonstrate how mesoporous silica architectures can be rationally designed to achieve either controlled release or magnetically guided delivery by tuning pore structure and magnetic functionality, highlighting the versatility of porous materials for advanced functional and application-oriented systems.

Acknowledgements

This work was supported by the EU NextGenerationEU through the Recovery and Resilience Plan for Slovakia, project No. 09I03-03-V04-00722. and by the Slovak Research and Development Agency under Contract APVV-23-0097.

References

[1] F. da S. Bruckmann, F. B. Nunes, T. da R. Salles, C. Franco, F. C. Cadoná, C. R. Bohn Rhoden, Magnetochemistry **8** (2022).

DESIGN AND SYNTHESIS OF MATERIALS

From Pristine to Functionalized MIL-101(Cr): Impact of PEI on Gas Adsorption

N. Hlávková[a]*, T. Zelenka[b], P. Sharda[c], A. Sharma[d], M. Almáši[a]

[a]Department of Inorganic Chemistry, Institute of Chemistry, Faculty of Science, Pavol Jozef Šafárik University in Košice, Moyzesova 11, 040 01 Košice, Slovak Republic
[b]Department of Chemistry, Faculty of Science, University of Ostrava, 30. Dubna 22, 702 00 Ostrava, Czech Republic
[c]Department of Physics, School of Applied Science, Centre for Renewable Energy & Storage, Suresh Gyan Vihar University, Jaipur 302017, India
[d]Department of Applied Sciences and Humanities, School of Engineering & Technology, Central University of Haryana, 123031 Mahendragarh, India

*nina.hlavkova@student.upjs.sk

Porous materials are currently being widely investigated in many scientific fields as potential solutions to major global challenges, including energy storage, the replacement of fossil fuels, and the reduction of greenhouse gas emissions. Among these materials, metal–organic frameworks (MOFs) represent one of the largest and most important classes. Their potential arises from their crystalline architectures, composed of metal ions or metal-based clusters coordinated to organic linkers, resulting in highly ordered porous networks. After synthesis, MOFs can be further modified to enhance their adsorption capacity and other functional properties. One approach for improving gas adsorption involves introducing a substance with strong gas-binding ability, such as polyethyleneimine (PEI) onto the pore surfaces of MOFs. This polymer exhibits excellent CO_2 capture performance and can modify the pore environment to increase surface polarity, which is beneficial for hydrogen adsorption [1].

In this study, we concentrated on a specific subclass of MOFs belonging to the MIL (Materials Institute Lavoisier) family and their post-synthetic modification aimed at enhancing H_2 and CO_2 sorption capacities. Seven different MIL-101 materials were synthesized and initially evaluated based on their adsorption properties. From this series, MIL-101 containing chromium (III) in the metal clusters, MIL-101(Cr), exhibited the most favourable overall sorption behaviour and was therefore selected for further investigation. This material was functionalized with PEI of three different average monomeric units (800, 1300, and 2000) and loadings (25, 50, 75, and 100 wt%).

The pristine MIL-101(Cr) and all modified samples were characterized by infrared spectroscopy, powder X-ray diffraction, nitrogen adsorption @77 K, hydrogen adsorption @77 K, and carbon dioxide adsorption @273 K (see Figure 1). These measurements showed that, in all cases, post-synthetic modification did not lead to degradation of the material, and that the amount of PEI in the final materials was directly proportional to both the number of monomeric units and the concentration at which it was introduced into MIL-101(Cr). The sorption capacities for both H_2 and CO_2 decreased with a higher number of PEI monomeric units and with increasing PEI loading. However, although the raw sorption data may suggest a decrease in adsorption capacities with increasing PEI loading and polymer chain length, this trend must be interpreted in relation to the accessible surface area and pore volume obtained from nitrogen adsorption measurements. Incorporation of PEI into the pores leads to partial pore filling, resulting in a reduction of the BET surface area and total pore volume. Therefore, the adsorption capacities of CO_2 and H_2 should be considered with respect to the available surface area of each material. After normalization to surface area, an opposite trend is observed, in which increasing PEI loading and a higher number of monomeric units lead to enhanced adsorption performance. The improved CO_2 uptake can be attributed to the increased number of amine functional groups providing strong specific interactions with CO_2 molecules, while the reduced pore size caused by polymer incorporation strengthens confinement effects, which is beneficial for adsorption of small gas molecules such as H_2. These results confirm that PEI functionalization enhances the intrinsic affinity of MIL-101(Cr) toward both gases, despite the reduction in overall surface area. The highest sorption capacities for both H_2 and CO_2 were achieved by MIL-101(Cr) modified with 100% PEI-2000, reaching a capacity of 22.1 ×

10^{-2} cm³ m⁻² for H_2, which is more than three times the adsorption capacity of the unmodified material. In the case of CO_2 adsorption, a capacity of 17.87×10^{-2} cm³ m⁻² was obtained, representing almost a 7.5-fold increase compared with pristine MIL-101(Cr).

Post-synthetic functionalization of MIL-101(Cr) with polyethyleneimine successfully modified the pore environment and introduced additional amine active sites. Despite a reduction in surface area due to partial pore filling, PEI incorporation enhanced the intrinsic affinity of the material toward CO_2 and H_2. These findings demonstrate that PEI-functionalized MIL-101(Cr) is a promising material for gas capture and storage applications.

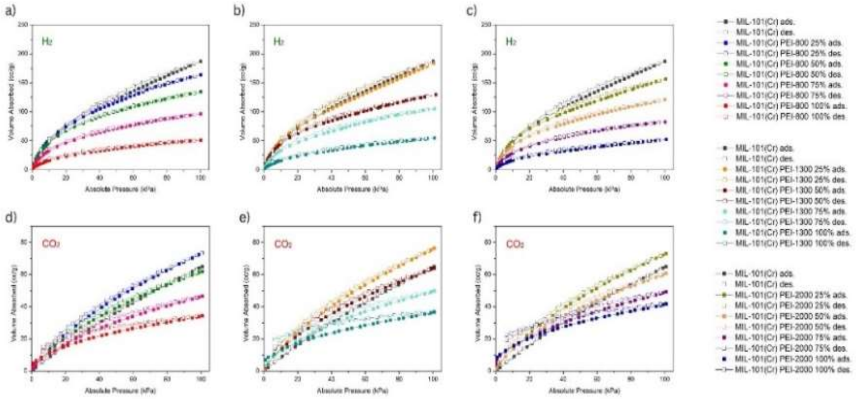

Figure 1 a) b) c) H_2 and d) e) f) CO_2 adsorption isotherms of prepared MIL-101(Cr) PEI modified materials.

Acknowledgements

This work was supported by the projects VEGA 1/0058/25, VEGA 1/0442/25, APVV SK-CZ-RD-21-0068 and LUASK22049 (INTER-EXCELLENCE II, MŠMT).

Refrences

[1] X. Shen, H. Du, R. H. Mullins, R. R. Kommalapati, Energy Technol. **5** (2017) 822 – 833.

Structural Engineering of Metal Organic Frameworks for Water Remediation

M. Hmadeh[a]*

[a]Department of Chemistry, American University of Beirut, Beirut, Lebanon

*mh210@aub.edu.lb

Access to clean water is a growing global challenge, with nearly one-third of the world's population lacking safe drinking water. Climate change, pollution, and unsustainable water management practices are worsening the crisis, making it crucial to develop efficient water purification technologies. This work addresses these challenges by designing, synthesizing, and implementing advanced porous materials, particularly metal organic frameworks (MOFs),[1] for scalable and energy-efficient water decontamination systems. By leveraging the exceptional adsorption properties of MOFs through structural engineering by cation doping and /or defect incorporation, the obtained materials showed an improved water decontamination process. We first apply a reaction-diffusion process in a 1 D system to produce MOF crystals in a controlled manner.[2,3] This method occurs at room temperature by diffusing the metal salt into an agar gel matrix containing the organic linker to form nanocrystals of MOFs with tailored structural features that include crystal size distribution, surface area, and defect number. We show how this process can be used to control the size, morphology, composition and defects in MOFs.[4] In addition to this new process, we use modulated solvothermal synthesis to create defects in UiO-66 based MOF structures.[5] The nature of defects, their density, and distribution in the UiO-66 structure were characterized through set of spectroscopic and microscopic techniques and were proven to be very effective to tune the physical and chemical properties of UiO-66 without altering the main building blocks of the MOF structure. Finally, we integrate the defected crystals into electrospun membranes for enhanced performance and separation.[6] This novel type of material engineering was further applied for catalysis and water remediation.

Acknowledgements

This work was supported by American University Research Board.

References

[1] H. Furukawa, K. E. Cordova, M. O'Keeffe, O. M. Yaghi, Science **341** (2013) 1230444.
[2] D. Saliba, M. Ammar, M. Rammal, M. Al-Ghoul, M. J. Hmadeh, J. Am. Chem. Soc. **140** (2018) 1812– 1823.
[3] R. Issa, F. A. Ibrahim, M. Al-Ghoul, M. Hmadeh, Nano Res. **14** (2021) 423– 431.
[4] P. Damacet, K. Hannouche, A. Gouda, M. Hmadeh, ACS Appl. Mater. Interfaces (2024).
[5] O. Haidar, T. Roques-Carmes, A. Gouda, N. Tabaja, J. Toufaily, M. Hmadeh. ACS Applied Nano Mater. **7** (2024) 10003-10015.
[6] M. H. Hashem, M. Hammoud, M. N. Ahmad, M. Hmadeh, ACS Appl. Mater. Interfaces **17** (2025) 16275-16286.

Post-Synthetically Modified GaTCPP Metal–Organic Framework as an Efficient Electrochemical Sensing Platform

N. Király[a]*, P. Obšatník[a], J. Shepa[b], J. Demeterová[b], D. Volavka[c], M. Almáši[a], R. Oriňaková[b], V. Zeleňák[a]

[a]Department of Inorganic Chemistry, Institute of Chemistry, University of Pavol Jozef Safarik in Kosice, Moyzesova 11, 041 54 Kosice, Slovak Republic
[b]Department of Physical Chemistry, Institute of Chemistry, University of Pavol Jozef Safarik in Kosice, Moyzesova 11, 041 54 Kosice, Slovak Republic
[c]Depertment of Condensed Matter Physics, University of Pavol Jozef Safarik in Kosice, Jesenná 9, 041 54 Kosice, Slovak Republic

*nikolas.kiraly@upjs.sk

Metal–organic frameworks (MOFs) represent a rapidly expanding class of crystalline porous materials constructed from metal ions or metal clusters interconnected by multifunctional organic ligands. Owing to their exceptionally high specific surface area, tunable pore architecture, structural diversity, and chemical tailorability, MOFs have attracted considerable attention in a wide range of applications, including gas storage and separation, catalysis, energy storage, drug delivery, and chemical sensing [1]. In recent years, particular emphasis has been placed on the rational design of MOF materials for electrochemical sensing, where their porosity, abundance of active sites, and capability for specific host–guest interactions can be exploited to enhance sensitivity and selectivity toward target analytes [2].

This work focuses on the synthesis, post-synthetic modification, comprehensive characterization, and application of a porphyrin-based MOF material, GaTCPP, as a functional platform for electrochemical sensing. The parent framework, GaTCPP, is based on gallium(III) ions coordinated by the tetrakis(4-carboxyphenyl)porphyrin (H_6TCPP) linker, forming a three-dimensional microporous network. A microporous porphyrin-based metal–organic framework, GaTCPP ($\{[Ga_2(H_2TCPP)(OH)_2]\cdot 5DMF\cdot 2H_2O\}_n$), was prepared via solvothermal synthesis using gallium(III) nitrate (0.7 mmol) and tetrakis(4-carboxyphenyl)porphyrin (0.022 mmol) as building units, following a previously reported method [3]. The synthesized GaTCPP was characterized by single-crystal X-ray diffraction (SC-XRD) (Figure 1).

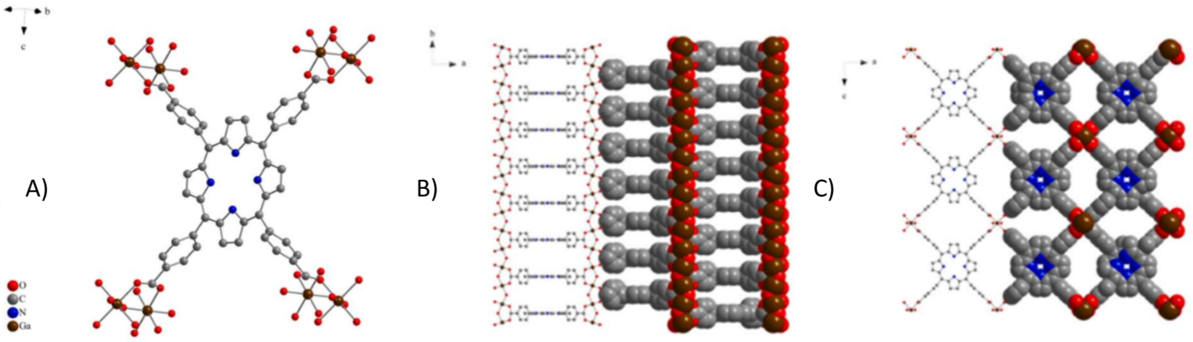

Figure 1 A) Coordination environment of $\{[Ga_2(H_2TCPP)(OH)_2]\cdot 5DMF\cdot 2H_2O\}_n$, molecules of solvents were removed for better clarity. B) A view along the c-axis showing half of the space-fill model of porous system. C) A view along the *b*-axis showing half of the space-fill model of porous system.

Post-synthetic metalation of the porphyrin core with M(II) = Ni(II), Cu(II), Zn(II) and Co(II) ions was carried out by immersing 200 mg of GaTCPP in 10 mL of dimethyl sulfoxide containing metal nitrate ($M(NO_3)_2$) at a concentration of 20 mg mL^{-1}. The suspension was stirred at 90 °C for 72 h to facilitate coordination of metal ions to the porphyrinic nitrogen atoms. Both synthesis steps proceeded with high yields, providing a stable, microporous material suitable for further physicochemical characterization and electrochemical applications. The structural integrity and successful post-synthetic modification of the GaTCPP framework were confirmed by a combination of powder X-ray diffraction, infrared spectroscopy, and X-ray photoelectron spectroscopy (Figure 2). Microscopic analyses revealed well-defined MOF crystallites with homogeneous distribution of M(II) within the framework. Gas adsorption measurements demonstrated that the material retained its microporous character and high specific surface area after metalation, confirming that the post-synthetic modification preserved the essential structural and textural properties required for electrochemical applications.

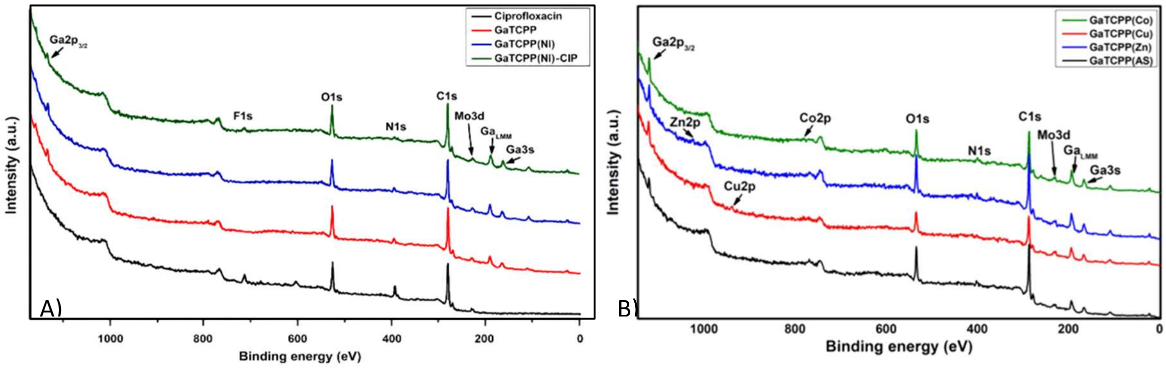

Figure 2 A) XPS survey of Ciprofloxacin, GaTCPP, GaTCPP(Ni) and GaTCPP(Ni) + Ciprofloxacin. B) XPS survey of GaTCPP(AS), GaTCPP(Zn), GaTCPP(Cu) and GaTCPP(Co).

Electrochemical studies showed that ciprofloxacin oxidation proceeds via an irreversible, diffusion-controlled process involving approximately three electrons. The enhanced sensing performance is attributed to specific interactions between ciprofloxacin and the MOF framework, leading to a broad linear detection range, good selectivity, and satisfactory stability, as well as reliable performance in real serum samples. These results highlight the potential of post-synthetically modified porphyrin-based MOFs for practical electrochemical sensing applications. The successful synthesis of the porphyrin-based metal–organic framework GaTCPP and its subsequent post-synthetic modification with Ni(II), Cu(II), Zn(II), and Co(II) ions were demonstrated. Structural and spectroscopic characterization confirmed the preservation of the MOF framework and the effective incorporation of the metal ions into the porphyrin core. Preliminary electrochemical investigations performed with the Ni-modified GaTCPP(Ni) material revealed very promising sensing performance, including enhanced electrochemical response and favorable interaction with the target analyte. These results suggest a high potential of post-synthetically metalated GaTCPP frameworks as functional electrochemical materials and indicate that analogous modifications with Cu(II), Zn(II), and Co(II) ions are likely to exhibit similarly advantageous electrochemical properties, warranting further systematic investigation.

Acknowledgements

This work was supported by VEGA 1/0058/25, 1/0442/25 and Funded by the EU NextGenerationEU through the Recovery and Resilience Plan for Slovakia under the project No. 09I03-03-V05-00008 (VVGS-ESGV-2923).

References

[1] H. Zhou, S. Kitagawa, Chem. Soc. Rev. **43** (2014) 5415.

[2] M. Yin, L. Zhang, X. Wei, J. Sun, D. Xu, Microchem. J. **183** (2022) 107946.

[3] N. Király, D. Capková, M. Almáši, et al. RSC Adv. **12** (2022) 23989.

How Porosity Affects Superconducting Properties in EuBCO Bulk Material

V. Kuchárová[a]*, D. Volochová[a], P. Diko[a]

[a]Institute of Experimental Physics, Slovak Academy of Sciences, Watsonova 47, 040 01 Košice, Slovakia

*kucharova@saske.sk

Bulk $REBa_2Cu_3O_{7-\delta}$ (REBCO, RE = rare earth) single grain bulks produced by top-seeded melt growth process can trap magnetic fields well beyond conventional permanent magnets and are therefore considered for compact trapped-field magnet assemblies in rotating machines, bearings, and cryogenic magnet systems [1-2]. Field homogeneity is a critical requirement in several of these applications and places constraints on the choice of the rare-earth element, because the paramagnetic moment of RE ions can distort the trapped-field profile. In this respect, EuBCO bulks are attractive candidates compared with strongly paramagnetic systems [3-4].

Despite steady progress in processing, the performance of EuBCO bulks remains limited by microstructural defects formed during melt growth and subsequent oxygenation. Porosity is among the most consequential of these defects. Pores reduce the effective superconducting cross-section, interrupt current percolation paths, and act as stress concentrators that promote cracking during thermal cycling and oxygen uptake [5]. They also couple to other microstructural features that control the macroscopic response, including the size and distribution of non-superconducting Eu_2BaCuO_5 (Eu211) particles and Ag inclusions, both of which influence flux pinning and mechanical integrity.

The present work examines how porosity, alongside Eu211 and Ag features, correlates with the superconducting properties of EuBCO bulks prepared either with engineered through-holes (Figure 1) or with controlled BaO_2/$BaCeO_3$ additions (Figure 2). Introducing holes into the green body provides escape paths for gases released during heating and can facilitate oxygen diffusion during the tetragonal to orthorhombic conversion. Adjusting the melt chemistry by additives can modify phase formation and coarsening during growth. In EuBCO, BaO_2 additions alter the Ba–O activity of the melt, while BaCeO3 (used as an alternative to CeO_2) provides a Ce source that tends to decorate RE211 particle surfaces and suppress Ostwald ripening, thereby refining pinning-active inclusions. These processing levers change not only Eu211 and Ag populations but also the pore size distribution and volume fraction, which in turn governs trapped field, levitation force, and magnetic critical current density.

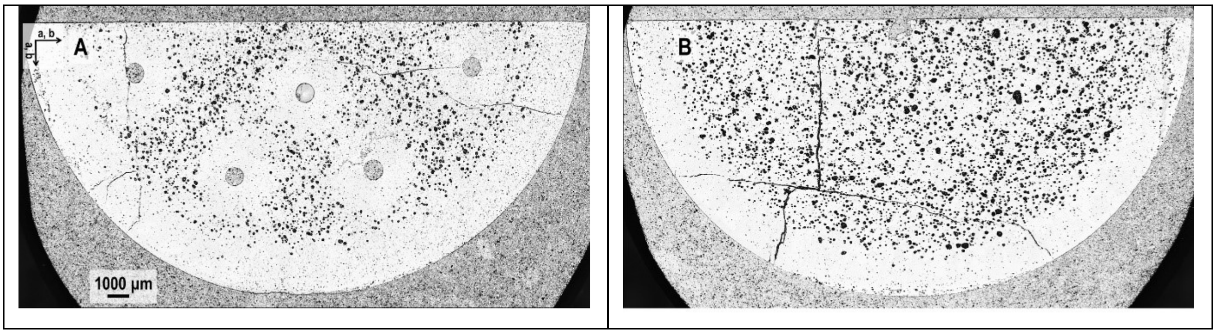

Figure 1 Polished a/b surface of the sample with holes (A) and sample without holes (B) at the half of the sample height.

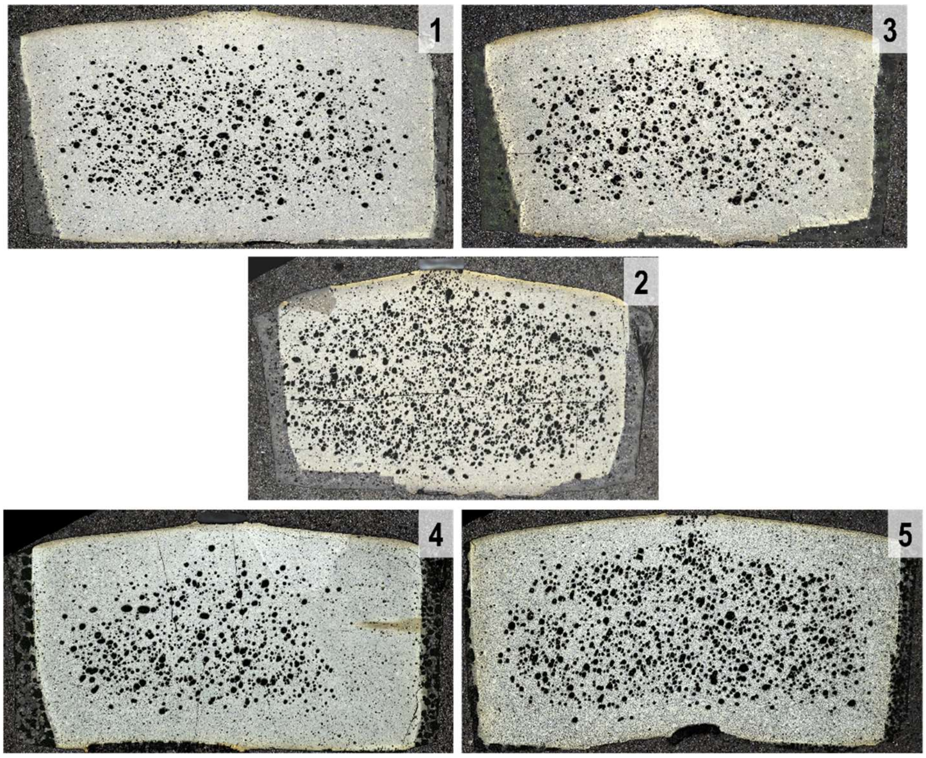

Figure 2 Polished a/c-sections of samples 1 – 5 observed under polarized light.

Acknowledgements

This work was supported by the European Union NextGenerationEU through the Recovery and Resilience plan for Slovakia under project No. 09I03–03-V04–00303.

References

[1] J. H. Durrell, M. D. Ainslie, D. Zhou, P. Vanderbemden, T. Bradshaw, S. Speller, M. Filipenko, D. A. Cardwell, Supercond. Sci. Technol. **31** (2018) 103501.
[2] D. K. Namburi, Y. Shi, D. A. Cardwell, Supercond. Sci. Technol. **34** (2021) 053002.
[3] Y. Yanagisawa, M. Hamada, K. Hashi, H. Maeda, Supercond. Sci. Technol. **35** (2022) 044006.
[4] P. Wikus, W. Frantz, R. Kümmerle, P. Vonlanthen, Supercond. Sci. Technol. **35** (2022) 033001.
[5] H. Y. Lee, C. J. Kim, G. W. Hong, J. Am. Ceram. Soc. **79** (1996) 2912-2916.

Porous Biocompatible MMCs: Synthesis and Effect of Reinforcement Particle Size

I. Laszko[a]*, I. Matuła[a], A. Barylski[a], W. Michalik[a], G. Dercz[a]**

[a]University of Silesia in Katowice, Institute of Materials Engineering, 75 Pułku Piechoty Street 1A, 41-500 Chorzów, Poland

*izabella.laszko@us.edu.pl, **grzegorz.dercz@us.edu.pl

The growing elderly population has increased the demand for advanced biomaterials in orthopedic and dental treatments, thereby stimulating the development of innovative solutions. Materials such as metal-based composites and modern alloys are being intensively studied due to their potential use in these clinical applications. These materials must exhibit high mechanical strength, wear resistance, and fatigue durability. Furthermore, they must actively support biological processes such as tissue repair, osseointegration, and integration with surrounding bone tissue [1]. Achieving an optimal balance between mechanical performance and biological response remains a major challenge, particularly in the case of long-term implants subjected to cyclic loading and corrosive physiological environments. Titanium alloys, particularly Ti6Al4V, are widely used due to their strength, corrosion resistance and biocompatibility. They account for over 50% of medical titanium application, compared to approximately 20-30% for commercially pure titanium [2,3]. A promising strategy for achieving a balance of mechanical performance, economic viability and biological safety is the development of biocompatible composites combining Ti6Al4V with pure titanium.

In this study, titanium-based metal-metal composites were successfully produced via powder metallurgy. Pure titanium was used as the matrix and Ti6Al4V particles were used as reinforcement. The effect of different particle sizes (~45 µm and ~450 µm) and weight fractions (20 wt.% and 40 wt.%) on the microstructure and properties was investigated. The microstructural analysis revealed a non-uniform particle distribution with agglomeration, particularly for larger particles (450 µm). The investigation revealed that an increase in reinforcement content was found to promote porosity. The Ti6Al4V particles exhibited a lamellar structure with a hardness gradient, higher in the cores and lower near the particle-matrix interface. The EDS analysis confirmed interdiffusion processes and the formation of diffusion-type bonds, indicating effective particle-matrix bonding but also the presence of local chemical and mechanical heterogeneities. Phase analysis confirmed that the composites have a biphasic nature, consisting of α-titanium and β-titanium.

Acknowledgements

This work was supported by the Polish National Science Centre, Poland (Polish: Narodowe Centrum Nauki, abbr. NCN) under the research project OPUS-27 no. UMO-2024/53/B/ST11/00431

Conference participation was supported by the GreenMat project, co-funded by the European Union under the program “European Funds for Silesia 2021-2027”

References

[1] L. Chen, et al., Front. Bioeng. Biotech. **11** (2023) 1206806.
[2] M. Najafizdaeh, et al., J. Alloys Comp. Commun. **3** (2024) 100019.
[3] N. Koju, S. Niraula and B. Fotovvati, Metals **12** (2022) 687.

Synthesis-Driven Design of Porous Carbon Adsorbents for Enhanced CO_2 Uptake

M. A. O. Lourenço[a]*, I. Correia[a], M. Odenot[b], N. P. F. Goncalves[a], M. Ilkaeva[a], M. Castellino[c], S. Bocchini[c], M. Fontana[c], F. C. Pirri[c], P. Ferreira[d], R. M. Novais[d], T. Frade[e], M. Bordonhos[e], M. Pinto[e], L. Mafra[a]

[a]University of Aveiro, Chemistry Department, CICECO, Aveiro, Portugal,
[b]Grenoble INP - Phelma, UGA, Graduate School of Engineering in Physics, Electronics, Materials Sciences, Grenoble, France;
[c]Politecnico di Torino, DISAT, Turin, Italy;
[d]University of Aveiro, DEMaC, CICECO, Aveiro, Portugal; [e]CERENA, Chemistry Engineering Department, IST, University of Lisbon, Lisboa, Portugal

*mirtha@ua.pt

The growing impact of CO_2 emissions on climate change has accelerated the development of efficient and sustainable capture technologies, with biochar emerging as a particularly promising adsorbent. Produced via the pyrolysis of biowaste, biochar offers highly tunable physicochemical properties through careful control of feedstock selection and synthesis conditions [1].

In this work, we focus on the optimization of chitosan-derived biochar adsorbents through innovative synthesis strategies aimed at enhancing CO_2 adsorption performance. A comprehensive suite of advanced characterization techniques, including X-ray photoelectron spectroscopy, gas sorption isotherms, electron microscopy, and operando thermogravimetric analysis coupled with infrared spectroscopy (TGA-IR), was employed to unravel the relationships between synthesis, microstructure, and CO_2 adsorption mechanisms.

A systematic study was conducted to assess the influence of polymerization routes, drying protocols, heating methods, and pyrolysis temperatures on the textural properties and adsorption behavior of the resulting biochars [2–4]. In parallel, the feasibility of producing self-standing, 3D-printed biochar composites incorporating inorganic polymers was explored [4] (Figure 1). The results demonstrate the strong potential of these materials for CO_2 capture and separation, particularly in CO_2/CH_4 and CO_2/N_2 mixtures, under both dry and humid conditions [2–4].

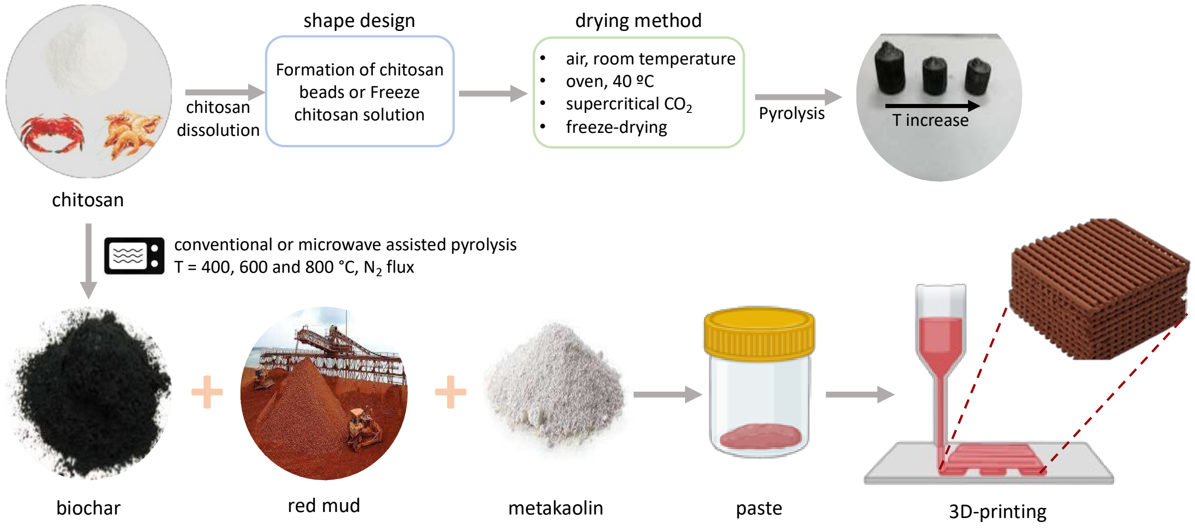

Figure 1 Schematic representation of the methodologies used to produce porous adsorbents.

By developing both powder and monolithic N-doped biochar adsorbents with tailored microstructures, clear correlations between porosity, surface chemistry, and CO_2 capture efficiency were established. These moisture-tolerant materials operate predominantly via physisorption and can be produced sustainably without additional activation or chemical modification, highlighting biochar as a highly attractive candidate for scalable CO_2 capture applications.

Acknowledgements

This work was developed within the scope of the project CICECO-Aveiro Institute of Materials, UID/50011/2025 (DOI 10.54499/UID/50011/2025) & LA/P/0006/2020 (DOI 10.54499/LA/P/0006/2020), funded by FCT/MEC (PIDDAC). It has received funding from the European Research Council under the European Union's Horizon Europe research and innovation program (Grant Agreement 865974) and by FCT/MCTES, I.P., through national funds (PIDDAC), co-financed by the European Regional Development Fund (ERDF) of the European Union, through the FEDER program and national funds related to operation no. 16589 (operation code: COMPETE2030-FEDER-00776600) of Portugal 2030 (CharM project). FCT is acknowledged by MAOL for a Junior Researcher Position (CEECIND/01158/2021). NG and MAOL acknowledge funding from the European Union's Horizon 2020 research and innovation programme No. 101065059 and 101090287, respectively.

References

[1] Y. Qiao and C. Wu, Carbon Capture Sci. Tech. **2** (2022) 100018.
[2] M. Lourenço et al., Chem. Eng. J. **362** (2019) 364.
[3] M. Lourenço et al., Chem. Eng. J. **470** (2023) 144005.
[4] I. Correia et al., J. Environ. Chem. Eng. **12** (2024) 113875.

Porous, Biocompatible Metal-Metal Composites Reinforced with *β*-Titanium Alloy

W. Michalik[a*], I. Matuła[a], A. Barylski[a], I. Laszko[a], G. Dercz[a**]

[a]University of Silesia in Katowice, Institute of Materials Engineering, 75 Pułku Piechoty Street 1A,
41-500 Chorzów, Poland

*wiktoria.michalik@us.edu.pl, **grzegorz.dercz@us.edu.pl

The continuous development and aging population are driving the ongoing increase in interest in engineering materials that can be successfully applied in medicine. Particular attention should be paid to composite materials, whose properties are determined by the phases consisting their structure [1]. Metal matrix composites (MMC) are the most widely used as implant materials. One of the most important problems with these materials is the risk of implant loosening caused by differences between the elastic modulus of human bone and the implant. With this in mind, it appears that titanium and its alloys are a particularly promising candidate material for biomedical applications [2]. Unfortunately, numerous studies have reported that vanadium and aluminium present in the Ti6Al4V alloy may result in negative biological effects including the potential for a correlation with the development of Alzheimer's disease [3, 4]. Based on this information, a study was carried out to examine the impact of adding biocompatible molybdenum on the properties of titanium matrix composites.

In this study, six composite variants were fabricated via powder metallurgy using commercially pure titanium (CP-Ti) and Ti16Mo reinforcement. The samples, designated 0TM to 50TM, contained increasing amounts of Ti16Mo powder in 10 wt.% increments, ranging from 0 to 50 wt.%. Samples were characterized using X-ray diffraction (XRD), optical microscopy (OM), and scanning electron microscopy (SEM) equipped with EDXS for elemental analysis.

X-ray diffraction analysis of the powder mixtures showed that higher molybdenum concentrations promoted the β-Ti phase, evidenced by the increased intensity of its reflections at the expense of the α-Ti phase. Post-sintering analysis revealed the emergence of an additional β-Ti phase not present in the initial powders. The shift in diffraction peaks suggests that this newly formed phase possesses a lower lattice parameter than the primary β phase originating from the Ti16Mo reinforcement, likely due to partial diffusion of Mo into the Ti matrix. Optical microscopy observations of the sintered materials revealed in the 0TM sample a characteristic α-Ti microstructure. A lamellar structure was observed in samples with a Ti-16Mo content of between 10-30%. This indicates the presence of transition zones between the α and β phases of titanium. Stereological calculations reveals that the addition of molybdenum, present in the reinforcing fraction, results in minimal porosity increase. SEM observations confirmed the porosity of the composites, as previously observed through OM imaging. Using SEM-EDS, elemental distribution maps were obtained. By comparing the distribution maps of titanium and molybdenum, it was evident that diffusion had occurred between the matrix and the reinforcing particles.

Acknowledgements

This work was supported by the Polish National Science Centre, Poland (Polish: Narodowe Centrum Nauki, abbr. NCN) under the research project OPUS-27 np. UMO-2024/53/B/ST11/00431.

Conference participation was supported by the GreenMat project, co-funded by the European Union under the program "European Funds for Silesia 2021–2027".

References

[1] L. A. Dobrzański, Warszawa (2002) 28, 46.
[2] E. M. Karakurt, Y. Cetin , A. Incesu, H. Demirtas, M. Kaya, Y. Yildizhan, M. Tosun, Y. Huang. Materials **16** (2023) 4240.
[3] K. V. Sergienko, S. V. Konushkin, Y. A. Morozova, M. A. Kaplan, A. D. Gorbenko, B. A. Rumyantsev, M. E. Prutskov, E. E. Baranov, E. O. Nasakina, T. M. Sevostyanova, et al., J. Funct. Biomater. **16** (2025) 126.
[4] H. Wu, T. Jiang, L. Kong, X. Chen, P. Liu. Materials **18** (2025) 602.

The Effects of Porosity on the Superconducting Properties of Bulk Single-Grain GdBCO-Ag Superconductors

M. Radušovská[a]*, D. Volochová[a] , V. Kuchárová[a], P. Diko[a]

[a]Department of Material Physics, Institute of Experimental Physics, SAS Košice, Watsonova 47, 040 01 Košice, Slovak Republic

*radusovska@saske.sk

Bulk single-grain superconductors composed of GdBCO ($GdBa_2Cu_3O_{7-\delta}$) belong to the group of high-temperature REBCO superconductors, where RE represents a rare earth element or Y [1]. These superconductors become superconductive at temperatures higher than those of liquid nitrogen. Because they have favourable electromagnetic properties, such as a higher critical temperature, critical current density, and the ability to trap large magnetic fields, they are a group of materials that can be used in advanced technology. GdBCO-Ag is a better superconductor and more stable mechanically than other REBCO systems. This is especially important for practical uses. Due to these characteristics, GdBCO-Ag bulk superconductors are being thoroughly studied for application in flywheel energy storage devices, magnetic levitation systems, and the generation of strong permanent magnetic fields [2].

Bulk GdBCO-Ag single-grain superconductors are usually prepared by growth from a molten mixture of superconductor components. The Top-Seeded Melt Growth (TSMG) method is used to produce bulk single-grain superconductors. The presence of finely dispersed secondary phases, specifically Gd_2BaCuO_5 (Gd-211) particles, plays an important role for flux pinning, which significantly increases the critical current density of the material. A characteristic microstructural deficiency of bulk GdBCO single-grain superconductors is porosity, which primarily results from the crystal growth process during melting. Pores are caused by the release of gases, typically oxygen, during the peritectic process. Porosity significantly influences the superconducting and mechanical properties of GdBCO-Ag materials. The existence of pores results in a reduction of the effective cross-section for superconducting current flow, hence decreasing the critical current density [3]. By modifying growth conditions, porosity can be partially reduced, leading to a more compact and mechanically stable microstructure [4].

This study examines the microstructure and superconducting characteristics of GdBCO-Ag single-grain superconductors with varying heights, emphasising porosity. GdBCO-Ag bulk superconductors were synthesised using the TSMG technique in an air atmosphere. The nominal composition of all samples consisted of 1 mol $GdBa_2Cu_3O_{7-\delta}$ (Gd-123) + 1/2 mol Gd_2BaCuO_5 (Gd-211) + 20 wt.% Ag_2O + 0.945 wt.% $BaCeO_3$. $GdBa_2Cu_3O_7$ (Solvay, particle size 30μm), Gd_2BaCuO_5 (CAN Superconductors, particle size 1-2 μm), Ag_2O (Chempur, 99%) and $BaCeO_3$ powder prepared in the laboratory Department of Material Physics (IEP SAS Kosice) were mixed in appropriate amounts in a mixer for 30 min and then intensively milled for 15 min in a friction mill.

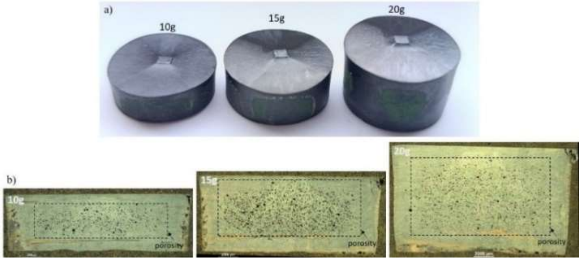

Figure 1 a) Macrostructure of GdBCO bulk superconductors and b) microstructure with visible pore region in the middle of the crystal.

The addition of silver improves the mechanical properties of GdBCO-Ag single grains and the addition of $BaCeO_3$ provides an inhibitor of Gd-211 particle growth in this system. The powder mixtures with weights of 10 g, 15 g, and 20 g were uniaxially compressed into cylindrical pellets with a diameter of 20 mm. GdBCO single grains were epitaxially grown from a thin-film NdBCO seed on the surface of the compressed tablet (see Figure 1a).

GdBCO-Ag pellets were heated to a melting temperature of 1062°C at a rate of 100°C per hour, held there for one hour, cooled to 1022°C at a rate of 100°C per hour, and then gradually cooled to 978°C at a rate of 0.4°C per hour. After that, it was cooled to 900°C at a rate of 100°C per hour, and then it was finally cooled to room temperature in a furnace. The GdBCO sample was cooled to liquid nitrogen temperature (77 K) in an external magnetic field of 1.4 T in order to measure superconducting characteristics as a trapped magnetic field. A Hall probe positioned 0.5 mm above the sample surface detected the trapped magnetic field (see Figure 2).

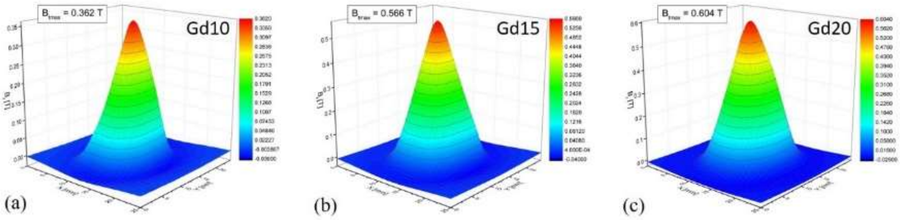

Figure 2 Trapped magnetic field for: a) Gd10, b) Gd15, and c) Gd20 bulk GdBCO-Ag superconductors.

An optical microscope and a scanning electron microscope were used to conduct microstructural examination along the crystallographic a/c plane (see Figure 1b). Image analysis was used to assess how the size and volume fraction of pores varied with distance from the seed (see Figure 3a, 3b).

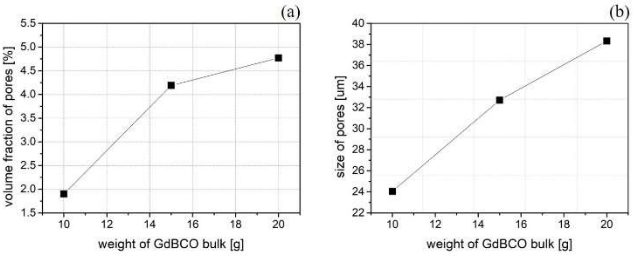

Figure 3 Dependence of a) volume fractions and b) size of pores for GdBCO-Ag with different weight of bulks.

From the calculated values of critical current density for whole the sample, J_{cs}, (Table 1), it can be seen that the smaller sample, Gd10, exhibits a lower value of critical current density, J_{cs}, compared to the samples with higher weight, Gd15 and Gd20. In the sample Gd10 we observe a lot of solidified melt along the edges of the crystal, which is related to the higher loss of melt from the sample into the substrate during crystal growth.

Table 1 Calculated values of critical current density for the whole sample, J_{cs}, for GdBCO-Ag with different weight of bulks.

Sample	*Sample height [mm]*	B_{tmax} *[T]*	$J_{cs} \times 10^4$ *[A/cm²]* *z = 0,5 mm*
Gd10	5.12	0.388	1.19
Gd15	7.6	0.566	1.54
Gd20	10.7	0.604	1.54

Acknowledgements

This work was supported by Slovak Grant Agency APVV-21-0387, VEGA No. 2/0018/26 and by the European Union NextGenerationEU through the Recovery and Resilience plan for Slovakia under project No. 09I03-03-V04-00303.

References

[1] D. A Cardwell, Mat. Sci. Eng. **B 53** (1998) 1–10.
[2] J. Durrell, M. Ainslie, D. Zhou, P. Vanderbemden, T. Bradshaw, S. Speller, M. Filipenko and D. Cardwell, Supercond. Sci. Technol. **31** (2018) 103501.
[3] J. Baumann, Y. Shi, D. Weerakonda, J. H. Durrell, D. A. Cardwell, J. Eur. Ceram. Soc. **43** (2023) 542-1547.
[4] P. Diko, W. Gawalek, T. Habisreuther, P. Gornert, Applied Superconductivity **1** (1995) 123-126.

DESIGN AND SYNTHESIS OF MATERIALS

Grignard Grafting on Titania – Mechanistic Insights into the Modification and Surface Properties

F. Tharakan[a], L. Bergh[a,b], N. Gauquelin[c], C. Chandran[a,d], J. Verbeeck[c], S. V. Doorslaer[b], V. Meynen[a,*]

[a]Laboratory of Adsorption and Catalysis, Department of Chemistry, University of Antwerp, Antwerp, 2020 Belgium
[b]Theory and Spectroscopy of Molecules and Materials, Department of Chemistry, University of Antwerp, Antwerp, 2610 Belgium
[c]Electron microscopy for Materials Science, Department of Physics, University of Antwerp, Antwerp 2020 Belgium
[d]Electrochemical and Surface Engineering, Department of Materials and Chemistry, Vrije Universiteit Brussel, Brussels, 1050 Belgium.

*vera.meynen@uantwerpen.be

Metal oxides like titania are applied in separation technology, such as in sorption and membrane processes [1]. The applicability of these metal oxide membranes are limited due to their hydrophilic nature and the limited specific surface interactions, hampering affinity separation capabilities. To avoid these issues, metal oxides can be modified with organic groups, introducing hydrophobicity and specific interactions from a wide diversity of organic (functional) groups to their surface. These organic grafted metal oxides, provide unique properties in applications. One such interesting surface modification involves using Grignard reagents to graft organic groups on titania [2, 3] as schematically represented in Figure 1.

The organic groups are introduced to the surface of titania via reaction with Grignard reagents, make the resulting material applicable in a wide range of solvents and allow regulating separation selectivity by altering solute and solvent interaction with the surface, a property needed for organic solvent nanofiltration [1] as well as for anti-fouling purposes [4]. However, the mechanism of the Grignard grafting remains elusive and complex, as there are multiple processes ongoing including grafting of the organic group and a titania reduction process (evidenced by a color change of titania in solution after addition of the Grignard reagent). The current work focusses on grafting organic groups on titania using various Grignard reagents such as ethyl and octyl magnesium chlorides, phenyl magnesium bromide and others in order to study the reduction behavior of titania during Grignard modification and its correlation with the modification degree (using EPR, TGA-MS, IR, XPS and EELS measurements). In specific, the influence of crystal phases on the modification process (using phase pure titania powders) is evaluated.

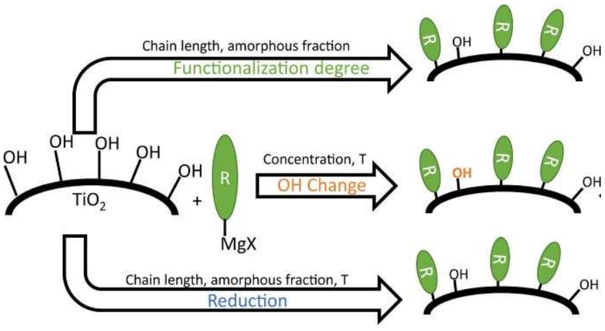

Figure 1 Schematic representation of Grignard surface grafting on titaniae [2].

Acknowledgements

This work was funded by Uantwerpen BOF project Grignard 2.0.

References

[1] S. R. Hosseinabadi, K. Wyns, A. Buekenhoudt, B. Van der Bruggen, D. Ormerod, Sep. Purif. Technol. **147** (2015) 320–328.

[2] J. Van Dijck, P. Mampuys, H. Y. V Ching, D. Krishnan, K. Baert, T. Hauffman, J. Verbeeck, S. V. Doorslaer, B. U. W. Maes, M. Dorbec, A. Buekenhoudt, V. Meynen, Appl. Surf. Sci. **527** (2020) 146851.

[3] P. Van Heetvelde, E. Beyers, K. Wyns, P. Adriaensens, B. U. W. Maes, S. Mullens, A. Buekenhoudt, V. Meynen, Chem. Commun. **49** (2013) 6998–7000.

[4] G. Mustafa, K. Wyns, P. Vandezande, A. Buekenhoudt, V. Meynen, J. Memb. Sci. **470** (2014) 369-377.

Porosity in SDMG-Processed YBCO Bulk Superconductors: Effect of the Time–Temperature Processing Profile

K. Zmorayová[a]*, L. Vojtková[a], P. Diko[a]

[a]Institute of Experimental Physics, Slovak Academy of Sciences, Watsonova 47, 04001 Košice, Slovak Republic

*zmoray@saske.sk

$YBa_2Cu_3O_{7-\delta}$ (YBCO) and related $REBa_2Cu_3O_{7-\delta}$ (REBCO, where RE denotes a rare-earth element) bulk superconductors are widely studied high-temperature superconducting materials due to their ability to operate at liquid-nitrogen temperatures and to trap high magnetic fields. The properties of bulk YBCO are strongly influenced by the microstructure, which is controlled by the applied processing conditions, particularly the time–temperature profile during melt processing. Extended dwelling in the molten state, typically associated with slower growth rates, promotes oxygen release and leads to a reduction in porosity. However, prolonged processing simultaneously results in coarsening of the secondary Y_2BaCuO_5 (Y-211) phase. While finely dispersed Y-211 particles act as effective flux pinning centres, excessive particle growth is generally associated with a decrease in the effective critical current density, potentially limiting the trapped magnetic field and levitation force. Porosity in YBCO bulk samples is mainly generated by oxygen evolution during the peritectic decomposition of the $YBa_2Cu_3O_x$ (Y-123) phase, with additional contributions arising from carbonate decomposition and air entrapped during powder compaction. Although a limited level of porosity can facilitate oxygen diffusion during post-processing oxygenation, excessive porosity has an adverse effect on both the mechanical integrity and superconducting properties of bulk REBCO materials [1, 2, 3].

In this work, the formation of porosity was investigated as a function of the applied time–temperature processing regime, with particular emphasis on its influence on the size, volume fraction, and distribution of Y-211 particles in bulk YBCO samples. Bulk YBCO samples were prepared from commercially available $YBa_2Cu_3O_x$ (Y-123) and Y_2BaCuO_5 (Y-211) powders (Can Superconductors), with the addition of CeO_2 (as a Y-211 particle refining agent), mixed in a weight ratio of 70 wt.% Y-123, 30 wt.% Y-211, and 0.5 wt.% CeO_2. The powder mixture was homogenized in a shaker for 30 min and subsequently milled for 15 min. The resulting powder mixture was sieved using a vibrating sieve and uniaxially pressed into pellets with a mass of 15 g, a diameter of 20 mm, and a height of 10 mm. The pressed pellets were synthesized at 1005 °C for 2 h in air. Bulk single-grain superconductors were grown using the SDMG (single-direction melt growth) process [4], in which growth proceeds from a large-area seed placed under of the synthesized pellet. An $EuBa_2Cu_3O_x$ (EuBCO) bulk superconductor grown by the TSMG process was used as the large-area seed. Before to growth by SDMG proces, the surfaces of both the EuBCO seed and the synthesized YBCO pellets were ground and polished to ensure intimate contact, and a suspension of Y-211 powder in ethanol was applied as a bonding layer. Growth was carried out in a muffle furnace using three different time–temperature processing regimes (Figure 1a (S1), 1b (S2), 1c (S3)).

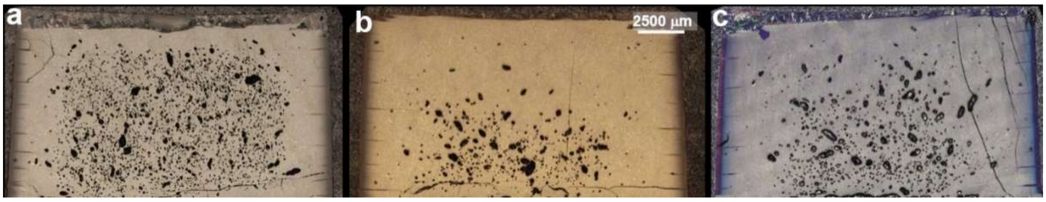

Figure 1 Macrostructure of SDMG-processed YBCO bulk samples observed in polarized light, illustrating differences in porosity distribution and pore volume fraction (Vp) resulting from different applied time–temperature processing regimes: (a) S1 (Vp = 15%), (b) S2 (Vp = 4%), and (c) S3 (Vp = 8%).

The microstructure was characterized by optical polarization microscopy (Nikon UDMLV 100 D-U) on sections cut along the a/c growth direction (i.e., a cut perpendicular to the top surface of the sample). Quantitative data on the size and volume fraction of Y-211 particles and pores were obtained by image analysis using NIS-Elements software. It was observed that processing regimes involving a high maximum temperature of 1011 °C led to an increase in the average and maximum size of Y-211 particles, indicating pronounced particle coarsening (Table 1). In contrast, for sample S3, where the maximum processing temperature was reduced to 1006 °C while maintaining a slow cooling rate, a slight increase in porosity was detected; however, the average Y-211 particle size reached values generally considered favourable for flux pinning, suggesting a potentially beneficial balance between porosity and secondary-phase particle morphology with respect to the resulting superconducting properties.

Table 1 Processing parameters and microstructural characteristics of SDMG-processed YBCO bulk samples. The average and maximum sizes of Y-211 particles (d_{211}) and the volume fraction of pores (Vp) were determined by image analysis.

Sample	Maximum temperature (°C)	Cooling rate (°C / h)	Average d_{211} (μm)	Maximum d_{211} (μm)	Vp (%)
S1	1011	0.5	2	7.5	15
S2	1011	0.25 / 0.4	2.5	9.5	4
S3	1006	0.25 / 0.4	1.2	6	8

Acknowledgements

This work was supported by APVV project no. 21-0387, VEGA No. 2/0018/26 and APD0204.

References

[1] D. K. Namburi, Y. Shi, D. A. Cardwell, Supercond. Sci. Technol. **34** (2021) 053002.
[2] N. Sakai, D. Ishihara, K. Inoue, M. Murakami, Supercond. Sci. Technol. **15** (2002) 698–701.
[3] K. Zmorayová, P. Diko, D. Volochová, V. Antal, T.Hlásek, V. Plecháček, F. Antončík, Ceram. Int. **49** (2023) 22177-22186.
[4] T. Motoki, R. Sasada, T. Tomihisa, M. Miwa, S. Nakamura, J. Shimoyama, Supercond. Sci. Technol. **35** (2022) 094003.

ENVIRONMENTAL ADSORPTION AND SEPARATION

Long-Term Environmental Behaviour of Functionalized SBA-15 Mesoporous Silica: Implications for Drug Delivery Sustainability and Environmental Fate

M. Almáši[a]*, Ľ. Zauška[a], T. Zelenka[b], E. Beňová[a], V. Zelenák[a], M. Balintová[c], A. Eštoková[c]

[a]Department of Inorganic Chemistry, Institute of Chemistry, Faculty of Science, Pavol Jozef Šafárik University in Košice, Moyzesova 11, 040 01 Košice, Slovak Republic
[b]Department of Chemistry, Faculty of Science, University of Ostrava, 30. Dubna 22, 702 00 Ostrava, Czech Republic
[c]Department of Material Engineering, Faculty of Civil Engineering, Technical University of Košice, Vysokoškolská 4, 042 00 Košice, Slovak Republic

*miroslav.almasi@upjs.sk

Mesoporous silica materials, particularly SBA-15, represent an important class of drug delivery carriers due to their high specific surface area, tunable pore architecture, and versatile surface chemistry. While extensive research has focused on optimizing drug loading, release kinetics, and biological performance, the long-term environmental stability of these materials after their life cycle remains insufficiently understood. This aspect is critical because silica-based carriers inevitably enter wastewater streams and may accumulate in soil environments. Therefore, understanding their long-term structural and chemical evolution is essential for evaluating environmental safety and sustainability. The present study systematically investigates the long-term behaviour of pristine and functionalized SBA-15 under accelerated ageing conditions simulating multi-year exposure in aqueous acidic and soil environments [1].

Pristine SBA-15 and SBA-15 functionalized with polar ($-NH_2$, $-SH$, polyethyleneimine (PEI)) and non-polar ($-CH_3$, $-Ph$) groups were prepared via post-synthetic grafting. The successful incorporation of functional groups was confirmed by thermogravimetric analysis, showing organic loadings ranging from 0.66 wt% for SBA-15-CH_3 to 16.91 wt% for SBA-15-PEI. Functionalization strongly influenced textural properties. While pristine SBA-15 exhibited a BET surface area of approximately 625 $m^2\ g^{-1}$ and total pore volume of 0.753 $cm^3\ g^{-1}$, PEI-functionalized SBA-15 showed a dramatic decrease to 18.3 $m^2\ g^{-1}$ and 0.024 $cm^3\ g^{-1}$ due to pore blocking by bulky polymer chains. These results confirm that functional group size and density directly control pore accessibility.

Long-term environmental behaviour was evaluated using accelerated ageing in a salt spray chamber simulating acid rain ($pH \approx 4$) through cyclic exposure for 100 days (2400 h), corresponding to multi-year natural exposure based on Q10 modelling extended with a pH stress factor. Parallel soil exposure experiments enabled comparison between hydrolytic degradation and complex multiphase environmental interactions.

Nitrogen sorption analysis revealed significant degradation of textural properties under aqueous conditions. Pristine SBA-15 exhibited a decrease in BET surface area from 625 $m^2\ g^{-1}$ to approximately 321 $m^2\ g^{-1}$ (≈49% reduction). Hydrophilic functionalization significantly reduced stability. SBA-15-NH_2 showed surface area losses exceeding 60% after aqueous exposure ($69.6 \rightarrow 24.7$ $m^2\ g^{-1}$). In contrast, SBA-15-PEI exhibited an apparent increase in surface area ($18.3 \rightarrow 113.2$ $m^2\ g^{-1}$), attributed to hydrolytic degradation and leaching of PEI chains, which reopened previously blocked pores. Hydrophobic functionalization markedly improved environmental resistance. SBA-15-CH_3 retained approximately 82% of its original surface area, while SBA-15-Ph retained approximately 76% after aqueous ageing. These results indicate that hydrophobic surface chemistry limits water penetration and suppresses hydrolytic degradation processes. Soil exposure produced more complex degradation patterns compared to aqueous ageing. XRF analysis revealed adsorption of soil-derived ions and organic compounds. Unmodified SBA-15 exposed to soil showed SiO_2 content decreasing to approximately 77.6%, while hydrophobic derivatives retained near-pristine composition (>97%). Polar-functionalized samples exhibited incorporation of soil-derived elements, particularly iron, detected as Fe_2O_3 at concentrations up to ~0.36 wt%, indicating strong interactions between functional groups and soil mineral phases. Thermogravimetric analysis revealed distinct functional group stability trends. Thiol-functionalized samples showed partial degradation (3.89 wt% → 2.61 wt% in water → 1.95 wt% in soil). PEI-functionalized samples exhibited the highest hydrolytic instability, losing approximately 11–13 wt% organic content. Interestingly, NH_2-functionalized samples showed apparent organic content increase in soil (~14.16 wt%), attributed to adsorption of humic substances and multivalent cations rather than increased functional group concentration. Small-angle X-ray scattering confirmed progressive structural degradation during environmental exposure. Domain size decreased from ~47–48 nm in pristine samples to ~21.8–33.5 nm after aqueous ageing. Hydrophobic functionalization again provided improved structural protection, with SBA-15-CH_3 showing the highest retained domain size. Correlation analysis identified strong relationships between key textural parameters. BET surface area and total pore volume showed very strong correlation ($r \approx 0.97$), confirming that these parameters represent reliable indicators of structural degradation. In contrast, correlations between chemical composition (SiO_2 content) and textural parameters were weaker, indicating that pore collapse is the primary degradation driver.

Mechanistically, aqueous ageing is dominated by hydrolysis-driven siloxane bond cleavage and functional group degradation, resulting in relatively uniform degradation behaviour. Soil exposure introduces additional processes including ion exchange, mineral deposition, adsorption of organic matter, and microbial activity, producing more heterogeneous and sometimes more severe long-term degradation. Despite these changes, the silica matrix itself remained structurally intact even under accelerated ageing conditions, confirming the intrinsic stability and environmental compatibility of SBA-15-type materials. Considering the natural abundance and biocompatibility of amorphous silica, SBA-15 remains a promising platform for sustainable drug delivery systems.

From a materials design perspective, hydrophobic functionalization (–CH_3, –Ph) offers superior long-term environmental stability and should be prioritised for environmentally resilient drug delivery systems. Polar functional groups remain essential for drug–carrier interactions and stimuli responsiveness but should be selectively applied or protected using hybrid coatings. Structural reinforcement strategies such as thicker pore walls or hierarchical porosity represent additional approaches for improving long-term durability. Overall, this study establishes a predictive relationship between surface chemistry and environmental fate of mesoporous silica materials. The findings provide essential guidance for designing next-generation sustainable drug delivery carriers with improved environmental safety and regulatory compliance.

Acknowledgements

This work was supported by APVV project no. APVV-23-0097 and VEGA 1/0286/25.

References

[1] Ľ. Zauška, T. Zelenka, E. Beňová, M. Zelinská, M. Cambal Hološová, V. Zelenák, M. Balintová, A. Eštoková, M. Almaši, J. Environ. Chem. Eng. **13** (2025) 119561.

Studies on Membrane-Cascade Pervaporation for Recovery and Reincorporation of Aroma Compounds in Wine Dealcoholization

R. Cândido[a]*, A. Catarina Faria[a,b]

[a]Fraunhofer Portugal Center for Advanced Water, Energy, and Resource Management - AWAM, Régia Douro Park, 5000-033 Vila Real, Portugal
[b]Centre for the Research and Technology of Agroenvironmental and Biological Sciences, CITAB, Inov4Agro, Universidade de Trás-os-Montes e Alto Douro, UTAD, Quinta de Prados, 5000-801 Vila Real, Portugal

*rodrigo.candido@awam.fraunhofer.pt

The increase in alcohol content in wines, driven by climate change and modern vinification practices, has intensified interest in effective dealcoholization strategies. Among the available technologies, membrane-based processes are often preferred due to their non-thermal operation and potential for enhanced retention of thermolabile and volatile compounds compared to thermal methods. Pervaporation (PV) is a particularly attractive technique, offering high selectivity for ethanol at low temperatures and moderate energy demand, and operational simplicity and flexibility [1].

Following our previous work demonstrating the feasibility of pervaporation for the partial (7.5% vol.) and total (1.0% vol.) dealcoholization of red, wine, and rosé wines, the present study aims to test different membrane-cascade system configurations to minimize volatile compounds losses and improve the dealcoholization process performance. PV experiments were conducted in a laboratory-scale setup (Figure 1) using a commercial *Pervap*™ 4060 flat-sheet organophilic membrane. White, red, and rosé wines were dealcoholized at low temperatures (13-17 °C), and the membrane permeate site was maintained at a vacuum pressure of 10 mbar. Such conditions were selected to preserve wine quality, particularly the appearance of white wine, as higher temperatures were found to favor the degradation of compounds, evidenced by visible darkening of the wine’s color. The results showed that total dealcoholization had a more pronounced impact on wine volatile compounds, providing a higher loss when compared to partial dealcoholization. White wine showed the greatest potential for the next study, as it exhibited better retention of esters (20 - 40%) (cf. (see Figure 2)), which are key contributors to wine aroma, compared with the other wines.
In the previous study, it was observed that, despite the organophilic nature of the membrane, significant water permeation occurred alongside ethanol and other volatile organic compounds (VOCs), which can be attributed to the higher water partial vapor pressure gradient across the membrane. Besides that, ethanol removal carried along key esters and higher alcohols, negatively affecting the taste and complexity/body of the dealcoholized wine.

To address this limitation and recover organic compounds and water for reincorporation into the final dealcoholized wine, the present work investigates a multi-stage membrane pervaporation strategy (Figure 3) that combines an organophilic membrane (*Pervap*™ 4060) with a hydrophilic membrane (*Pervap*™ 4100) for the dealcoholization of white wine. The process consists of three sequential stages: (1) initial wine partial dealcoholization using *Pervap*™ 4060, (2) dehydration of the resulting permeate with *Pervap*™ 4100 to concentrate ethanol and organic compounds as much as possible, and (3) separation of ethanol from organic compounds in the retentate mixture. Finally, water and VOCs are reincorporated into the dealcoholized wine to preserve its original sensory profile. Both the treated wine and intermediate streams are characterized semi-quantitatively by GC–MS to assess aroma retention.

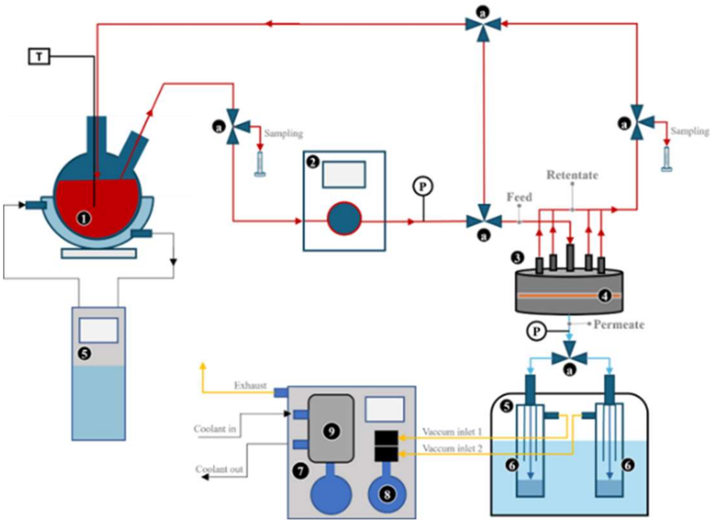

Figure 1 Pervaporation experimental set-up (1. Round-bottom flask; 2. Peristaltic pump; 3. Membrane module; 4. Membrane; 5. Thermostatic bath; 6. Vacuum cold sample trap; 7. Vacuum pump; 8. Inlet separator; 9. Exhaust vapor condenser; T. Thermometer; P. Pressure gauge; a. two and three-way valves).

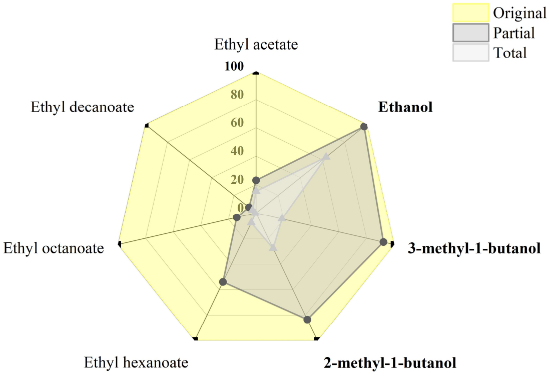

Figure 2 Retention of key volatile compounds in white wine after partial and total dealcoholization.

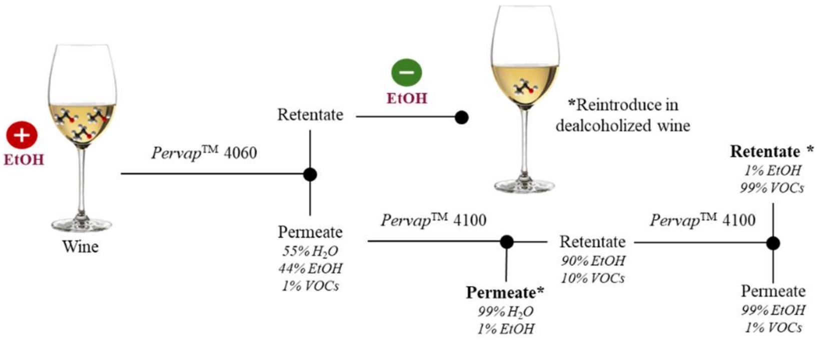

Figure 3 Multi-stage pervaporation process schematic.

Acknowledgements

This work was supported by the project “Vine and Wine Portugal – Driving Sustainable Growth Through Smart Innovation”, with reference no. C644866286-00000011, co-financed by the Recovery and Resilience Plan and NextGeneration EU Funds, and by National Funds by FCT, under the projects UI/04033 and LA/P/0126/2020.

References

[1] A. Basile et.al, Elsevier (2015).

ENVIRONMENTAL ADSORPTION AND SEPARATION

Adsorption of Anionic Water Pollutants on Amino-Functionalized UiO-66 and UiO-67: Effects of Conditions and Mechanistic Insights

L. M. Holeczyová[a]*, L. Zauška[a], M. Almáši[a]

[a]Department of Inorganic Chemistry, Institute of Chemical Sciences, Faculty of Science,
Pavol Jozef Safarik University, Moyzesova 11, 040 01 Kosice

*lara.mia.holeczyova@student.upjs.sk

In recent years, there has been growing interest in developing metal-organic frameworks (MOFs) for environmental applications. These porous structures represent a promising approach in battling pollution of aqueous matrices [1]. MOFs, also known for high porosity and large surface area, are networks that can be modified for specific applications. Our work focuses on applying zirconium-based MOFs, UiO-66-NH_2 and UiO-67-NH_2, for heavy metal adsorption in water systems.

The UiO-66-NH_2 was synthesized via the solvothermal method and applied for metal ions adsorption from aqueous environment under varying conditions, e.g. mass concentration (50, 200 and 500 mg L^{-1}), *pH* (7, 5, 3) and UV irradiation (254 and 366 nm). The studied metals (manganese and chromium) in their anionic forms (MnO_4^-, CrO_4^{2-} and $Cr_2O_7^{2-}$) were selected due to their distinct colour in solution, which can be detected by UV/VIS spectroscopy. Applied methods of characterization were infrared spectroscopy, powder X-ray diffraction and ultraviolet and visible light spectrophotometry. To further demonstrate the suitability of UiO-66-NH_2 to capture previously mentioned anionic pollutants second material, UiO-67-NH_2, was synthesised and characterized by the available methods.

The infrared spectroscopy measured using the ATR technique, revealed characteristic bands of a primary amine at 3473 (v_{as}(NH)) and 3376 (v_s(NH)) cm^{-1}, the carboxylate was displayed at 1565 (v_{as}(COO^-)) and 1381 (v_s(COO^-)) cm^{-1}, in comparison with the starting material of 2-aminoterephthalic acid new signal was observed at 654 (v(ZrO)) cm^{-1} which corresponds to the zirconium oxygen bond. Observed absorption bands are consistent with the literature describing UiO-66-NH_2 structure [2]. The measured PXRD pattern aligned with the previously described record [2] with peaks at 7.40°, 8.55° and 25.70°, which correspond to (111), (200) and (600) crystal planes, respectively. The characterization was complete through the techniques mentioned above.

Table 1 Evaluated kinetic models.

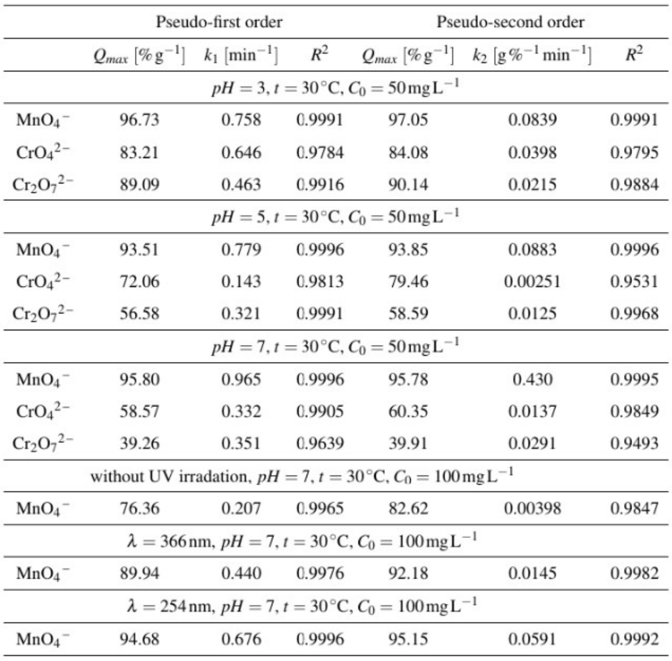

	Pseudo-first order			Pseudo-second order		
	Q_{max} [$\% \, g^{-1}$]	k_1 [min^{-1}]	R^2	Q_{max} [$\% \, g^{-1}$]	k_2 [$g \, \%^{-1} \, min^{-1}$]	R^2
$pH = 3, t = 30\,°C, C_0 = 50\,mg\,L^{-1}$						
MnO_4^-	96.73	0.758	0.9991	97.05	0.0839	0.9991
CrO_4^{2-}	83.21	0.646	0.9784	84.08	0.0398	0.9795
$Cr_2O_7^{2-}$	89.09	0.463	0.9916	90.14	0.0215	0.9884
$pH = 5, t = 30\,°C, C_0 = 50\,mg\,L^{-1}$						
MnO_4^-	93.51	0.779	0.9996	93.85	0.0883	0.9996
CrO_4^{2-}	72.06	0.143	0.9813	79.46	0.00251	0.9531
$Cr_2O_7^{2-}$	56.58	0.321	0.9991	58.59	0.0125	0.9968
$pH = 7, t = 30\,°C, C_0 = 50\,mg\,L^{-1}$						
MnO_4^-	95.80	0.965	0.9996	95.78	0.430	0.9995
CrO_4^{2-}	58.57	0.332	0.9905	60.35	0.0137	0.9849
$Cr_2O_7^{2-}$	39.26	0.351	0.9639	39.91	0.0291	0.9493
without UV irradiation, $pH = 7, t = 30\,°C, C_0 = 100\,mg\,L^{-1}$						
MnO_4^-	76.36	0.207	0.9965	82.62	0.00398	0.9847
$\lambda = 366\,nm, pH = 7, t = 30\,°C, C_0 = 100\,mg\,L^{-1}$						
MnO_4^-	89.94	0.440	0.9976	92.18	0.0145	0.9982
$\lambda = 254\,nm, pH = 7, t = 30\,°C, C_0 = 100\,mg\,L^{-1}$						
MnO_4^-	94.68	0.676	0.9996	95.15	0.0591	0.9992

UiO-66-NH_2 has semiconductive properties due to its favourable band gap energy. The energy was determined from UV/VIS spectra by Tauc plot analysis. Both direct and indirect transitions were calculated with values being 2.82 eV and 2.52 eV, respectively. Arising from this fact, photocatalytic degradation of MnO_4^- was investigated. Adsorption capacity increased significantly under 254 nm UV irradiation compared to no UV irradiation (see Table 1).

The pseudo-first and pseudo-second order models were applied to the obtained data with the aim of a better understanding of the adsorption kinetics. Determined values of the maximum adsorption capacity, i.e. capacity in equilibrium and corresponding rate constants, are shown in Table 1. Due to the higher value of R^2 the pseudo-first kinetic model provided a better description of adsorption kinetics. This indicates that the prevailing mechanism is dependent on the presence of accessible adsorption sites, namely the positively charged amino groups. To confirm this mechanistic hypothesis, a new adsorbent, UiO-67-NH_2, was synthesised and tested. Pseudo-first order Q_{max} values (see Figure 1) confirmed that the larger pores present in UiO-67-NH_2 do not have a positive impact on the adsorbed amount of the pollutant.

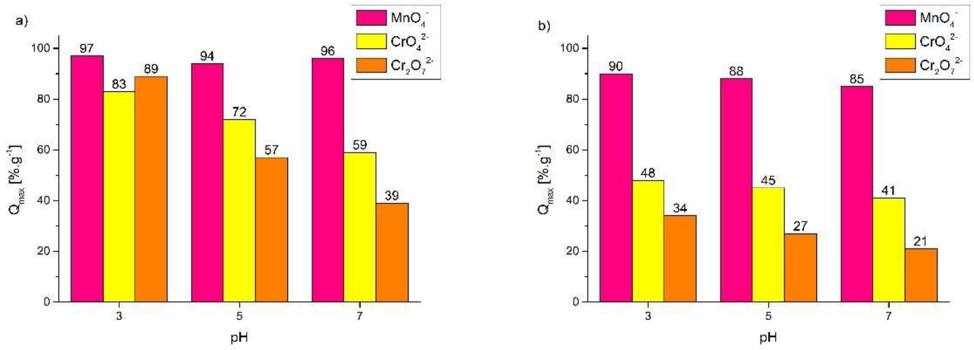

Figure 1 Comparison of maximum adsorption capacity of anionic pollutants of a) UiO-66-NH_2 and b) UiO-67-NH_2.

After successful synthesis, characterization, and adsorption studies of anionic heavy metals MnO_4^-, CrO_4^{2-} and $Cr_2O_7^{2-}$, findings indicated that in acidic conditions, the adsorption was more efficient compared to neutral *pH* conditions. There was an evident correlation between decreasing *pH* and increasing adsorption capacity. Similarly, UV irradiation had an influence on the amount of adsorbate (MnO_4^-) left in solution. Decreasing the UV wavelength led to a reduction in the amount of anionic metal left in the aqueous phase. Higher adsorbate concentration led to a higher amount of pollutant adsorbed. Insight into the occurring mechanism was provided, indicating that the accessible amino groups have direct impact on the adsorption.

Acknowledgements

This work was supported by the projects APVV SK-CZ-RD-21–0068, LUASK22049 (INTER-EXCELLENCE II, MŠMT) and VEGA 1/0058/25.

References

[1] Y. Wen, P. Zhang, V. K. Sharma, X. Ma, H. - C. Zhou, Cell Rep. Phys. Sci. **2** (2021) 100348.
[2] C. L. Luu; T. T. V. Nguyen, T. Nguyen, T. C. Hoang, Adv. Nat. Sci.: Nanosci. Nanotechnol. **6** (2015) 025004.

Sodium Poly(heptazine imides)-Based Adsorbents for CO_2 Capture

P. Ouro[a], D. Pereira[a], M. Sardo[a], I. Krivtsov[b], I. Marin-Montesinos[a], L. Mafra[a], and M. Ilkaeva[b]*

[a]Department of Chemistry, CICECO – Aveiro Institute of Materials, University of Aveiro, Campus Universitário de Santiago, 3810-193 Aveiro, Portugal
[b]Department of Chemical and Environmental Engineering, University of Oviedo, 33006 Oviedo, Spain

*ilkaevamarina@uniovi.es

A new class of polymeric carbon nitrides (PCNs), called poly(heptazine imides) (PHIs), has shown great potential for CO_2 capture. These materials are appealing due to their (i) cost-effectiveness, (ii) ability to withstand temperatures up to 450°C, and (iii) resistance to moisture - qualities that set them apart from metal-organic frameworks (MOFs), for example, which can collapse when exposed to humidity. PHIs can be synthesized quickly and easily using a molten-salt method (Figure 1), and they feature a microporous structure that allows for a high CO_2 adsorption capacity of about 4 mmol/g, according to our initial findings [1]. Despite these advantages, the semi-crystalline nature of PHIs has complicated our efforts to understand how they absorb CO_2. To clarify the nature of CO_2 capture in PHIs, advanced techniques such as solid-state nuclear magnetic resonance (ssNMR) and X-ray absorption spectroscopy (XAS) were employed, among others. By probing local atomic environments, ssNMR allowed for the identification of specific adsorbate-adsorbent interactions. Then, XAS revealed how the presence of CO_2 affected PHIs' structural cations and their local environment. By generating such an in-depth understanding of PHI and its interaction with CO_2, this study intends to pave the way for a new generation of PHI-based adsorbents better suited for carbon capture applications.

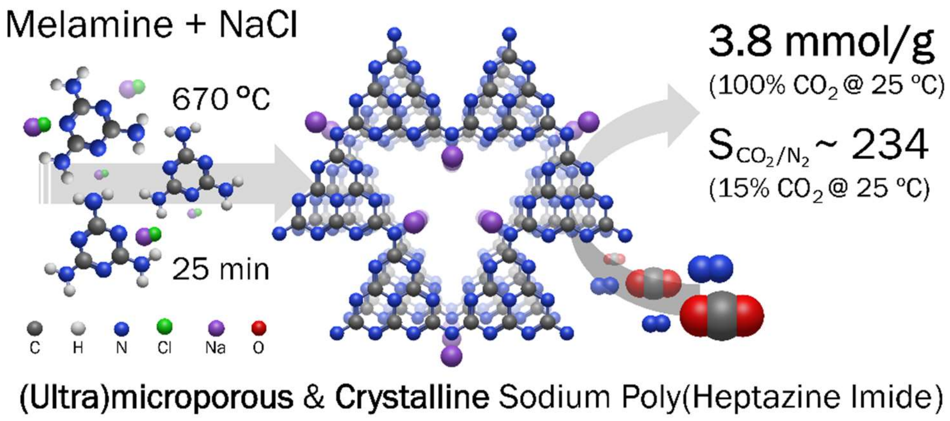

Figure 1 Overview of sodium PHI (NaPHI), its synthesis, structural properties, and performance in CO_2 capture.

Acknowledgements

The authors acknowledge Spanish Ministry of Science, Innovation and Universities, State Research Agency and the FEDER (Projects PID2023-148187OB-I00) for financing this work. This work was developed within the scope of the project CICECO Aveiro Institute of Materials, UID/50011/2025 (DOI 10.54499/UID/50011/2025) and LA/P/0006/2020 (DOI 10.54499/LA/P/0006/2020), financed by national funds through the FCT/MCTES (PIDDAC). The NMR spectrometers are part of the National NMR Network (PTNMR) and are partially supported by Infrastructure Project 022161 (cofinanced by FEDER through COMPETE 2020, POCI and PORL and FCT through PIDDAC). MI also acknowledges the Spanish Ministry of Science, Innovation and Universities for the “Beatriz Galindo” Scholarship (MU-23-BG22/00145).

References

[1] P. Ouro, Á. Cuevas, J. Liessem, D. Mitoraj, R. Beranek, E. Díaz, S. Ordóñez, I. Marin-Montesinos, D. Pereira, M. Sardo, I. Krivtsov, L. Mafra, M. Ilkaeva, ChemSusChem **18 (**2025).

Ceramic Membrane Filtration for Winery Wastewater Reclamation: Experimental Performance and Economic Assessment

V. E. Mendes[a,b,c*], D. Morais[a,d], M. Rio[a,d], J. A. Peres[d], M. S. Lucas[d], B. M. Esteves[a,e]

[a]Fraunhofer Portugal AWAM, Régia Douro Park – Parque de Ciência e Tecnologia, 5000-033 Vila Real, Portugal
[b]LSRE-LCM – Laboratory of Separation and Reaction Engineering - Laboratory of Catalysis and Materials, Faculty of Engineering, University of Porto, Rua Dr. Roberto Frias, Porto, 4200-465, Portugal
[c]ALiCE – Associate Laboratory in Chemical Engineering, Faculty of Engineering, University of Porto, Rua Dr. Roberto Frias, Porto, 4200-465, Portugal
[d]Chemistry Centre Vila Real (CQVR), Department of Chemistry, Universidade de Trás-os-Montes e Alto Douro, UTAD, Quinta de Prados, Vila Real 5000-801, Portugal
[e]Centre for the Research and Technology of Agroenvironmental and Biological Sciences, CITAB, Inov4Agro, Universidade de Trás-os-Montes e Alto Douro, UTAD, Quinta de Prados, 5000-801 Vila Real, Portugal

*vanessa.mendes@fraunhofer.pt

The increasing pressure on water resources has raised interest in the use of reclaimed water within industrial sectors. Winemaking, for example, generates substantial volumes of winery wastewater (WWW) characterized by seasonal flow rates, elevated organic loads, nutrients, suspended solids, and recalcitrant compounds such as polyphenols [1]. However, achieving regulatory compliance for water reuse remains challenging, requiring treatment solutions that can adapt to wastewater variability while meeting quality standards at acceptable costs. This study evaluates the applicability of ceramic membrane filtration for WWW treatment and reuse in the Douro Valley, Portugal, focusing on the performance limits of ultrafiltration (UF) and nanofiltration (NF).

On-site aerobic biological treatment effectively removed biodegradable organic matter, consistently achieving BOD_5 reductions above 90%, producing effluents compliant with discharge regulations, however unsuitable for non-potable reuse (e.g., irrigation, urban uses) according to the Portuguese Decree-Law No. 119/2019. When applied as a polishing step, UF membranes with a nominal pore size of 10 nm enabled the production of reuse-compliant permeates from biologically treated effluents with moderate residual loads (COD ≤ 550, $BOD_5 \leq 120$ mg O_2 L^{-1}), achieving quality suitable for vine irrigation (Figure 1). Stable hydraulic performance was maintained, with permeate fluxes of approximately 140 L m^{-2} h^{-1}, alongside effective removal of suspended solids, nutrients, and *Escherichia coli*. For effluents with higher residual organic loads (COD < 1000, $BOD_5 <$ 500 mg O_2 L^{-1}), tighter UF and NF membranes (5 nm, 5 kDa, and 1 kDa) enhanced overall organic removal; nonetheless, permeate quality was constantly limited by elevated BOD_5 residual levels.

A membrane-based treatment cascade was assessed as an alternative to biological processes, targeting the control of the biodegradable organic fraction (BOD_5) from raw winery wastewater. The configuration UF (10 nm) → NF (0.9 nm) → NF (low cut-off 400 Da) achieved substantial reductions in electrical conductivity and BOD_5 (>85 %); nevertheless, final BOD_5 concentrations (~400 mg O_2 L^{-1}) remained above reuse thresholds. These findings confirm that membrane filtration improves effluent quality and process robustness but cannot replace biological oxidation for the removal of biodegradable organic matter. Pre-filtration significantly mitigated fouling and enhanced flux stability, whereas the final low-cut-off NF step resulted in marked permeability losses with limited additional treatment benefit.

An economic assessment of a ceramic membrane system – designed for an average flow rate of 70 m^3 day^{-1} – estimated operating costs of approximately 1.6 € m^{-3}, with energy consumption accounting for the largest share (37 %). Overall, the results demonstrate that ceramic membranes constitute a technically viable and economically competitive complementary, rather than standalone, technology for enabling WWW reuse within sustainable and circular water management strategies.

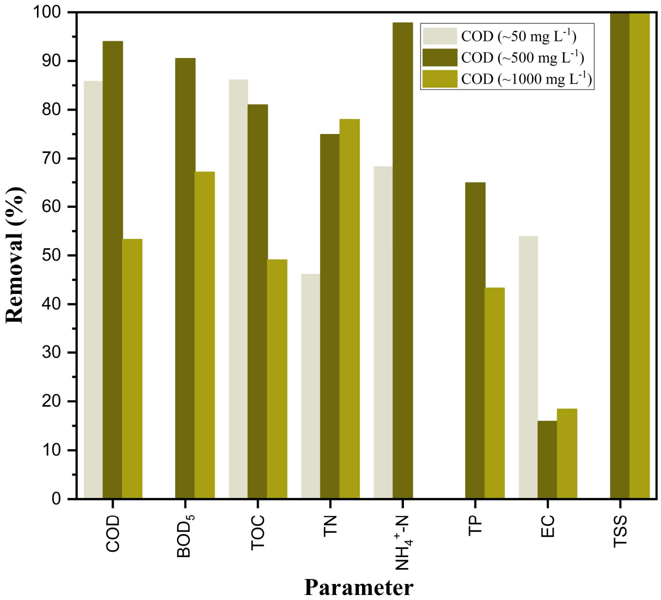

Figure 1 Removal efficiencies of selected parameters for WWW samples with different initial COD when treated using UF 10 nm ceramic membrane.

Acknowledgements

This work was financially supported by the project “Vine and Wine Portugal – Driving Sustainable Growth Through Smart Innovation” with reference number C644866286–00000011, co-financed by the Recovery and Resilience Plan and NextGeneration EU Funds, and by National Funds by FCT – Portuguese Foundation for Science and Technology, under the projects UID/04033/2025: Centre for the Research and Technology of Agro-Environmental and Biological Sciences, UID/ 00616/2025: Chemistry Centre Vila Real (CQVR https://doi.org/10.54499/UID/00616/2025) and LA/P/0126/2020 (https://doi.org/10.54499/LA/P/0126/2020).

References

[1] L. A. Ioannou, G. L. Puma, D. Fatta-Kassinos, J. Hazard. Mater. **286** (2015) 343–368.

Surface Chemistry-Driven Adsorption Kinetics of Co(II) Ions and Congo Red on Schiff Base-Functionalized MIL-101(Fe)

Ľ. Zauška[a,b]*, P. Pillárová[c], M. Almáši[a].

[a]Department of Inorganic Chemistry, Faculty of Science, P. J. Šafárik University, Moyzesova 11, SK-041 01, Košice, Slovak Republic
[b]BovaChem s.r.o, Laboratory-1, Kirejevská 22, SK-979 01, Rimavská Sobota, Slovak Republic
[c]Institute of Experimental Physics, Slovak Academy of Sciences, Watsonova 47, SK-041 01, Košice, Slovak Republic

*lubos.zauska@upjs.sk

Metal–organic frameworks (MOFs) have emerged as advanced adsorbent materials for water remediation due to their high porosity, modular chemistry, and structural stability. Among them, MIL-101(Fe) derivatives are particularly attractive because of their large mesoporous cages and robust framework. In this contribution, we present a detailed kinetic, thermodynamic, and mechanistic study of cobalt(II) ions and the azo dye Congo red adsorption on pristine MIL-101(Fe)-NH_2 and its Schiff base–modified analogue, MIL-101(Fe)-Pyr.

The parent MIL-101(Fe)-NH_2 was synthesized solvothermally and subsequently post-synthetically modified via condensation of surface amino groups with 2-pyridinecarboxaldehyde, yielding imine-containing coordination sites capable of chelating metal ions. Structural integrity after modification was confirmed by PXRD, which showed preservation of the MIL-101 topology, while FT-IR and XPS analyses evidenced the formation of C=N bonds and pyridinic nitrogen species. Nitrogen adsorption–desorption measurements revealed a decrease in BET surface area from 1359 $m^2\ g^{-1}$ for MIL-101(Fe)-NH_2 to 234 $m^2\ g^{-1}$ for MIL-101(Fe)-Pyr, indicating partial pore blocking by organic moieties; nevertheless, functionalization significantly altered adsorption performance.

Adsorption isotherms demonstrated that Co(II) uptake was strongly enhanced by Schiff base functionalization. The maximum adsorption capacity for Co(II) increased from 1.01 $mg\ g^{-1}$ for MIL-101(Fe)-NH_2 to 3.74 $mg\ g^{-1}$ for MIL-101(Fe)-Pyr, accompanied by a substantial increase in the Freundlich constant ($K_f = 6.71$ for MIL-101(Fe)-Pyr vs. 0.28 for MIL-101(Fe)-NH_2), indicating stronger affinity toward metal ions. In contrast, Congo red adsorption capacities were comparable for both materials ($\approx$2.1–2.7 $mg\ g^{-1}$), suggesting that dye adsorption is governed primarily by pore accessibility and electrostatic interactions rather than specific coordination.

Kinetic experiments revealed rapid adsorption within the first 30 minutes for all systems, followed by gradual equilibration. The pseudo-second-order (PSO) model provided the best overall fit (see Figure 1), with correlation coefficients R^2 up to 0.998, indicating that chemisorption plays a dominant role, particularly for Co(II) ions on MIL-101(Fe)-Pyr. The calculated equilibrium adsorption capacity (q_e) for Co(II) reached 61.9 $mg\ g^{-1}$ for the Schiff base–modified material, compared to 60.7 $mg\ g^{-1}$ for the pristine MOF. Boyd diffusion analysis further suggested that external mass transfer is a rate-limiting step during the initial adsorption stage, while intraparticle diffusion becomes relevant at longer contact times.

Thermodynamic parameters derived from Van't Hoff analysis (see Figure 2) showed that Co(II) adsorption on MIL-101(Fe)-Pyr is spontaneous and exothermic ($\Delta G° \approx -27\ kJ\ mol^{-1}$, $\Delta H° = -14.6\ kJ\ mol^{-1}$), consistent with coordination bond formation between cobalt ions and imine/pyridyl sites. Conversely, Co(II) adsorption on MIL-101(Fe)-NH_2 exhibited positive $\Delta G°$ values, indicating less favorable binding. Congo red adsorption was spontaneous for both materials, with $\Delta G°$ values ranging from −15 to −20 $kJ\ mol^{-1}$, reflecting mixed physical–chemical interactions.

Reusability tests over five adsorption–desorption cycles confirmed good structural stability and retention of adsorption capacity, supported by post-cycle PXRD analysis. Overall, this study demonstrates that targeted surface functionalization of MIL-101(Fe) enables precise tuning of adsorption kinetics and mechanisms, transforming a high-surface-area MOF into a chemically selective adsorbent for heavy metal ions while maintaining effective removal of organic dyes.

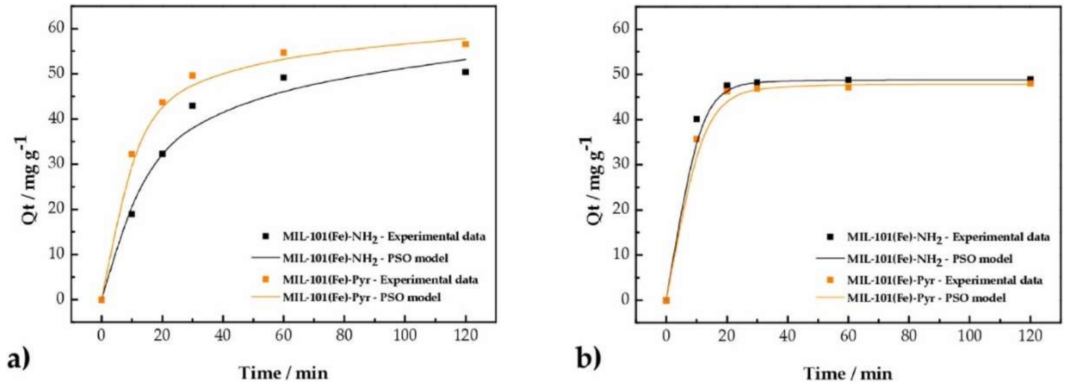

Figure 1 Pseudo-second-order kinetic fitting of Co(II) ions (a) and Congo red (b) adsorption on MIL-101(Fe)-NH₂ and MIL-101(Fe)-Pyr.

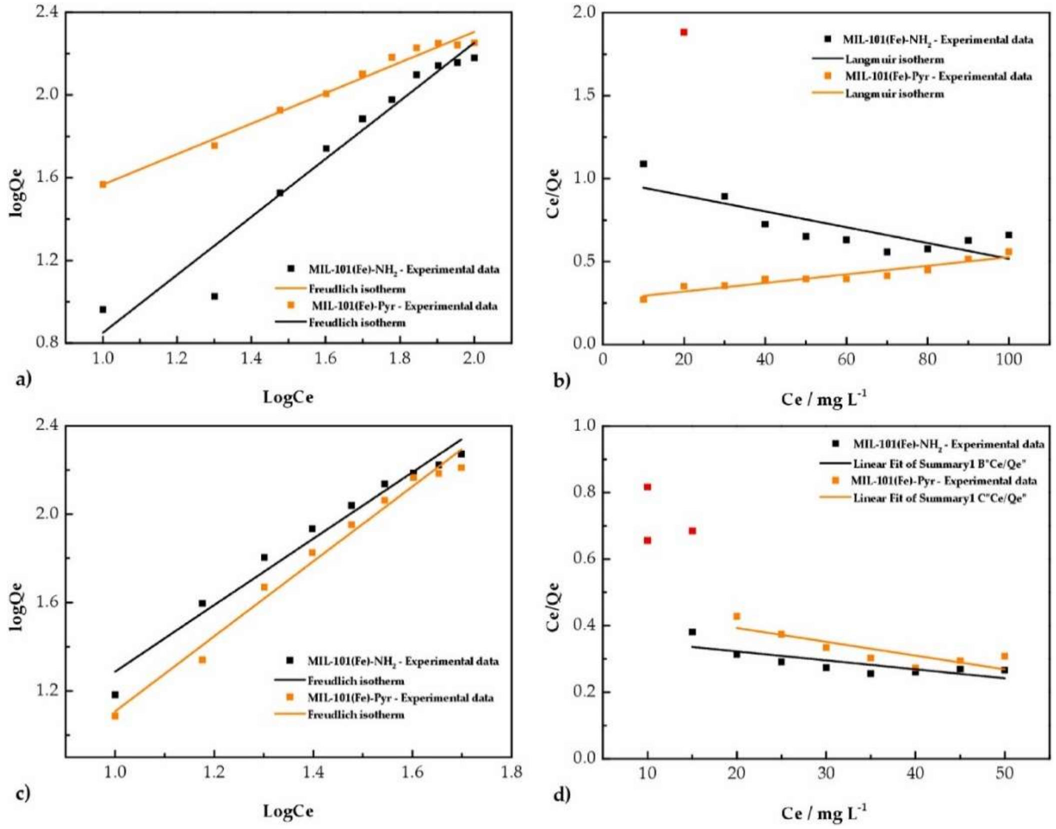

Figure 2 Comparison of Freundlich and Langmuir adsorption models for Co(II) ions and Congo red on pristine and Schiff base-modified MIL-101(Fe), highlighting heterogeneous surface adsorption and deviations from ideal monolayer behavior.

Acknowledgements

This work was supported by VEGA 1/0058/25.

References

[1] Ľ. Zauška, P. Pillárová, D. Volavka, E. Kinnertová, J. Bednarčík, J. Brus, V. Hornebecq, M. Almáši, Microp. Mesop. Mater. **386** (2025) 113493.

Synthesis of Porous g-C_3N_4@MOF Composites for the Capture of Toxic Volatile Compounds

Ľ. Zauška[a,b]*, M. Almáši[a]

[a]Department of Inorganic Chemistry, Institute of Chemistry, Faculty of Science, Pavol Jozef Šafárik University
in Košice, Moyzesova 11, 040 01 Košice, Slovak Republic
[b]BovaChem s.r.o, Laboratory-1, Kirejevská 22, SK-979 01, Rimavská Sobota. Slovak Republic

*lubos.zauska@upjs.sk

The increasing occurrence of toxic volatile compounds in industrial emissions and indoor environments has stimulated the development of advanced porous materials capable of their efficient capture. Hybrid systems combining chemically and structurally complementary components represent a promising approach, as they allow tailoring of pore architecture, surface chemistry, and adsorption-active sites within a single material platform. In this context, composites based on graphitic carbon nitride and metal–organic frameworks (g-C_3N_4@MOF) have attracted growing interest due to the synergistic combination of chemical stability, nitrogen-rich surfaces, and well-defined porosity.

Graphitic carbon nitride was selected as a robust matrix material owing to its thermal and chemical stability and its ability to provide nitrogen-containing functional sites. In this work, porous g-C_3N_4 was prepared via thermal condensation of melamine–urea crystalline precursors. This precursor system enabled homogeneous molecular mixing and promoted gas evolution during calcination, resulting in a layered g-C_3N_4 framework with developed mesoporosity and enhanced surface accessibility. The obtained g-C_3N_4 served as a suitable structural and chemical platform for the formation of hybrid composites.

Porous g-C_3N_4@MOF composites were synthesized using a controlled in situ strategy, in which g-C_3N_4 was directly introduced into the MOF synthesis medium. This approach enabled nucleation and growth of MOF crystals in close contact with the g-C_3N_4 surface, promoting intimate interfacial interactions and avoiding simple physical mixing. Three representative MOF structures were employed, namely HKUST-1 (Figure 1), MIL-100(Cr), and MIL-100(Fe), selected for their distinct metal centers, pore architectures, and relevance for gas adsorption applications. The MOF content in the composites was systematically varied in the range of approximately **10–30 wt.%**, allowing evaluation of the influence of MOF loading on the structural and textural properties of the hybrids.

Structural characterization confirmed the successful formation of graphitic carbon nitride and the preservation of the crystalline structure of the incorporated MOFs. The presence of g-C_3N_4 did not suppress MOF crystallization, while the in situ synthesis ensured uniform distribution of MOF particles within and on the surface of the g-C_3N_4 matrix. Morphological analysis indicated that MOF crystallites with typical sizes in the sub-micrometer to low micrometer range were well dispersed throughout the composite, with increasing MOF content leading to higher surface coverage of g-C_3N_4 without compromising the overall structural integrity of the material.

Textural analysis revealed that the g-C_3N_4@MOF composites exhibit hierarchical porosity arising from the combination of mesopores associated with the g-C_3N_4 framework and micropores characteristic of the MOF structures. The specific surface areas of the composites increased with increasing MOF content and typically fell within the range of ~200 to 800 $m^2\,g^{-1}$, depending on the type and fraction of the MOF phase. Pore size distribution analysis confirmed the coexistence of micro- and mesoporous domains, with their relative contribution governed by the nature of the incorporated MOF.

Incorporation of MOFs into the g-C_3N_4 matrix also modified the surface chemistry of the composites by introducing coordinatively unsaturated metal sites in addition to the nitrogen-rich functionalities of g-C_3N_4. This combination of structural and chemical features provides favorable conditions for interactions with volatile guest molecules. Preliminary adsorption experiments with selected toxic volatile compounds indicated enhanced uptake compared to pristine g-C_3N_4, with adsorption behavior strongly dependent on MOF identity and loading, suggesting contributions from both physical adsorption within the porous network and specific surface interactions.

Overall, the presented in situ synthetic strategy offers a versatile and modular route to porous g-C_3N_4@MOF composites with tunable composition, porosity, and surface functionality. By adjusting the MOF type and content within the 10–30 wt.% range, hybrid materials with tailored structural properties can be obtained, providing a robust platform for further systematic studies focused on adsorption-based capture of toxic volatile compounds under environmentally relevant conditions.

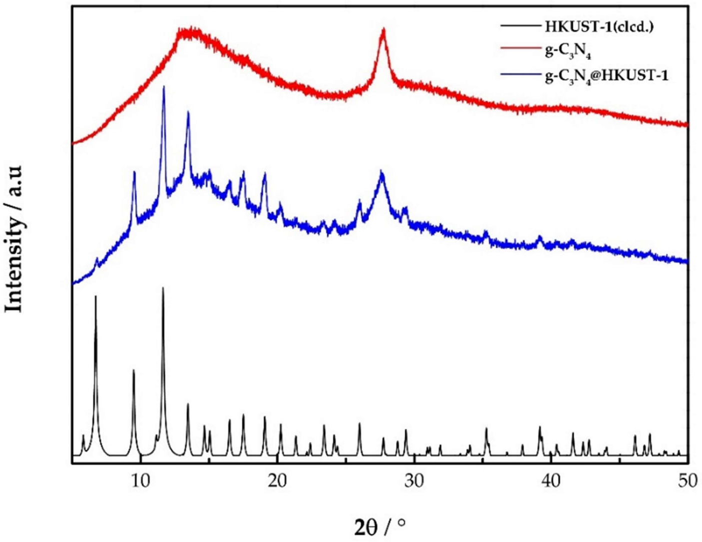

Figure 1 PXRD patterns of pristine g-C_3N_4, crystalline HKUST-1, and the g-C_3N_4@HKUST-1 composite. The composite exhibits characteristic reflections of HKUST-1 together with the broad diffraction features of g-C_3N_4, confirming the successful formation of a hybrid material while preserving the crystalline structure of the MOF phase.

Acknowledgements

This work was supported by VEGA 1/0058/25.

References

[1] Y. Gong, X. Zhao, H. Zhang, B. Yang, K. Xiao, T. Guo, J. Zhang, H. Shao, Y. Wang, G. Yu, Appl. Catal. B: Environ. **233** (2018) 35–45.

[2] C. Cheng, H. Jing, H. Ji, Y. Li, L. Ma, J. Hao, J. Colloid Interface Sci. **678** (2025) 1112–1121.

ENVIRONMENTAL ADSORPTION AND SEPARATION

Study of Synergistic Effects in MOF/Carbon Composites for VOC Capture: Comparative Sdsorption Behavior of Pristine UiO-66, HPCM, and their Hybrid

A. Migasová[a], M.Želinská[a]*, T. Zelenka[b], M. Almáši[a]

[a]Department of Inorganic Chemistry, Institute of Chemistry, Faculty of Science, Pavol Jozef Šafárik University in Košice, Moyzesova 11, 040 01 Košice, Slovak Republic
[b]Department of Chemistry, Faculty of Science, University of Ostrava, 30. Dubna 22, 702 00 Ostrava, Czech Republic

*milica.zelinska@gmail.com

Rapid industrialization and urban development have led to a significant increase in atmospheric pollution, creating an urgent demand for efficient technologies capable of removing hazardous contaminants from air streams. Among the available approaches, gas-phase purification based on adsorption has attracted considerable attention due to its low energy consumption, operational simplicity, and cost-effectiveness. However, conventional adsorbents such as activated carbon and zeolites frequently suffer from limited recyclability, structural instability, and performance losses under practical conditions [1]. In this regard, metal–organic frameworks (MOFs) and their composites have emerged as promising alternatives. Their exceptionally high surface areas, tunable pore geometries, and chemically tailorable compositions enable the rational design of specific binding sites and enhanced interactions with target molecules [2]. These features are particularly advantageous for removing volatile organic compounds (VOCs), high-vapor-pressure pollutants widely emitted from industrial activities, vehicles, solvents, paints, and consumer products. Many exhibit significant toxicity and contribute to smog formation and secondary aerosol generation, leading to adverse respiratory and neurological effects upon prolonged exposure. Consequently, the development of efficient, selective, and regenerable adsorbents for VOC capture remains a pressing environmental priority [3,4].

Here, three sorbents—pristine UiO-66, hierarchically porous carbon (HPCM), and a UiO-66@HPCM composite—were synthesized and compared to assess the influence of MOF–carbon integration on VOC capture. The composite was prepared via repeated in situ growth of UiO-66 on the carbon support to increase MOF loading. All materials were obtained using solvothermal synthesis and characterized by PXRD, SEM, BET surface area analysis, TGA, and FTIR prior to adsorption testing. Vapor uptake was evaluated at 25 °C in sealed chambers as an initial screening of twelve VOCs (methanol, formaldehyde, pyridine, benzene, toluene, aniline, DMF, benzyl bromide, benzaldehyde, salicylaldehyde, dimethyl adipate, and triethyl phosphate).

All three adsorbents followed nearly comparable uptake behavior over time for a given compound, suggesting similar adsorption mechanisms, while differences were reflected mainly in the achieved capacities. Near-saturation was observed only for methanol, toluene, and benzene within the experimental time window, while most other compounds showed a continuous increase in uptake without reaching equilibrium. Pyridine showed a distinct uptake pattern, suggesting a more complex interaction or partial chemisorption. Across the series, small, low-boiling and high-vapour-pressure molecules reached the highest capacities, whereas larger and less volatile compounds exhibited lower uptake. Among the tested materials, carbon provided the highest adsorption capacities for most VOCs, particularly for methanol (13.7 $\mathrm{mmol{\cdot}g^{-1}}$), formaldehyde (8.1 $\mathrm{mmol{\cdot}g^{-1}}$), and pyridine (6.95 $\mathrm{mmol{\cdot}g^{-1}}$). The UiO-66@HPCM composite generally exhibited intermediate performance, frequently exceeding pristine UiO-66 but not uniformly for all adsorbates. Pristine UiO-66 showed the lowest overall capacities, reaching ~6.5 $\mathrm{mmol{\cdot}g^{-1}}$ for methanol and formaldehyde, moderate values of approximately 1.9–3.5 $\mathrm{mmol{\cdot}g^{-1}}$ for pyridine, benzene, toluene, and DMF, and below 1 $\mathrm{mmol{\cdot}g^{-1}}$ for compounds with higher boiling points (≈178–230 °C), including aniline, benzaldehyde, salicylaldehyde, benzyl bromide, dimethyl adipate, and triethyl phosphate, reflecting their lower volatility and consequently reduced vapor-phase concentration.

These results demonstrate the beneficial effect of combining MOF microporosity with carbon hierarchical porosity and provide a basis for further systematic studies of adsorption mechanisms, regenerability, and temperature-dependent behavior.

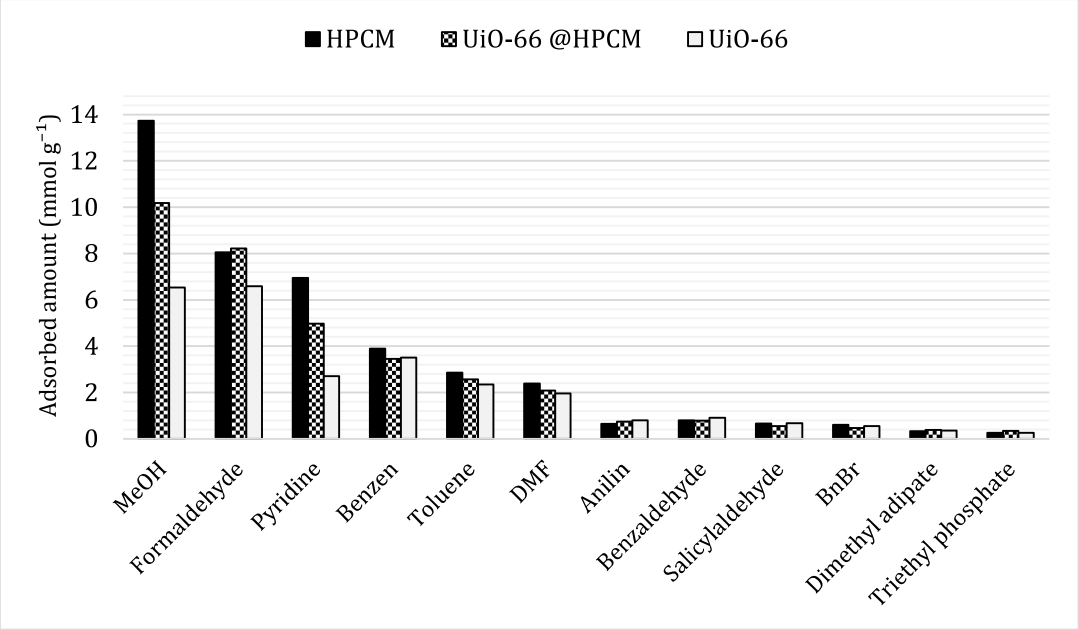

Figure 1 Comparison of VOC adsorption capacities after 6 h exposure on UiO-66, UiO-66@HPCM, and HPCM.

Acknowledgements

This work was supported by the Ministry of Education, Science, Research and Sport of the Slovak Republic, VEGA project no. 1/0058/25.

References

[1] R. Wen, E. Barea, J. A. R. Navarro, Microp. Mesop. Mater. **305** (2020) 110331.
[2] L. Li, J. Song, X. Yao, J. Cent. South Univ. **19** (2012) 3530–3539.
[3] B. Siu, A. R. Chowdhury, Z. Yan, S. M. Humphrey, T. Hutter, Coord. Chem. Rev. **485** (2023) 215119.
[4] S. Rehman, X. Zheng, M. I. Aujla, T. Mehmood, Chem. Eng. J. **505** (2025) 159257.

ENVIRONMENTAL ADSORPTION AND SEPARATION

Performance Comparison of MIL-101(Cr), MIL-101/C Composites, and Porous Carbon for VOC Adsorption

M. Želinská[a]*, T. Zelenka[b], M. Almáši[a]

[a]Department of Inorganic Chemistry, Institute of Chemistry, Faculty of Science, Pavol Jozef Šafárik University in Košice, Moyzesova 11, 040 01 Košice, Slovak Republic
[b]Department of Chemistry, Faculty of Science, University of Ostrava, 30. Dubna 22, 702 00 Ostrava, Czech Republic

*milica.zelinska@gmail.com

Volatile organic compounds (VOCs) are highly volatile organic pollutants originating mainly from anthropogenic sources that readily evaporate under ambient conditions and pose significant environmental and health risks due to their toxicity, carcinogenicity, and contribution to atmospheric smog formation, making their efficient removal from air streams a critical global challenge [1,2]. Among available abatement technologies, adsorption is considered one of the most energy-efficient and practical approaches, however, conventional adsorbents such as activated carbons and zeolites often suffer from limited stability and regenerability [3]. In contrast, metal–organic frameworks (MOFs) and their composite materials offer high surface areas, tunable porosity, and chemically functionalizable structures, making them promising candidates for selective VOC capture [4].

Within this context, chromium-based MIL-101 and its carbon-based composites were selected as high-porosity and structurally robust adsorbents for VOC capture. Accordingly, MIL-101(Cr), hierarchically porous carbon (HPCM), and a MOF–carbon composite (prepared by *in situ* growth of MIL-101 in the carbon support) were synthesized and fully characterized by PXRD, SEM, BET surface area analysis, TGA, and FTIR to confirm their successful formation and structure and to subsequently study structure–adsorption property relationships.

Their adsorption performance toward representative VOCs—methanol, formaldehyde, benzene, toluene, pyridine, DMF, aniline, benzaldehyde, salicylaldehyde, benzyl bromide, dimethyl adipate, and triethyl phosphate—was systematically evaluated under closed-box conditions at 25 °C as a preliminary screening study to identify adsorption trends and select the most promising sorbents. For each adsorbate, the three materials displayed nearly identical uptake profiles, indicating comparable adsorption mechanisms, while differing mainly in absolute capacity. Kinetic analysis showed that several systems reached apparent equilibrium within the experimental time frame (benzene, toluene, methanol, and pyridine), whereas formaldehyde and the remaining compounds exhibited a continuous increase over 6 h without clear saturation. Because the experiments were conducted in sealed chambers, the measured uptake depended not only on adsorbent affinity but also on the rate at which vapor accumulated and saturated the space, meaning that the observed kinetics were influenced by both vapor availability and adsorption. Although no universal relationship between polarity and kinetic behavior was identified, comparison of the maximum uptake values after 6 h revealed clear capacity trends: small, low-boiling and highly volatile molecules exhibited the highest adsorption, whereas bulkier and less volatile species showed only minimal uptake, indicating a stronger dependence on molecular size and volatility than on polarity alone. Quantitatively, the adsorption performance consistently followed the order MIL-101 > MIL-101/C > HPCM for all tested compounds, identifying MIL-101 as the most efficient adsorbent. These preliminary results provide a basis for further systematic investigations, including thermodynamic analysis, adsorbent regenerability and cycling stability, evaluation of vapor concentration effects, and temperature-dependent measurements at 35 °C and 45 °C to elucidate adsorption mechanisms under different conditions.

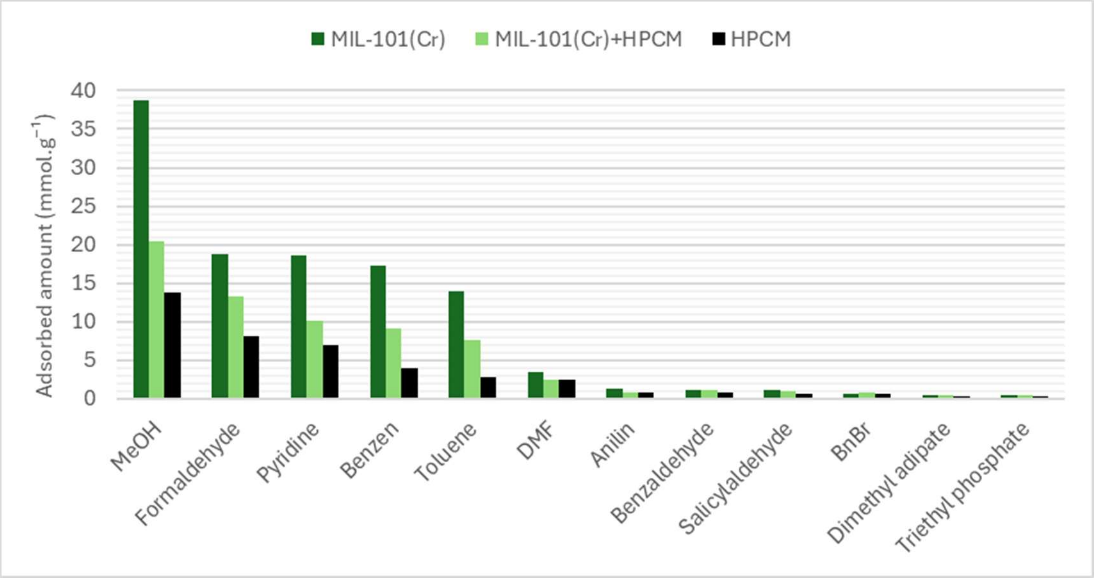

Figure 1 Comparison of VOC adsorption capacities after 6 h exposure on MIL-101(Cr), MIL-101(Cr)/HPCM, and HPCM.

Acknowledgements

This work was supported by the Ministry of Education, Science, Research and Sport of the Slovak Republic, VEGA project no. 1/0058/25.

References

[1] R. Wen, E. Barea, J. A. R. Navarro, Microp. Mesop. Mater. **305** (2020) 110331.
[2] L. Li, J. Song, X. Yao, J. Cent. South Univ. **19** (2012) 3530–3539.
[3] B. Siu, A. R. Chowdhury, Z. Yan, S. M. Humphrey, T. Hutter, Coord. Chem. Rev. **485** (2023) 215119.
[4] S. Rehman, X. Zheng, M. I. Aujla, T. Mehmood, Chem. Eng. J. **505** (2025) 159257.

Adsorption Behavior of Volatile Organic Vapors on HKUST-1 under Confined Conditions

N. Vargová[a], M. Želinská[a]*, T. Zelenka[b], M. Almáši[a]

[a]Department of Inorganic Chemistry, Institute of Chemistry, Faculty of Science, Pavol Jozef Šafárik University in Košice, Moyzesova 11, 040 01 Košice, Slovak Republic
[b]Department of Chemistry, Faculty of Science, University of Ostrava, 30. Dubna 22, 702 00 Ostrava, Czech Republic

*milica.zelinska@gmail.com

HKUST-1 ($Cu_3(BTC)_2$, MOF-199) is one of the most representative members of the metal–organic framework (MOF) family, which comprises crystalline porous materials constructed from metal ions or clusters connected by organic linkers and is distinguished by high surface area, tunable porosity, and versatile surface chemistry, making them highly attractive for adsorption-based environmental applications. The structure of HKUST-1 is composed of dicopper ‘paddle-wheel’ units bridged by benzene-1,3,5-tricarboxylate ligands, forming a three-dimensional microporous framework with accessible Cu^{2+} open metal sites after activation, which are crucial for its adsorption performance [1,2].

HKUST-1 has been intensively explored in environmental applications, including gas separation and air purification, and has recently attracted significant interest as an adsorbent for volatile organic compounds (VOCs) [1,3]. VOCs are organic compounds with high vapor pressure at ambient conditions, originating mainly from industrial processes, solvents, fuels, and building materials, and are recognized as major air pollutants with harmful effects on human health and the environment [1,2]. In this context, MOFs—and HKUST-1 in particular—have emerged as promising alternatives to conventional adsorbents, offering enhanced adsorption capacity and selectivity for VOC capture through rational design of pore structure and surface chemistry [1–3].

Based on these considerations, HKUST-1 was chosen as a representative MOF, and its vapor adsorption performance toward selected VOCs was systematically studied. HKUST-1 was prepared by a conventional solvothermal synthesis and characterized by PXRD, SEM, BET surface area analysis, TGA, and FTIR prior to adsorption measurements. Vapor uptake was evaluated at 25 °C in sealed chambers under constant temperature as an initial screening of twelve volatile organic compounds (methanol, formaldehyde, pyridine, benzene, toluene, aniline, DMF, benzyl bromide, benzaldehyde, salicylaldehyde, dimethyl adipate, and triethyl phosphate). Because the experiments were performed in closed volumes, the adsorption profiles reflect both adsorption on HKUST-1 and the rate of vapor generation. Highly volatile compounds such as methanol and formaldehyde rapidly saturated the gas phase and reached the highest capacities within 1 h, achieving 17.16 and 17.74 mmol g^{-1} after 6 h, respectively. Benzene, toluene, and pyridine also equilibrated quickly and showed clear plateaus with capacities of 7.83, 5.96, and 7.98 mmol g^{-1}. In contrast, higher-boiling and functionalized VOCs (DMF, benzaldehyde, salicylaldehyde, benzyl bromide, aniline, dimethyl adipate, and triethyl phosphate) exhibited slower and continuous uptake without reaching equilibrium within the experimental time (Figure 1a). Pyridine induced a visible color change of HKUST-1 from blue to green, suggesting coordination to Cu^{2+} open metal sites and possible framework modification, indicating that rapid equilibration does not necessarily correspond to purely physisorptive behavior.

Kinetic analysis revealed size-dependent adsorption behavior, small VOCs reached equilibrium rapidly, whereas larger molecules adsorbed more gradually with diffusion-like uptake. The PSO model provided the closest agreement with experimental capacities (Figure 1b). Overall, the adsorption performance correlates with vapor pressure and boiling point, confirming that vapor availability and adsorbate–surface interactions jointly govern uptake under confined conditions.

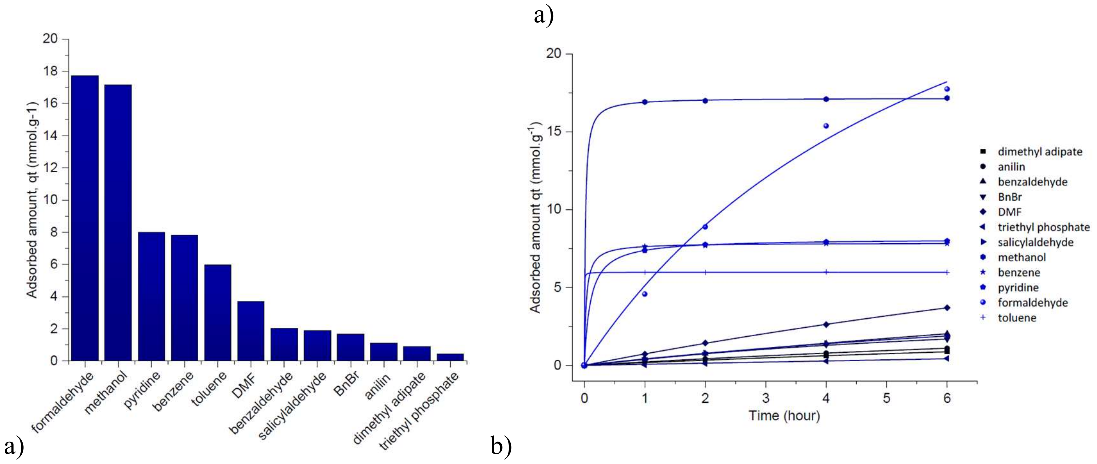

Figure 1 a) Comparison of VOC adsorption capacities after 6 h; b) Time-dependent VOC uptake on HKUST-1.

Acknowledgements

This work was supported by the Ministry of Education, Science, Research and Sport of the Slovak Republic, VEGA project no. 1/0058/25.

References

[1] S. Rehman, X. Zheng, M. I. Aujla, T. Mehmood, Chem. Eng. J. **505** (2025) 159257.
[2] B. Siu, A. R. Chowdhury, Z. Yan, S. M. Humphrey, T. Hutter, Coord. Chem. Rev. **485** (2023) 215119.
[3] R. Chen, Z. Yao, N. Han, X. Ma, L. Li, S. Liu, H. Sun, S. Wang, ACS Omega **5** (2020) 15402–15408.

ENERGY STORAGE AND CONVERSION

Activated and Calcinated MOF-74(Co) as Sulfur Hosts for Li-S Energy Storage Systems

D. Capková[a], M. Želinská[b], A. Straková-Fedorková[c], T. Kazda[d], M. Almáši[b]*

[a]Department of Chemical Sciences, Bernal Institute, University of Limerick, IR-V94 T9PX Limerick, Ireland
[b]Department of Inorganic Chemistry, Institute of Chemistry, Faculty of Science, Pavol Jozef Šafárik University in Košice, Moyzesova 11, SK-040 01 Košice, Slovak Republic
[c]Department of Physical Chemistry, Faculty of Sciences, Pavol Jozef Šafárik University in Košice, Moyzesova 11, SK-041 54, Košice, Slovak Republic
[d]Department of Electrical and Electronic Technology, Faculty of Electrical Engineering and Communication, Brno University of Technology, Technická 10, CZ-616 00, Brno, Czech Republic

*miroslav.almasi@upjs.sk

Lithium–sulfur (Li–S) batteries are among the most promising next-generation energy-storage systems due to their very high theoretical specific capacity and energy density, as well as the abundance, low cost, and environmental friendliness of sulfur [1]. However, their practical application is strongly limited by the insulating nature of sulfur, large volume changes during cycling, and especially by the dissolution and migration of lithium polysulfides (the so-called shuttle effect), which lead to rapid capacity fading, low Coulombic efficiency, and poor cycling stability [2]. In this context, metal–organic frameworks (MOFs) have recently attracted considerable attention as advanced host materials for Li–S cathodes [3]. Owing to their exceptionally high surface areas, well-defined and tunable porosity, and the presence of chemically active metal sites, MOFs can physically confine sulfur species and chemically immobilize polysulfides, thereby suppressing the shuttle effect, buffering volume expansion, and promoting more efficient redox conversion [4].

In this contribution, we explore the application of MOF-74(Co) in sulfur cathodes and evaluate the effect of its structural state on the electrochemical performance of Li–S batteries. The study is based on the hypothesis that the porous structure and open Co(II) sites of MOF-74 enable effective sulfur and polysulfide confinement, while additional thermal treatment (calcination) can improve material stability and rate performance. Accordingly, two related host materials were investigated: activated MOF-74(Co) with an open framework and a calcinated MOF-74(Co)-derived porous composite.

MOF-74(Co)(AS) was synthesized by a standard solvothermal route, and its structural properties were investigated by PXRD, IR spectroscopy, TG analysis, nitrogen adsorption–desorption measurements, and SEM. A portion of the material was subsequently calcinated under nitrogen to obtain MOF-74(Co)(C). Both materials exhibited predominantly microporous character, however, calcination resulted in a marked decrease in surface area and pore volume. Sulfur composites based on both hosts were then fabricated and assembled into Li–S cells, where they were systematically electrochemically evaluated.

Electrochemical performance was assessed by cyclic voltammetry, galvanostatic charge–discharge tests, and rate capability measurements. Both materials demonstrated the ability to function as effective sulfur host, however, notable differences were observed. The calcinated MOF-74(Co)(C) cathode delivered a higher initial discharge capacity of about 690 mAh g^{-1} at 0.2 C, which increased to ~722 mAh g^{-1} after 20 cycles, and maintained capacities of ~616, 524, and 408 mAh g^{-1} at 0.5, 1, and 2 C, respectively. In comparison, the activated MOF-74(Co)(AC) electrode exhibited an initial capacity of ~652 mAh g^{-1}, decreasing to ~568 mAh g^{-1} after 20 cycles, and ~477, 408, and 308 mAh g^{-1} at 0.5, 1, and 2 C. The MOF-74(Co)(C) cathode showed higher current responses and superior rate performance. This behavior may be a consequence of improved electrical conductivity and the associated higher probability of polysulfide conversion. In contrast, the MOF-74(Co)(AC) electrode displayed more stable cyclic voltammograms and better capacity retention. Overall, the two materials showed different but complementary electrochemical behaviors, with one favoring rate performance and the other cycling stability.

This study demonstrates that MOF-74(Co)-derived materials are promising multifunctional components for Li–S battery cathodes, combining physical confinement, chemical adsorption, and catalytic activity.

Acknowledgements

Funded by the EU NextGenerationEU through the Recovery and Resilience Plan for Slovakia under the project No. 09I03-03-V03-00034 (MASS-PRAM).

References

[1] Z. - C. Lv, P. - F. Wang, J. - C. Wang, S. - H. Tian, T. - F. Yi, J. Ind. Eng. Chem. **124** (2023) 68–88.
[2] J. Ke, Z. Wang, H. Zhu, M. Chen, R. Song, Q. Ji, D. Liu, S. Lan, Commun. Mater. **6** (2025) 237.
[3] Y. Yan, X. Zhou, J. He, C. Yue, X. Liu, X. Shang, X. Yu, Z. Sun, H. K. Liu, S. X. Dou, Coord. Chem. Rev. **548** (2026) 217218.
[4] Z. Xie, B. Cao, X. Yue, R. Wang, Z. Xue, J. Wang, G. Guan, W. Chen, Nano Res. **17** (2024) 2592–2618.

MIL-101(Cr)-Derived Carbon Materials as a Platform for Next-Generation Lithium-Ion Battery Anodes

D. Capková[a], N. Hlávková[b], N. Király[b], K. M. Ryan[a], M. Almáši[b]

[a] Department of Chemical Sciences and Bernal Institute, University of Limerick, Limerick, V94 T9PX, Ireland
[b] Department of Inorganic Chemistry, Institute of Chemistry, Faculty of Science, Pavol Jozef Šafárik University in Košice, Moyzesova 11, 040 01 Košice, Slovak Republic

*miroslav.almasi@upjs.sk

The continuous advancement of portable electronics, electric mobility, and large-scale energy storage systems has intensified the demand for high-performance lithium-ion batteries (LIBs) with enhanced energy density, rate capability, and long-term cycling stability. Although graphite remains the commercial benchmark anode material due to its structural stability and low operating potential, its theoretical capacity (372 mAh g^{-1}) inherently limits further improvements in energy density. Consequently, considerable research efforts have focused on developing alternative anode materials capable of delivering higher reversible capacities while maintaining structural integrity during repeated lithiation/delithiation processes.

Metal–organic frameworks (MOFs) have emerged as attractive candidates for next-generation electrode materials owing to their exceptionally high specific surface area, tunable porosity, structural diversity, and chemical versatility. Their well-defined crystalline architectures enable controlled ion diffusion pathways and offer the possibility of structural modification at the molecular level. In particular, chromium(III)-based MIL-101(Cr) (Figure 1) is a robust MOF characterized by large mesoporous cages, high surface area, and remarkable thermal and chemical stability, making it a promising precursor or active component for electrochemical applications.

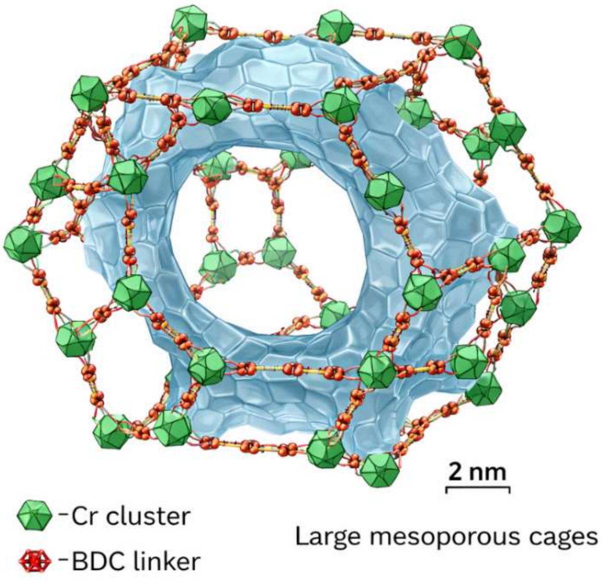

Figure 1 Crystal structure of micro/mesoporous material MIL-101(Cr).

In this study, MIL-101(Cr) was synthesized using tetramethylammonium hydroxide (TMAOH) as a structure-directing agent, followed by carbonization to enhance electrical conductivity and electrochemical performance. The resulting composite electrode consisted of 80 wt% carbonized MIL-101(Cr), 10 wt% Super P conductive carbon, and eco-friendly 10 wt% carboxymethyl cellulose (CMC) binder. Electrodes were assembled into CR2032 coin cells with lithium metal as the counter/reference electrode, and 1 M $LiPF_6$ dissolved in an EC/DEC solvent mixture as the electrolyte.

Electrochemical characterization was performed using galvanostatic charge–discharge cycling. Prior to long-term cycling, the cells underwent a formation cycle at 50 mA g^{-1} to promote stable solid electrolyte interphase (SEI) formation. Subsequent cycling was conducted at a current density of 100 mA g^{-1}. The initial coulombic efficiency reached approximately 44%, reflecting irreversible processes associated primarily with SEI formation and surface-related reactions typical for high-surface-area materials. From the second cycle onward, the average coulombic efficiency stabilized near 99%, indicating good reversibility of the lithiation/delithiation reactions.

The specific capacity reached 232 mAh g^{-1} at 50 mA g^{-1} and 201 mAh g^{-1} at 100 mA g^{-1}. After 500 cycles at 100 mA g^{-1}, the material retained 76% of its capacity, demonstrating moderate cycling stability. Although the achieved capacity does not exceed that of graphite, the results confirm that MIL-101(Cr)-derived materials exhibit stable long-term electrochemical behavior and structural resilience. The porous architecture likely facilitates electrolyte penetration and lithium-ion transport, while the carbonized framework improves electronic conductivity.

To further enhance performance, future work will focus on hybridization strategies, particularly the incorporation of silicon nanoparticles into the MIL-101(Cr) matrix. Silicon offers a significantly higher theoretical capacity (4200 mAh g^{-1}), but its large volume expansion during cycling leads to rapid degradation. Embedding silicon within a porous MOF-derived matrix may effectively buffer volumetric changes, mitigate particle pulverization, and stabilize the electrode structure.

Overall, this work demonstrates the feasibility of utilizing MIL-101(Cr) as a functional anode material and provides a foundation for further optimization of MOF-based hybrid electrodes for advanced lithium-ion battery systems.

Acknowledgements

Funded by the EU NextGenerationEU through the Recovery and Resilience Plan for Slovakia under the project No. 09I03-03-V03-00034 (MASS-PRAM).

ENERGY STORAGE AND CONVERSION

Ternary Cu-BTC/C/Pd Composites for Advanced Hydrogen Energy Storage

J. Vyhlídalová[b], T. Zelenka[b], M. Želinská[a]*, M. Almáši[a]

[a]Department of Inorganic Chemistry, Institute of Chemistry, Faculty of Science, Pavol Jozef Šafárik University in Košice, Moyzesova 11, 040 01 Košice, Slovak Republic
[b]Department of Chemistry, Faculty of Science, University of Ostrava, 30. Dubna 22, 702 00 Ostrava, Czech Republic

*milica.zelinska@gmail.com

Hydrogen is widely considered a key future energy carrier due to its high gravimetric energy density (~142 MJ kg^{-1}) and zero emissions at the point of use, offering a promising route toward the decarbonization of transport, industry, and power systems [1]. Nevertheless, its large-scale implementation is still limited by the lack of efficient and safe storage technologies. Conventional approaches based on compressed or liquefied hydrogen require high pressures or cryogenic conditions, resulting in low volumetric energy density, significant energy consumption, safety concerns, and increased costs [2].

In this context, adsorption-based storage using porous materials has emerged as an attractive alternative to traditional storage methods. Among them, metal–organic frameworks (MOFs) have gained particular attention due to their exceptionally high surface areas, tunable pore architectures, and chemically designable structures. These features enable enhanced hydrogen physisorption through weak host–guest interactions, making MOFs and MOF-based composites promising candidates for advanced hydrogen storage systems [3][4].

In this study, a series of ternary composites Cu-BTC@C/Pd(IS) with different palladium contents (2, 5, and 10 wt%) and surface-modified analogues (2 and 5 wt% Pd treated with thioglycolic acid) were developed as functional platforms for hydrogen storage. All materials were prepared by an *in situ* approach involving palladium incorporation during C synthesis, followed by carbonization and subsequent *in situ* growth of Cu-BTC. This strategy yielded ternary composites with close contact between the porous carbon matrix, palladium nanoparticles, and MOF phase, favorable for efficient gas transport and storage.

Comprehensive characterization using FT-IR spectroscopy, PXRD, SEM/EDX, TEM, thermal and elemental analyses, and gas sorption measurements confirmed the successful formation of the ternary composite, the presence of the Cu-BTC phase and Pd nanoparticles, the preservation of hierarchical porosity, and the introduction of additional surface functionality after thiol modification.

Hydrogen adsorption was investigated at 77, 273, and 298 K up to 100 kPa. At 77 K, all ternary composites exhibited significant hydrogen uptake at 77 K, with the highest capacity of ~7.0 mmol g^{-1} obtained for the 10 wt% Pd sample, demonstrating efficient utilization of the hierarchical porous structure. Next, hydrogen sorption at elevated temperatures was investigated in detail for the Cu-BTC@C/Pd(IS)-10% composite in comparison with Pd-free reference materials. This material exhibited measurable hydrogen uptake under near-ambient conditions (~0.22 mmol g^{-1} at 298 K), confirming the positive effect of palladium incorporation on hydrogen uptake at elevated temperatures.

The results suggest that the ternary composite represents a promising, modular material concept for next-generation hydrogen storage. The synergistic combination of hierarchical porosity, MOF functionality, and palladium activity provides a versatile platform for further optimization toward practical energy-storage and hydrogen-technology applications.

Acknowledgements

Funded by the EU NextGenerationEU through the Recovery and Resilience Plan for Slovakia under the project No. 09I03-03-V03-00034 (MASS-PRAM).

References

[1] A. S. Mekonnin, K. Wacławiak, M. Humayun, S. Zhang, H. Ullah, Catalysts **15** (2025) 260.
[2] L. Qiao, C. Lu, W. Fan, Z. Xue, X. Wang, Z. Kang, D. Sun, Int. J. Hydrogen Energy **93** (2024) 805–821.
[3] L. Jimenez-Lopez, R. M. Ospino, L. G. de Araujo, A. Celzard, V. Fierro, Nanoscale **17** (2025) 6390–6413.
[4] A. I. Osman, W. Abd-Elaziem, M. Nasr, M. Farghali, A. K. Rashwan, A. Hamada, Y. M. Wang, M. A. Darwish, T. A. Sebaey, A. Khatab, A. H. Elsheikh, Environ. Chem. Lett. **22** (2024) 4764–4770.

Thiol-Engineered MOF–Carbon Composites with Palladium Nanoparticles: Interfacial Design for Temperature-Dependent Hydrogen Sorption

J. Vyhlídalová[a], M. Želinská[b*], J. Silvestre-Albero[c], T. Zelenka[a*], M. Almáši[b*]

[a]Department of Chemistry, Faculty of Science, University of Ostrava, 30. dubna 22, 702 00 Ostrava, Czech Republic
[b]Department of Inorganic Chemistry, Institute of Chemistry, Faculty of Science, Pavol Jozef Šafárik University in Košice, Moyzesova 11, 040 01 Košice, Slovak Republic
[c]Advanced Materials Laboratory, Department of Inorganic Chemistry, University Institute of Advanced Materials, University of Alicante, Alicante, Spain

*milica.zelinska@gmail.com, tomas.zelenka@osu.cz, miroslav.almasi@upjs.sk

Hydrogen storage in porous solids requires the rational integration of physisorption-active surfaces with catalytic sites capable of promoting dissociative chemisorption under near-ambient conditions. While metal–organic frameworks (MOFs) and porous carbons provide high surface area and well-defined microporosity for low-temperature hydrogen uptake, their performance at elevated temperatures remains limited by weak host–guest interactions. The incorporation of noble metal nanoparticles represents a viable strategy to enhance hydrogen affinity via spillover-related mechanisms. However, controlled metal dispersion and stabilization remain critical challenges.

In this study, hierarchically porous carbon monoliths (HPCM) were surface-engineered by thiol functionalization using silane- and thioglycolic acid-based approaches. The introduction of –SH groups was designed to promote strong metal–sulfur coordination, enabling controlled anchoring and homogeneous distribution of palladium nanoparticles. Palladium was incorporated either via *in situ* introduction during carbon synthesis or via post-synthetic modification. Subsequently, Cu-BTC was integrated to combine microporous physisorption domains with metal-active sites (Figure 1).

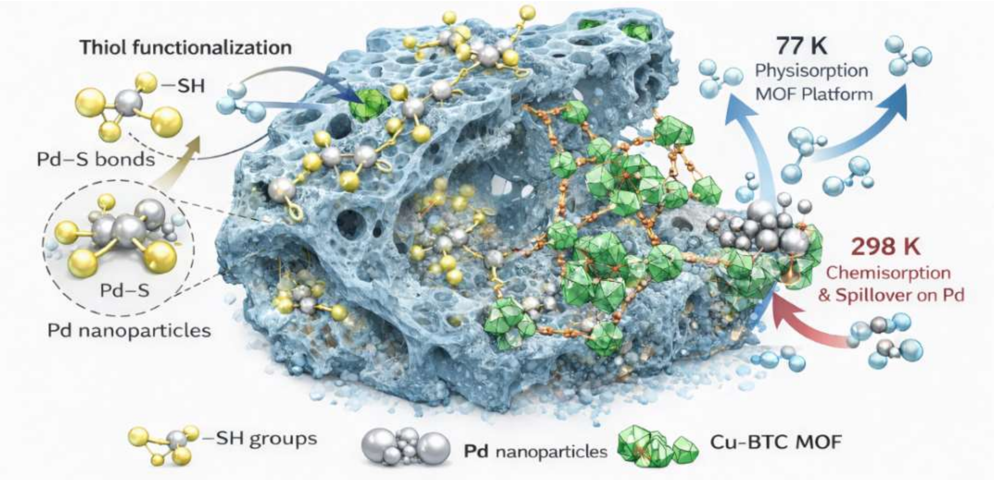

Figure 1 Interfacial design of Cu–BTC/HPCM–Pd composite enabling physisorption–chemisorption synergy.

Fourier-transform infrared spectroscopy confirmed successful surface functionalization and the presence of thiol-related vibrational features, while SEM/EDX and TEM analyses verified the dispersion of palladium nanoparticles and their stabilization within the carbon matrix. PXRD measurements demonstrated preservation of the crystalline Cu-BTC framework within the composite architecture.

Gas sorption analysis using N_2 (77 K) and CO_2 (273 K) adsorption combined with QSDFT and GCMC modelling revealed that thiol functionalization significantly alters micropore accessibility and surface chemistry. Hydrogen sorption measurements at 77, 273, and 298 K allowed differentiation between dominant physisorption and chemisorption contributions. At cryogenic temperature, uptake was primarily governed by microporosity, whereas at elevated temperatures, palladium-containing samples exhibited enhanced hydrogen adsorption relative to Pd-free analogues, indicating the role of metal-mediated interactions.

The results highlight the importance of interfacial engineering in MOF–carbon–metal composites and demonstrate that thiol-directed palladium incorporation provides a controlled route toward multifunctional porous materials. The synergistic integration of hierarchical porosity and metal-active sites offers a structurally robust platform for advancing hydrogen storage strategies under practical operating conditions.

Acknowledgements

Funded by the EU NextGenerationEU through the Recovery and Resilience Plan for Slovakia under the project No. 09I03-03-V03-00034 (MASS-PRAM).

Capture and Storage of CO_2 in Porous Molecular Framework Materials: Details Matter!

A. Adewale[a], J. S. K. R. Mudiyanselage[a], M. A. Addicoat[a]*

[a]Nottingham Trent University, Clifton Lane, NG11 8NS, UK

*matthew.addicoat@ntu.ac.uk

Porous framework materials have shown great promise in the capture, storage and valorization of atmospheric CO_2. Computational modelling is a key first step in the development of porous materials in order to elucidate the physical characteristics that determine the usefulness of any given material. The aim of this computational modelling is to prevent time, effort and chemicals being wasted in unsuccessful materials.

However, computational chemistry is not a panacea. Current computational approaches are firstly expensive, and secondly, only predict the properties of *ideal* materials, and fail to account for defects, edge effects and isomers. Mixed materials, which combine the properties of two or more distinct materials add a further dimension and further increase the challenge involved in predictive modelling. These defects, edges and interfaces often determine the real-world performance of materials and need to be accounted for from the beginning.

In this contribution, we describe our efforts to move beyond traditional computational chemistry approaches and develop mathematical models of defective and mixed porous materials combined with machine learning in order to accurately and efficiently identify and characterize the binding sites of CO_2 in as-manufactured porous materials.

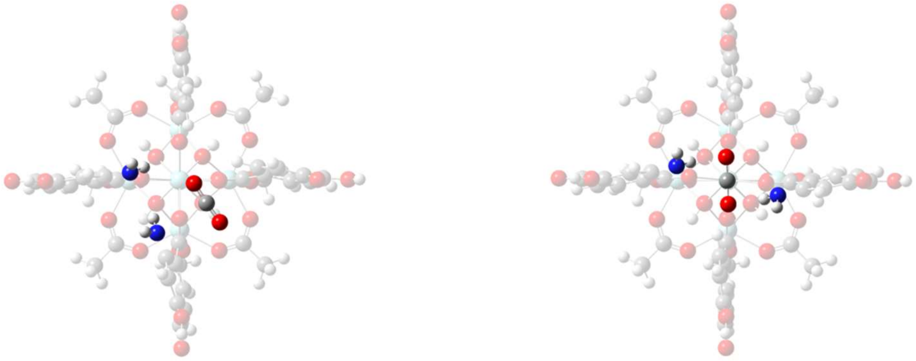

Figure 1

Acknowledgements

MAA is grateful to the Engineering and Physical Sciences Research Council for funding through grant no. EP/S015868/1 and HPC time *via* the UK Materials and Molecular Modelling Hub *via* grant no. EP/T022213.

References

[1] M. Nurhuda, Y. Hafidh, C. Dogan, D. Packwood, C. P. Perry, M. A. Addicoat, Inorg. Chem. Front. **10** (2023) 5379-5390.

Porous Biomaterials Based on Core–Shell Microparticles

G. Dercz[a]*, I. Matuła[a]

[a]Institute of Materials Science, University of Silesia in Katowice, 75 Pułku Piechoty Street 1 A,
41-500 Chorzów, Poland

*grzegorz.dercz@us.edu.pl

Porous metallic biomaterials with spatially controlled phase composition, mechanical gradients and designed heterogeneity represent a promising strategy for overcoming the limitations of conventional implant alloys, particularly stress shielding and insufficient biological integration. In this study, we present the design, synthesis and detailed characterization of porous Ti-Ta materials composed of diffusion-engineered core-shell microparticles consolidated into a porous bulk structure.

Mechanical alloying enables the formation of Ti-core/Ta-shell particles, which after consolidation create a structure composed of spherical and elliptical particles interconnected by diffusion necks. The resulting architecture exhibits two distinct but complementary levels of porosity. The first is interconnected macroporosity between particles, generated by incomplete densification and neck formation. This macroporosity provides space for tissue ingrowth, vascularization and bone trabeculae penetration, enabling mechanical interlocking and long-term biological fixation.

The second level is intraparticle porosity formed as a consequence of unequal diffusion rates of Ti and Ta. The faster diffusion of one species leads to vacancy accumulation and the formation of internal voids through the Kirkendall effect. This intraparticle porosity introduces microscale heterogeneity within individual particles and increases internal surface area. Such fine-scale porosity may promote protein adsorption, improve fluid permeability and create favorable microenvironments for osteoblast attachment and proliferation. While macropores facilitate bone tissue colonization and vascular supply, smaller pores and internal voids support cell adhesion, nutrient transport and early-stage cellular activity at the implant-bone interface.

Microstructural investigations reveal a continuous radial gradient consisting of a Ti-rich α core, an intermediate α + β Widmanstätten-type transition zone, and a Ta-rich β outer shell. This diffusion-driven architecture results in a functionally graded microstructure within each particle, where phase distribution and chemical composition evolve progressively from the center toward the surface. The inherent heterogeneity of phase arrangement and porosity distribution generates a complex structural landscape that may enhance both mechanical energy dissipation and biological responsiveness.

Nanoindentation mapping demonstrates that the mechanical response correlates directly with the phase sequence. The α + β transition region exhibits reduced Young's modulus values lower than those measured in the β-rich shell and α core. This spatial modulation of stiffness within a single microparticle introduces a hierarchical mechanical response at the microscale and can be extended to the macroscale design of a Functionally Graded Material implant mimicking the natural transition from cortical bone to trabecular tissue.

The Ta-rich β phase forming the external shell plays a crucial role in long-term biomedical performance. Tantalum is characterized by excellent biocompatibility and the formation of a stable passive oxide layer, ensuring corrosion resistance in physiological environments. The coexistence of chemically distinct zones, interconnected macroporosity and diffusion-generated intraparticle voids creates a heterogenic, hierarchically porous structure that may enhance osteointegration through synergistic mechanical compatibility and biological stimulation.

The combination of phase gradation, hierarchical porosity and controlled heterogeneity results in a porous metallic biomaterial in which structural complexity becomes a functional design parameter, opening pathways toward next-generation titanium-based implants with improved biomechanical compatibility and long-term biological performance.

Acknowledgements

This work was supported by the Polish National Science Centre (Narodowe Centrum Nauki, NCN) under the research project OPUS-27, no. UMO-2024/53/B/ST11/00431.

Conference participation was supported by the GreenMat project, co-funded by the European Union under the program "European Funds for Silesia 2021-2027"

Electron Tomography: From Pixels to Voxels Imaging

V. Girman[a,b]*, P. Indyka[c], M. Klementová[d], P. Sovák[a], J. Bednarčík[a,e]

[a]Department of Solid State Physics, Institute of Physics, Faculty of Science, Pavol Jozef Šafárik University in Košice, Moyzesova 11, 040 01 Košice, Slovak Republic
[b]Institute of Materials Research, Slovak Academy of Science, Watsonova 47, 040 01 Košice, Slovak Republic
[c]SOLARIS National Synchrotron Radiation Centre, Jagiellonian University, Czerwone Maki 98, 30-392 Krakow, Poland.
[d]FZU - Institute of Physics, Czech Academy of Sciences, Na Slovance 2, Prague 18221, Czech Republic.
[e]Institute of Experimental Physics, Slovak Academy of Science, Watsonova 47, 040 01 Košice, Slovak Republic

*vladimir.girman@upjs.sk

Transmission electron microscopy (TEM) has long been recognized as a versatile and indispensable analytical tool for the investigation of solid state and soft matter systems, providing structural information down to the atomic scale. Despite its remarkable capabilities, conventional TEM intrinsically suffers from a fundamental constraint: it yields only two-dimensional (2D) projections of specimens that are inherently three-dimensional (3D). As a consequence, key structural features may remain invisible or misinterpreted when relying solely on 2D projections. Electron tomography (ET) overcomes this limitation by enabling the reconstruction of the 3D volume from a tilt series of 2D images and significantly extends analytical capabilities of TEM. ET provides direct access to quantitative 3D information at the micro, nano and atomic scale. The reconstructed volumetric data allow researchers to visualize and measure complex structural motifs that remain hidden in standard TEM imaging, including structural defect networks, grain and phase boundaries, porosity, particle dispersion in composite materials, or intricate internal architectures in functional nanomaterials [1]. Such insights are essential for the study of accurate structure - property relationships and enable the rational design of advanced materials.

Principles of electron tomography

In ET, a specimen is incrementally tilted, typically over ±60° to ±80°, and 2D projection images are collected with high angular precision. Three essential steps define the workflow [2, 3]:

(i) Data acquisition: High-quality projections must be recorded under stable imaging conditions. The accuracy of tilt increments is crucial to achieving reliable reconstructions. The tilt series is typically recorded in angular increments of 1–2°, *(ii) Alignment*: Individual projections are aligned to correct for shifts, rotations, and mechanical instabilities during tilting. Cross-correlation and tracking of markers are commonly applied to ensure consistent geometry across the tilt series, *(iii) Reconstruction*: The aligned projections are converted into a 3D volume using algorithms such as weighted back-projection (WBP) or iterative reconstruction methods, particularly the simultaneous iterative reconstruction technique (SIRT). Alternative algorithms continue to be developed, providing ongoing improvements in reconstruction fidelity and efficiency.

The theoretical foundation of electron tomography rests on the Radon transform, which models each measured projection as a line integral of the object function. For a 2D object $f(x,y)$, the projection $Rf(p,\theta)$ can be written as:

$$R\,f(p,\theta) = \int_{-\infty}^{\infty}\int_{-\infty}^{\infty} f(x,y)\;\delta\,(p - x\cos\theta - y\sin\theta)\;dxdy$$

where $f(x,y)$ denotes the density function of 2D slice, $Rf(p,\theta)$ is projection along a line at signed distance p from the origin and rotated by angle θ, and δ is the Dirac delta function. The Central Slice Theorem (Fourier slice theorem) then establishes that the one-dimensional Fourier transform of a projection $Rf(p,\theta)$ with respect to p

equals a central radial slice through the two-dimensional Fourier transform of f taken at the same angle θ. This provides a direct spectral pathway from projections to the object's frequency domain and underpins both Fourier-domain reconstruction and filtered back-projection. In ET, this relationship also clarifies how limited tilt ranges map to anisotropic "missing-wedge" support in Fourier space, manifesting as elongation and resolution loss along the beam direction, and motivates sampling and filtering strategies to mitigate these artifacts [4].

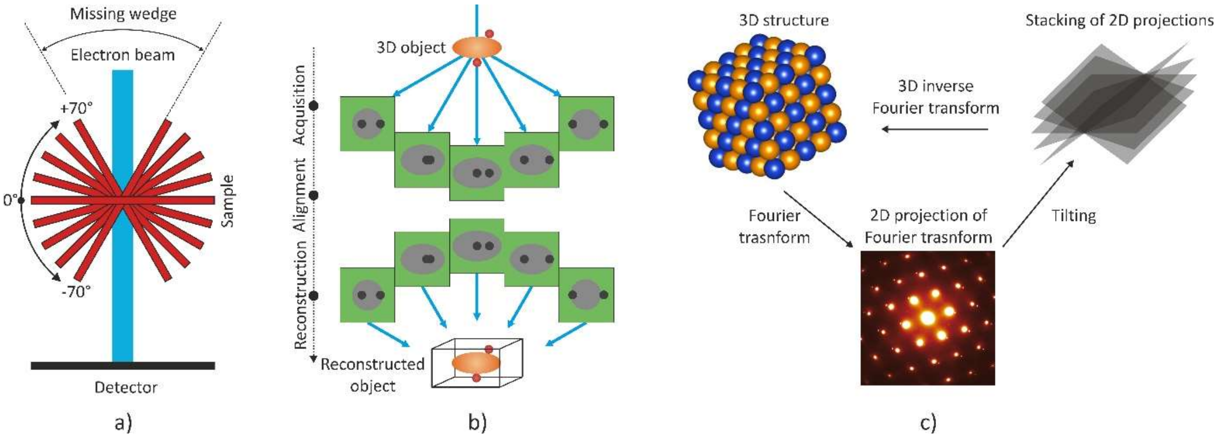

Figure 1 a) schematic illustration of the specimen-tilting geometry used during tomography, b) the process of direct reconstruction from real-space projections, c) reconstruction obtained from reciprocal-space information.

In general, two principal strategies for achieving 3D imaging in ET can be distinguished. These approaches differ primarily in the manner of data acquisition, the experimental constraints they impose, and the computational demands associated with image reconstruction. The first category, *image tomography* (Figure 2), relies on recording a series of real-space projections obtained by tilting the specimen, which are subsequently combined to produce a 3D representation of the sample. Image tomography is particularly suited for reconstructing morphological features on the submicro- to nanoscale, providing insights into the shape and spatial arrangement of structural domains. In contrast, the second category, *diffraction tomography*, aslo known as 3D Electron Diffraction, exploits reciprocal-space information collected from diffracted intensities, enabling reconstruction of the atomic structure itself and crystallographic relationships that cannot be achieved through real-space imaging [1, 5].

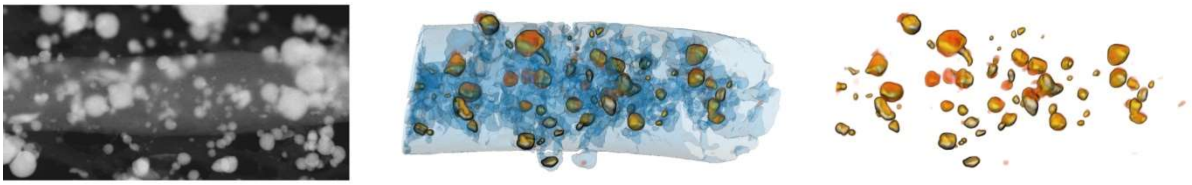

Figure 2 Carbon fibre decorated with CoP nanoparticles. From the left to right: TEM image, reconstructed segment of fibre and visualization of CoP nanoparticles distribution (V. Girman, Ana B. Hungría, Miguel L. Haro).

Acknowledgements

This research was funded by the EU NextGenerationEU through the Recovery and Resilience Plan for Slovakia under the project No. 09I03-03-V03-00034, and co-funded by the research project VEGA 1/0638/24. The authors are grateful for the: Research at the National Synchrotron Radiation Centre SOLARIS is supported by the Ministry of Science and Higher Education, Poland, under contract no. 1/SOL/2021/2.

References

[1] P. A. Midgley, S. Bals: Electron Tomography. In Handbook of Nanoscopy. Ch.7., Ed. by G. van Tendeloo et al., Wiley-VCH Verlag GmbH & Co. (2012).
[2] S. M. Collins: Electron Tomography. In Industrial Tomography: Systems and Applications. Ch.10, 2nd ed. (2022) 305-332.
[3] B. Goris, T. Roelandts, K. J. Batenburg, H. H. Mezerji, S. Bals, Ultramicroscopy **127** (2013) 40-47.
[4] A. C. Kak and M. Slaney, Principles of Computerized Tomographic Imaging, IEEE, Inc., NY: IEEE Press, 1987.
[5] U. Kolb, Y. Krysiak, S. Plana-Ruiz, Acta Cryst. **B75** (2019) 463-474.

Using of ^{1}H NMR Relaxometry for Characterization of Resorcinol-Formaldehyde Gels

E. Kinnertová[a]*, V. Slovák[a]

[a]Department of Chemistry, Faculty of Science, University of Ostrava, 30. Dubna 22, 702 00 Ostrava, Czech Republic

*eva.kinnertova@osu.cz

Low-field NMR relaxometry is a technique that detects the presence of water in a sample (specifically the relaxation of protons in water) and therefore can be used for the investigation of molecular dynamics during the synthesis processes and also for the final prepared samples for characterization of their porosity.

During material preparation, the technique can be used in the resorcinol-formaldehyde (RF) sol-gel polycondensation phase when forming 3D structure (gel) [1]. The values of relaxation time (T_2) and abundance of components enable to assign them to states of water in the studied systems. One component of water with typically longer relaxation and higher content at the start of the reaction, represents bulk water with more of less free mobility. Second component of water with shorter relaxation times is related to water molecules in close proximity to the emerging particles (gradually captured in polymeric gel) with a limited possibility of motion (Figure 1a).

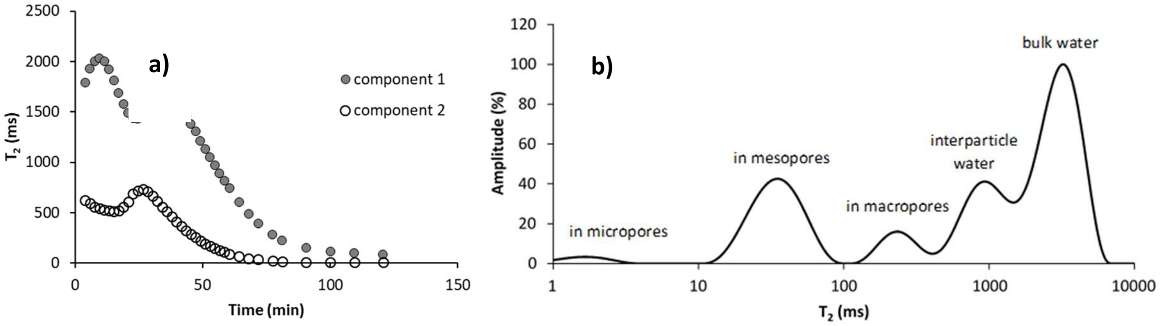

Figure 1 a) Relaxation times of two components during RF polycondensation, b) Distribution of T_2 for wet carbonaceous sample (logarithmic scale on horizontal axis).

Considering that porous materials as resorcinol-formaldehyde gels are used to purify water from various pollutants, it is useful to be aware of the porosity of the material in a wet state, and low-field NMR relaxometry can be helpful in this regard. The analysis relies on finding the number of components connected with different types of protons present in the studied system – sufficiently wetted samples. The appropriate parameters, amplitude, and relaxation time corresponding with given types of protons are optimized and can be used for the characterization of the pore size distribution (PSD) of various porous materials. Water in small pores (micropores) is relaxing very fast under 10 ms. As the amount of water increases, larger pores are gradually fill up. The relaxation times of water in mesopores can range in the order of tens milliseconds. The relaxation times of water in macropores or water in interparticle cavities range from hundreds to thousands of milliseconds. Long relaxation times (thousands ms, mostly above 1500 ms) are then related with relaxation of bulk water surrounding the samples (Figure 1b).

NMR relaxometry presents an interesting and not very often used method for studying resorcinol-formaldehyde polycondensation kinetics. The nucleation and growth of particles are well accessible by this method through their effect on the mobility of water molecules (related to measured relaxation). A limitation of the technique for characterizing porosity is that if we want to obtain PSD, we need to know an important parameter, namely surface relaxivity. This parameter depends on how water molecules interact with the pore surface, which affects the relaxation of protons. NMR relaxometry performed at negative temperatures, i.e. NMR cryoporometry, can be helpful in further research, e.g. the thickness of unfreezing water in samples.

References

[1] E. Kinnertová, V. Slovák, R. Maršálek, M. Mucha., Gels **8.1** (2022) 8.

CHARACTERIZATION AND MODELING

Systematic DSC Analysis of Melting of Water in Different Mesopore Sizes in Carbon Xerogels

L. Kořená[a]*, V. Slovák[a], S. L. Flores-López[b], A. Arenillas[b]

[a]Department of Chemistry, Faculty of Science, University of Ostrava, 30. Dubna 22, 702 00 Ostrava, Czech Republic
[b]Instituto de Ciencia y Tecnología del Carbono, INCAR-CSIC, Francisco Pintado Fe 26, 33011, Oviedo, Spain

*lucie.korena@osu.cz

Thermoporometry is an alternative method for pore size distribution (PSD) determination based on differential scanning calorimetry (DSC) observations of melting point depression of a probe liquid confined in pores. However, the accuracy of the method strongly depends on parameters which are applied while transforming DSC record into PSD and which are derived from the melting behaviour of probe liquid confined in pores.

Thus, in this study, the individual effect of pore size on the melting behaviour of a probe liquid confined within material pores and on the parameters used for PSD determination was systematically investigated. As a model system, water serving as the probe liquid and a series of carbon xerogels exhibiting uniform pore shape and surface chemistry and pore sizes ranging from 10 to 50 nm was used.

A decreasing trend between the melting point depression of confined water and pore radius of carbon xerogels was established, confirming the applicability of the modified Gibbs–Thomson equation for PSD determination. DSC pore peak area, corresponding to the heat of fusion of ice in pores, and pore volume showed a good linear correlation, which was found to be pore size dependent. Also, the experimentally obtained Gibbs–Thomson constant (39 nm·K) significantly deviated from the commonly accepted one. Moreover, the thickness of the non-freezable layer (δ layer) was observed to increase with increasing pore size.

These findings highlight the necessity to test the Gibbs-Thomson constant and δ layer values for each studied liquid-solid system individually, because applying appropriate values of these parameters is a key to obtain accurate PSD from DSC record.

Acknowledgements

The Czech team was supported by the European Union under the LERCO project no CZ.10.03.01/00/22_003/0000003 and by the project of University of Ostrava no SGS12/PřF/2023.

References

[1] L. Kořená, V. Slovák, S. L. Flores-López, A. Arenillas, Thermochim Acta **753** (2025) 180128.

When Molecules Feel Claustrophobic: Decoding CO_2 Behaviour in Nanoconfinement with Solid-State NMR & Computer Modeling

L. Mafra[a]*, M. Sardo[a], I. Marin-Montesinos[a], M. A. O. Lourenço[a], R. Vieira[b]

[a]CICECO - Aveiro Institute of Materials, University of Aveiro, Aveiro, Portugal
[b]Center for Physics of the University of Coimbra, Department of Physics, University of Coimbra, Rua Larga, 3004-516 Coimbra, Portugal

*lmafra@ua.pt

Porous CO_2-chemisorbent materials are critical for addressing rising atmospheric CO_2 levels, enabling applications such as direct air capture and industrial flue gas separation. However, understanding their reactivity and the atomic-level details of CO_2 adsorption at the gas-solid interface remains a significant challenge, hindering the design of improved materials. This presentation highlights our group's recent advancements in elucidating CO_2 speciation in confined spaces under both dry and humid conditions, combining surface-enhanced solid-state NMR spectroscopy with computational modelling.[1-5]

Our methodology quantitatively resolves multiple co-existing species (up to six distinct confined CO_2 species) - from physisorbed CO_2 to chemisorbed carbamates and moisture-induced CO_2 species (bicarbonates) - enabling the first-ever generation of "species-specific" adsorption isotherms.[2] Unlike conventional volumetric or gravimetric techniques, NMR uniquely resolves these species, enabling the generation of individual CO_2 isotherms for each adsorbed component.The first application of Magic-Angle Spinning Dynamic Nuclear Polarization (MAS-DNP) NMR to this problem is also presented. This overcomes the intrinsic low sensitivity from the 1% natural abundance of ^{13}C, allowing us to probe CO_2 chemisorption under direct air capture (400 ppm CO_2). The versatility of our methodology is showcased across diverse porous systems, including amine-modified silicas, covalemt organic frameworks (COFs), metal-organic frameworks (MOFs) and polysaccharide-based biopolymers.[1-5] thus providing a powerful framework for rationalizing adsorption mechanisms at confined material's surfaces.

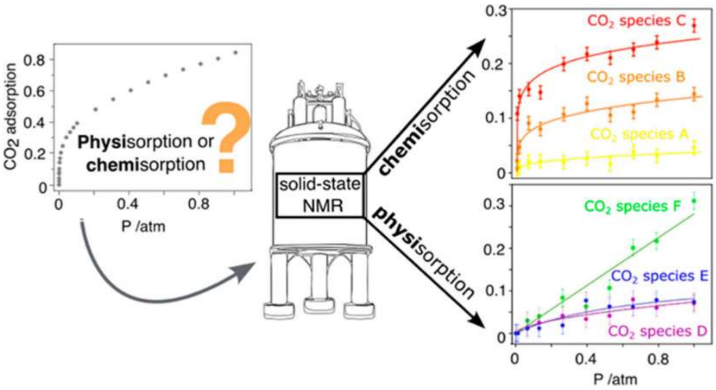

Figure 1 Solid-state NMR assisted adsorption methodologies to study CO_2 speciation in confinement.

Acknowledgements

This work has received funding from the European Research Council (ERC) under the European Union's Horizon 2020 research and innovation program (Grant Agreement 865974). We thank CICECO-Aveiro Institute of Materials and University of Aveiro, UIDB/50011/2020, UIDP/50011/2020 & LA/P/0006/2020.

References

[1] M. Sardo, T. Morais, M. Soares, R. Vieira, M. Ilkaeva, M. Lourenço, I. Marin-Montesinos, L. Mafra, Chem. Comm **60** (2024) 4015.

[2] M. Ilkaeva, R. Vieira, J. M. P. Pereira, M. Sardo, I. Marín-Montesinos, L. Mafra, J. Am. Chem. Soc. **145** (2023) 8764.

[3] L. Mafra, T. Čendak, S. Schneider, P. V. Wiper, J. Pires, J. R. B. Gomes, M. Pinto, J. Am. Chem. Soc. **139** (2017) 389-408.

[4] R. Vieira, I. Marín-Montesinos, J. Pereira, R. Fonseca, M. Ilkaeva, M. Sardo, L. Mafra, J. Phys. Chem. C **125** (2021) 14797-14808.

[5] D. Pereira, M. A. O. Lourenço, M. Sardo, A. Silvestre, I. Marin-Montesinos, L. Mafra, ACS Appl. Polym. Mater. **7** (2025) 12964.

CO_2 Speciation in Amine-Modified Porous Silicas for Direct Air Capture by DNP Enhanced Solid-State NMR

M. Soares[a], S. Akrial[b], D. Gajan[b], M. Sardo[a], A. Lesage[b], L. Mafra[a], I. Marín-Montesinos[a]*

[a]Department of Chemistry & CICECO−Aveiro Institute of Materials, University of Aveiro, 3810-193 Aveiro, Portugal
[b]Centre de RMN à Hauts Champs de Lyon, UMR 5082, Université de Lyon (CNRS/ENS Lyon/UCBL), 5 rue de la Doua, Villeurbanne, France

*imarin@ua.pt

Direct air capture (DAC) is a promising solution to mitigate atmospheric CO_2, especially in low-concentration environments. Amine-functionalized adsorbents are central to DAC efficiency, but optimizing their performance requires understanding molecular-level capture mechanisms. Chemisorption relies on strong chemical interactions with CO_2, yet precise speciation characterization under realistic conditions (~400 ppm CO_2) remains challenging. Traditional methods struggle to resolve adsorbed species at trace levels, limiting insights into material degradation or saturation. Solid-state (ss) NMR can distinguish chemisorbed and physisorbed CO_2 [1,2], but its sensitivity is limited by the low natural abundance of ^{13}C (~1%). Dynamic Nuclear Polarization (DNP) enhances sensitivity for studying adsorbed CO_2 in porous materials under DAC conditions. However, sample preparation must preserve the fragile gas-adsorbent interface. Current methods, like incipient wetness impregnation, risk displacing adsorbed CO_2 during radical doping, altering speciation. We present a novel radical impregnation method for MAS DNP NMR that minimizes perturbation of adsorbed CO_2. Our technique maintains speciation integrity while achieving high DNP signal enhancement. We demonstrate its application on amine-modified SBA-15 exposed to ambient air, resolving chemi- and physisorbed CO_2 species. This methodology enables DAC material characterization under operationally relevant conditions, guiding next-generation adsorbent design.

Acknowledgements

We thank CICECO-Aveiro Institute of Materials, UIDB/50011/2020, UIDP/50011/2020, and LA/P/0006/2020, financed by FCT/MCTES (PIDDAC). This work received funding from the ERC (Grant Agreement 865974) and the EU's H2020 programme (GA 101008500 "PANACEA").

References

[1] R. Vieira et al., J. Phys. Chem. C **125** (2021) 14797–14806.
[2] M. Ilkaeva et al., J. Am. Chem. Soc. **145** (2023) 8764–8769.

Fabrication of Functionally Graded Porous Materials Using Powder Metallurgy Techniques

I. Matuła[a]*, G. Dercz[a]

[a]Institute of Materials Science, University of Silesia in Katowice, 75 Pułku Piechoty Street 1 A, 41-500 Chorzów, Poland

*izabela.matula@us.edu.pl

Titanium-based materials have long been the gold standard in implantology due to their exceptional biocompatibility and corrosion resistance. However, the inherent stiffness of solid titanium remains a significant challenge, often leading to the "stress shielding" effect and subsequent bone resorption. To address this, the design of Functionally Graded Materials (FGMs) with tailored, spatially varying porosity has emerged as a crucial strategy. By precisely engineering the chemical composition, pore size and distribution, and thus the mechanical characterization across different regions of a single component, it is possible to mimic the complex architecture of natural bone.

Interestingly, the solutions and manufacturing protocols developed for these sophisticated medical structures can be successfully transferred to other industrial sectors. The ability to design and fabricate materials with controlled, gradient porosity opens new avenues in fields such as water purification and wastewater treatment, where porous metallic structures serve as highly efficient, durable filters or catalytic substrates. In these applications, as in medicine, the key lies in the precise control of the interconnected pore network, which facilitates fluid flow and maximizes active surface area. Thus, the advancement of powder metallurgy techniques for biomedical FGMs provides a versatile technological platform that transcends clinical applications, offering innovative solutions for modern environmental engineering and advanced industrial filtration.

A critical aspect of the production process is the milling and mechanical alloying stage, where controlling powder behavior is paramount to achieving desired material properties. Research indicates that the introduction of minor elemental additions, such as tin (Sn), silver (Ag), or copper (Cu) in concentrations of approximately 2–3 wt.%, significantly influences particle agglomeration and the synthesis of titanium-based alloys. These additions function as effective Process Control Agents (PCA), playing a key role in balancing cold-welding and fracturing mechanisms during high-energy milling. In particular, the addition of tin (Sn) limits excessive agglomeration and promotes significant particle refinement, leading to enhanced nanocrystallization of titanium phases and improved material homogenization.

The characterization was conducted in two distinct stages: evaluating the metallic powders following the modified powder metallurgy processes and analyzing the final sintered Functionally Graded Materials (FGMs). The powder properties were assessed using a laser particle size analyzer to determine volume distribution and mean diameters. Scanning Electron Microscopy (SEM) were employed to analyze morphology of powders and microstructure od sintered samoples. Phase were determined by X-ray Diffraction (XRD). Results confirmed the formation of interconnected pore networks suitable for osseointegration and a gradual change in microhardness across the sample cross-sections. These findings demonstrate that modified powder metallurgy is a highly effective route for engineering the next generation of porous, functionally graded implants with tailored biological and mechanical performance.

Acknowledgements

Conference participation was supported by the GreenMat project, co-funded by the European Union under the program “European Funds for Silesia 2021–2027”

CHARACTERIZATION AND MODELING

Efficient Removal of 17α-Ethinylestradiol from Water Using Silica-Based Adsorbents: Impact of Organic Functionalities and Water Matrices

T. Morais[a,b], D. Pereira[c], G. Sequera[a], A. C. Moreira[a], M. Ilkaeva[a,d], L. Mafra[a], M. Sardo[a]*, V. Calisto[c], M. A. O. Lourenço[a]

[a]CICECO – Aveiro Institute of Materials, Chemistry Depart., Univ. Aveiro, 3810-193, Aveiro, Portugal
[b]Chemistry Depart., Univ. Iceland, Science Institute, Dunhaga 3, 107 Reykjavik, Iceland
[c]CESAM, Chemistry Depart., Univ. Aveiro, 3810-193 Aveiro, Portugal
[d]Depart. of Chemical and Environmental Eng., Univ. Oviedo, Av. Julián Clavería 8, 33006 Oviedo, Spain

*msardo@ua.pt

Endocrine disruptors like 17α-ethinylestradiol (EE2) pose significant environmental risks due to their persistence in wastewater and increasingly stringent European discharge regulations. As conventional treatments remain largely ineffective, this study explores the potential of Periodic Mesoporous Organosilicas (PMOs) as a superior alternative to grafted silicas for efficient EE2 capture across diverse water matrices.

Three silica-based porous adsorbents – MCM-41 (pure silica), vinyl-MCM-41 (hybrid silica), and Ph-PMO (periodic mesoporous phenylene-silica) – were tested to evaluate the effect of organic functionalities on removing the hormone disruptor 17α-ethinylestradiol (EE2) from water. Adsorbent dosages were tested in ultrapure water spiked with 200 µg L-1 of EE2, and the results revealed that concentrations higher than 500 mg L-1 of adsorbent did not significantly enhance the EE2 removal efficiency. Both materials containing organic functionalities (using a dose of 500 mg L-1) were tested in ultrapure water, phosphate buffer at pH 5, 7, and 9, and wastewater effluent to evaluate the pH impact and effect of different water matrices on their adsorption performance. An increase in pH significantly improved the EE2 adsorption capacity of Ph-PMO, reaching 94 ± 2 % at pH 9, while it decreased the adsorption efficiency of vinyl-MCM-41 to 14 ± 7 % at the same pH. Following a comprehensive characterization of the materials, including assessments of chemical stability across varying pH conditions, point of zero charge, hydrophobicity, and textural properties such as specific surface area, pore volume, and pore diameter, the findings suggests that the homogenous distribution of organic functionalities in Ph-PMO enhances surface interactions, such as π-π stacking and hydrophobic interactions, with the EE2 hormone. Ph-PMO demonstrated superior performance in wastewater effluents, and kinetic studies showed rapid EE2 adsorption across all matrices, reaching equilibrium within 5 minutes. This study highlights the suitability of Ph-PMO for water remediation applications [1].

Acknowledgements

This work was developed within the scope of the project CICECO-Aveiro Institute of Materials, UIDB/50011/2020 (DOI 10.54499/UIDB/50011/2020), UIDP/50011/2020 (DOI 10.54499/UIDP/50011/2020) & LA/P/0006/2020 (DOI 10.54499/LA/P/0006/2020), financed by national funds through the FCT/MEC (PIDDAC). The authors also acknowledge financial support to CESAM by FCT/MCTES (UIDP/ 50017/2020+ UIDB/50017/2020+ LA/P/0094/2020), through national funds. The NMR spectrometers are part of the National NMR Network (PTNMR) and are partially supported by Infrastructure Project 022161 (cofinanced by FEDER through COMPETE 2020, POCI and PORL and FCT through PIDDAC). This work has received funding from the European Research Council (ERC) under the European Union's Horizon 2020 research and innovation program (Grant Agreement 865974). FCT is also acknowledged by D.P. for a Ph.D. Studentship (2020.05389. BD), M.I., M.A.O.L. and M.S. for Researcher positions (CEECIND/00546/2018, CEECIND/01158/2021 and CEECIND/00056/2020, respectively). M.A.O.L further acknowledges the funding from the European Union's Horizon Europe research and innovation programme (ERA-PF grant agreement No 101090287). MI also acknowledges Spanish Ministry of Science, Innovation and Universities for the “Beatriz Galindo” Scholarship (MU-23-BG22/00145).

References

[1] T. Morais et al., ACS Applied Mat. Interfaces (2026).

Effect of Cu on CO_2 Capture on Activated Carbon

M. Khonglek[a], P. Thongsuk[a], A. Wongkoblap[a]*, T. Khongkhuntian[b]

[a]School of Chemical Engineering, Suranaree University of Technology, Nakhon Ratchasima, 30000 Thailand
[b]Ratchaburi Learning Park, King Mongkut's University of Technology Thonburi, Bangkok, 10140, Thailand

*atichat@sut.ac.th

The commercial activated carbon (AC) derived from coconut shells was modified by adding copper (Cu) on its surfaces. Various concentrations of Cu on AC were used to investigate an enhancement of carbon dioxide (CO_2) capture on AC at 273K and high pressures. The activated carbon with 0.5, 1, 2 and 5% by weight of Cu on carbon's surfaces were prepared and the X-ray diffraction (XRD) was used to determine the amount of Cu on their surfaces. Nitrogen adsorption isotherm at 77K shown in Figure 1 was used to evaluate the specific pore volume of these AC. The specific pore volume was 0.021406, 0.000807, 0.005042, 0.036413 and 0.007809 cm^3/g, for original carbon, 0.5, 1, 2 and 5% Cu loading, respectively. It was observed that an increase of Cu could decrease the specific surface area, except at Cu loading of 2%. This may be due to the pore blocking effect preventing the diffusion of N_2 into the inner pore of modified AC with Cu. In the case of 2% Cu loading, the well distribution of Cu not only inside the pore but also at the pore mouth to form the outer pore, then the increase of pore volume led to an increase of surface area. Cu could increase the surface area and specific pore volume at suitable amount of Cu loading. The excess adsorption isotherms of CO_2 on activated carbon at 273K and pressures up to 35 bars for original carbon, AC having 2% and 5% of Cu loadings were presented in Figure 2. An early onset in adsorption isotherm for CO_2 was observed at low pressures, and the maximum adsorbed amount of CO_2 was 57.61, 59.77 and 56.46 cm^3/g at STP, for original AC, AC with 2 and 5% Cu, respectively. Increasing of Cu concentration could enhance the adsorption of CO_2 on AC compared with original AC, the improving of AC by adding copper can be used to enhance carbon dioxide capture. The adsorption at high pressures at various temperatures and optimum concentration of copper should be investigated for further improving AC for an environmental adsorption material and global warming issue.

.

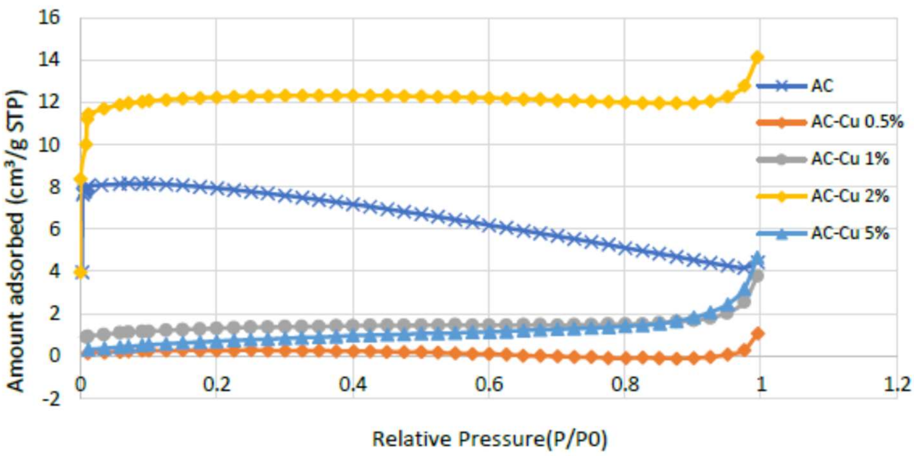

Figure 1 Nitrogen adsorption isotherm at 77K for original AC and AC with various Cu loadings.

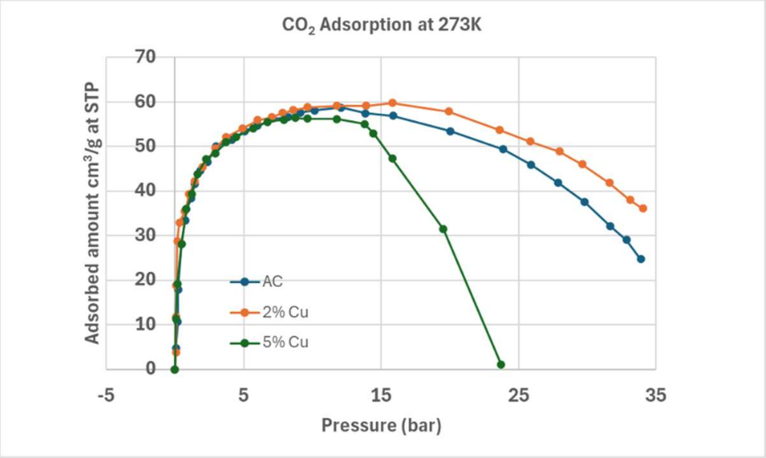

.

Figure 2 Adsorption isotherms for CO_2 at 273K on activated carbons with and without Cu.

Acknowledgements

This work was financial supported by Suranaree University of Technology via Capstone Design Project, we also acknowledged Ratchaburi Learning Park for analytical instrument.

Improved CO_2 Capture via Composites of Metal-Organic Framework and Nitrogen-Modified Hierarchically Porous Carbon Monoliths

T. Zelenka[a]*, M. Almáši[b], G. Zelenková[a], L. Kořená[a], E. Kinnertová[a], J. Silvestre-Albero[c]

[a]Department of Chemistry, Faculty of Science, University of Ostrava, 30. Dubna 22, 702 00 Ostrava, Czech Republic.
[b]Department of Inorganic Chemistry, Faculty of Science, Pavol Jozef Safarik University, Moyzesova 11, 040 01 Kosice, Slovak Republic.
[c]Department of Inorganic Chemistry, University of Alicante, San Vicente del Raspeig, 036 90 Alicante, Spain.

*tomas.zelenka@osu.cz

To address the critical need for effective carbon dioxide (CO_2) capture materials, this study explores the synthesis and performance of UiO-66-NH_2-integrated hierarchically porous carbon monolith (HPCM) [1] with nitrogen-based surface modifications. HPCM is carbon-based material structured with interconnected micro-, meso-, and macropores, which enhance surface area and gas transport properties. The objective of the study is to investigate the CO_2 sorption capacity of nitrogen-modified HPCM and their composites with nitrogen-rich UiO-66-NH_2 aiming to establish a synergistic platform with optimized characteristics tailored for carbon capture, storage, and other applications.

The composites (UiO-66-NH_2@HPCM) were synthesized by incorporating the microporous MOF into HPCM matrices pre-functionalized with various nitrogen groups, collectively referred to as HPCM-N. This was achieved through techniques such as nitration-reduction, melamine treatment, and (3-aminopropyl)triethoxysilane (APTES) grafting. This process yielded five distinct HPCM-N variants, each exhibiting unique structural and textural properties. Characterization techniques, including elemental analysis and X-ray photoelectron spectroscopy (XPS), confirmed successful nitrogen modifications, while nitrogen physisorption at -196 °C detailed the micropore and mesopore distributions. Powder X-ray diffraction (PXRD) and scanning electron microscopy (SEM) with energy dispersive X-ray (EDX) analysis confirmed the successful integration of UiO-66-NH_2 into the HPCM matrix. The MOF quantity in the resulting composite was calculated based on the weight loss changes between the HPCM and the composites using thermal analysis, with the amounts ranging from 15-30 wt. %. The composite prepared using HPCM modified by nitration-reduction exhibited the highest MOF content (30 wt.%), though with lower nitrogen content relative to other modifications. Adsorption of CO_2 at 0 °C up to 100 kPa was performed for all samples.

The CO_2 sorption studies demonstrated marked improvements across the composites compared to pristine HPCM/HPCM-N materials, where CO_2 capacity increased, reflecting the contribution of UiO-66-NH_2 micropores. However, composites with nitrogen-modified HPCM, particularly composite based on the HPCM treated with melamine, exhibited a notable adsorption capacity of 2.6 mmol g^{-1} at 100 kPa—a 1.5-fold improvement over unmodified HPCM. The enhanced performance is attributed to the strong CO_2 affinity of amine groups, maximizing interaction and retention within the hierarchical structure.

The study demonstrates that UiO-66-NH_2@HPCM composites, particularly those with targeted nitrogen modifications, can provide a scalable solution for CO_2 capture. These results emphasize the synergistic benefits of hierarchical porosity and nitrogen functionalities in HPCM and UiO-66-NH_2 materials for greenhouse gas mitigation.

Acknowledgements

This research was supported by LUASK22049 (INTER-EXCELLENCE II, MŠMT), APVV SK-CZ-RD-21-0068, and SGS09/PŘF/2024.

References

[1] P. Bulavová, J. Parmentier, V. Slovak, Microp. Mesop. Mater. **272** (2018) 155.

MAGNETIC AND FUNCTIONAL MATERIALS

Advantages of High-Energy X-Ray Radiation for Materials Research

J. Bednarčík[a]*

[a]Department of Condensed Matter Physics, Institute of Physics, Faculty of Science, Pavol Jozef Šafárik
University in Košice, Park Angelinum 9, 041 54 Košice, Slovak Republic

*jozef.bednarcik@upjs.sk

High-energy X-ray scattering at synchrotron radiation sources has become an indispensable tool for modern materials research, providing unique access to structural information across multiple length scales (see Table 1 below). The use of hard X-rays with high penetration depth enables *in situ* and *operando* investigations of bulk materials, complex sample environments, and realistic processing conditions that are often inaccessible to laboratory-based techniques.

Table 1 Experimental techniques sorted based on their sensitivity to characteristic correlation length.

Technique	Characteristic correlation length [m]								
	10^{-11}	10^{-10}	10^{-9}	10^{-8}	10^{-7}	10^{-6}	10^{-5}	10^{-4}	10^{-3}
XAS – X-ray Absorption Spectroscopy	●	●	●						
WAXS – Wide Angle X-ray Scattering	●	●	●	●	●				
PDF – Pair Distribution Function	●	●	●	●	●				
SAXS – Small Angle X-ray Scattering			●	●	●	●			
U-SAXS – Ultra-Small Angle X-ray Scattering					●	●	●		
X-TOMO – X-ray Tomography						●	●	●	●
TEM – Transmission Electron Microscopy	●	●	●	●	●				
SEM – Scanning Electron Microscopy				●	●	●	●	●	

This talk will present an overview of complementary high-energy X-ray methods available at synchrotron facilities, including X-ray diffraction (XRD), pair distribution function (PDF) analysis, small-angle X-ray scattering (SAXS), and X-ray absorption spectroscopy (XAS). Particular emphasis will be placed on their application to nanomaterials and highly disordered systems, such as amorphous and partially ordered materials, where conventional crystallographic approaches are limited. While XRD and SAXS provide insight into long-range order and nanoscale morphology, PDF analysis and XAS deliver element-specific information on local atomic structure, bonding, and electronic states.

In the final part of the talk, attention will be given to complementary **laboratory-based X-ray techniques**, including XRD, SAXS/WAXS, and XAS, which are currently being implemented and developed within the framework of the ongoing **MASS-PRAM project (Multimodal Approach to Study Structure–Property Relationships in Advanced Materials)**. This project aims to bridge synchrotron and laboratory capabilities by integrating multiple experimental modalities, enabling systematic and accessible studies of structure–property relationships in advanced and functional materials. The combined synchrotron–laboratory approach highlights the synergistic role of multimodal X-ray methods in addressing complex structural problems in contemporary materials science.

Acknowledgements

This study was funded by the EU Next,Generation-EU through the Recovery and Resilience Plan for Slovakia under the project No. 09I03-03-V03-00034

3D Hofmann-Type Clathrates as Diamagnetic Hosts for Single-Ion Magnets

J. Kuchár[a]*, A. Leško[a]

[a]Department of Inorganic Chemistry, Institute of Chemistry, Faculty of Science, Pavol Jozef Šafárik University in Košice, Moyzesova 11, 040 01 Košice, Slovak Republic

*juraj.kuchar@upjs.sk

Hofmann clathrates are historically important coordination solids often regarded as key structural predecessors of modern metal–organic frameworks (MOFs), since they already combine metal nodes with bridging ligands to generate extended architectures. In these compounds, the cyanide group (CN^-) plays a central role as a highly effective bridging linker, connecting metal centers into polymeric sheets or networks. This CN^--mediated metal-ligand connectivity creates robust host frameworks capable of trapping guest molecules, which is the essence of clathrate formation [1]. By enforcing directional bonding and efficient electronic/structural coupling between metals, cyanide bridges strongly influence framework topology and stability. Viewed in this way, Hofmann clathrates illustrate an early, conceptually MOF-like design principle: modular assembly of porous or guest-responsive solids from metal centers and bridging linkers dominated by cyanide. In the original Hofmann clathrates, nickel centers are linked into cyanide-bridged layers, while interlayer coupling is provided mainly by hydrogen bonding involving ammonia molecules coordinated to Ni, giving rise to distinct environments often described as NiC_4 and NiN_6. Building on this concept, the idea was to replace the hexacoordinated Ni sites with alkaline-earth metal ions and to engineer the interlayer connection through alternative pillars rather than NH_3-driven H-bonding. Specifically, bridging between the layers could be achieved using cyanide groups, terephthalate ligands, or 4,4′-bipyridine molecules, enabling tunable spacing and topology. Such substitutions would preserve the Hofmann-type layered motif while pushing the system toward a more explicitly MOF-like, modular framework design. These modifications also alter the charge balance compared with the original Hofmann clathrates. While classical Hofmann clathrates are overall electroneutral and therefore typically encapsulate neutral guest molecules, using 4,4′-bipyridine as a neutral pillar preserves this electroneutral framework character. In contrast, introducing linkers that carry a net charge can generate an anionic skeleton, so that charge compensation is achieved by extra-framework cations residing in the cavities (and potentially shaping the adsorption/encapsulation behavior). The original idea was inspired by the concept of glass corrosion, where Ca^{2+} ions are leached from the glass matrix and subsequently interact with species present in the surrounding solution. In our case, the solution contained cyanidometallate anions and complex cations, and its mildly alkaline character—arising from the presence of amine ligands in the complex cations—promoted such Ca^{2+} binding and reactivity. From the standpoint of magnetic studies, such framework is attractive because it serves as a diamagnetic host into whose cavities magnetically active ions can be incorporated. In this way, the ions can be immobilized at well-defined positions while being sufficiently separated to suppress direct magnetic coupling, including exchange interactions [2].

Building on this rationale, we prepared a series of compounds that can be described as 3D Hofmann-type clathrates, systematically varying the alkaline-earth metal centers as well as the guest/counterion species occupying the cavities. The present study reports the preparation and characterization of four novel compounds of the $[Ni(CN)_4]^{2-}$ - Ca^{2+}/Sr^{2+} - $[Ni(\mathit{ampy}/\mathit{en})_3]^{2+}$ type (where *ampy*: 2-aminomethylpyridine, *en*: ethylenediamine). Prepared compounds were characterized by elemental analysis, spectroscopic methods and SCXRD. Magnetic measurements indicate that exchange interactions are minimized, while simultaneously revealing behavior characteristic of single-ion magnets.

Acknowledgements

This work was supported by the Cultural and Educational Grant Agency MŠVVaM, project No. 013UPJŠ-4/2024.

References

[1] T. Iwamoto, Hofmann-Type Clathrates, In: Encyclopedia of Supramolecular Chemistry - Two-Volume Set (Taylor & Francis eBooks), 2013.
[2] Z. P. Ni, J. L. Liu, Md. N. Hoque,W. Liu, J. Y. Li, Y. C. Chen, M. L. Tong, Coord. Chem. Rev. **335** (2017) 28-43.

Exploring N-Donor Triazole Polymers for Potential Biomedical Use

K. Micheľová[a]*, J. Kuchár[a]

[a]Department of Inorganic Chemistry, Institute of Chemistry, Faculty of Science, Pavol Jozef Šafárik University
in Košice, Moyzesova 11, 040 01 Košice, Slovak Republic

*katarina.michelova@student.upjs.sk

Coordination polymers represent an important class of functional materials that have attracted sustained scientific interest due to their structural versatility and controllable architectures. Although their applications span multiple areas of research, these materials have also emerged as promising candidates for biomedical use. A major focus of current research is the development of reliable synthetic strategies and the elucidation of structure–property relationships, both of which remain challenging. Linear N,N′-donor ligands, particularly 4,4′-bipyridine and its analogues, have been widely employed as building blocks for constructing extended coordination polymers due to their ability to generate diverse frameworks. In contrast, bent ligands incorporating additional functional units between two pyridyl groups remain comparatively underexplored. Such ligands offer increased structural flexibility and allow fine tuning of polymer architectures. In particular, bent ligands containing 4-amino-1,2,4-triazole or 1*H*-1,2,4-triazole units between pyridyl moieties are especially attractive, as variations in the position of the pyridyl nitrogen atoms induce different degrees of molecular bending, influencing coordination topologies and potentially enhancing biomedical relevance [1].
Aromatic N-heterocyclic ligands are further advantageous due to their ability to adopt diverse coordination geometries. Beyond metal–ligand coordination, these ligands can participate in noncovalent interactions such as hydrogen bonding and π–π stacking, which are critical for directing the self-assembly of stable and structurally rich supramolecular coordination polymers [2,3].

This study primarily aims to synthesize and optimize the reaction conditions for products of anticipated polymeric character, based on 3*d* transition metal ions and triazole derivatives, specifically 4-amino-3,5-bis(4-pyridyl)-1,2,4-triazole. This ligand functions as a multi N-donor system and exhibits a conformationally favorable structure suitable for polymeric framework construction. The resulting products will be thoroughly characterized using a range of physicochemical techniques, including infrared IR and UV–Vis spectroscopy, elemental analysis, and thermal analysis. Compounds exhibiting promising properties may be further investigated for potential applications in the biomedical field.

Acknowledgements

This work was supported by the Cultural and Educational Grant Agency MŠVVaM, project No. 013UPJŠ-4/2024.

References

[1] F. - P. Huang, Q. Zhang, Q. Yu, H. - D. Bian, H. Liang, S. - P. Yan, D. - Z. Liao, P. Cheng, Cryst. Growth Des. **12** (2012) 1890.
[2] Y. Xu, Q. - H. Deng, F. Ding, R. An, D. Liu, T. - F. Miao, Polymers **11** (2019) 819.
[3] X. - F. Li, D. Cheng, X. - R. Meng, H. - X. Yang, Acta Crystallogr. C Struct. Chem. **75** (2019) 643.

Novel Lanthanoide Metal-Organic Frameworks: Synthesis, Sorption and Magnetic Properties

P. Obšatník[a]*, V. Zeleňák[a], A. Zeleňáková[b], L. Zelená[a,b], M. Litecká[c], M. Almáši[a], N. Király[a]

[a]Department of Inorganic Chemistry, Institute of Chemistry, University of Pavol Jozef Safarik in Kosice, Moyzesova 11, 041 54 Kosice, Slovak Republic
[b]Department of Chemistry, Faculty of Science, University of Ostrava, 30. dubna 22, Ostrava, CZ-702 00 Czech Republic
[c]Institute of Inorganic Chemistry of the Czech Academy of Science, Husinec-Řež 1001, 250 68, Řež, Czech Republic

*peter.obsatnik@student.upjs.sk

Metal–organic frameworks (MOFs) are hybrid coordination polymers that have attracted increasing attention due to their structural tunability and functional versatility [1]. Among them, lanthanide-based MOFs (Ln-MOFs) constitute an important class of porous materials combining permanent porosity with distinctive magnetic behaviour arising from 4f electrons. MOFs constructed from polydentate carboxylate ligands are particularly attractive, as they form robust and permeable frameworks with accessible active sites suitable for gas capture [2]. In this contribution, we report the synthesis and physicochemical characterization of a series of lanthanide coordination polymers based on the tetratopic azo-carboxylate ligand H_4MTA.

A series of lanthanide metal–organic frameworks was synthesized by coordination of the tetratopic azo-carboxylate ligand H_4MTA [3] with lanthanide ions. The LnMTA coordination polymers (Ln = La(III), Ce(III), Pr(III), Nd(III), Sm(III), Eu(III), Gd(III), Tb(III), Dy(III), Ho(III), Er(III), Tm(III), Yb(III), Lu(III)) were obtained via solvothermal synthesis, yielding orange needle-shaped crystals with the general formula $\{[Ln_4(MTA)_3]\cdot13H_2O\cdot14DMF\}_n$. The materials were prepared by reacting $Ln(NO_3)_3\cdot xH_2O$ (0.045 mmol) with H_4MTA (0.09 mmol) in a DMF and water solvent system at 80 °C.

The LnMTA materials were characterized by FT-IR spectroscopy, CHN elemental analysis, thermogravimetric analysis and powder and single-crystal X-ray diffraction. PXRD analysis confirmed that all compounds are isostructural. Single-crystal analysis confirmed that materials crystallize in the orthorhombic crystal system with four formula units per unit cell. Each Ln^{3+} center exhibits an eight-coordinate $[LnO_8]$ environment with a triakis tetrahedral coordination geometry. The tetratopic MTA^{4-} ligand connects eight lanthanide ions via a *chelate-anti* coordination mode, giving rise to a porous framework. The structure contains one-dimensional channels with pore dimensions of approximately 12.98 × 10.78 $Å^2$ propagating along the crystallographic c-axis (Figure 1).

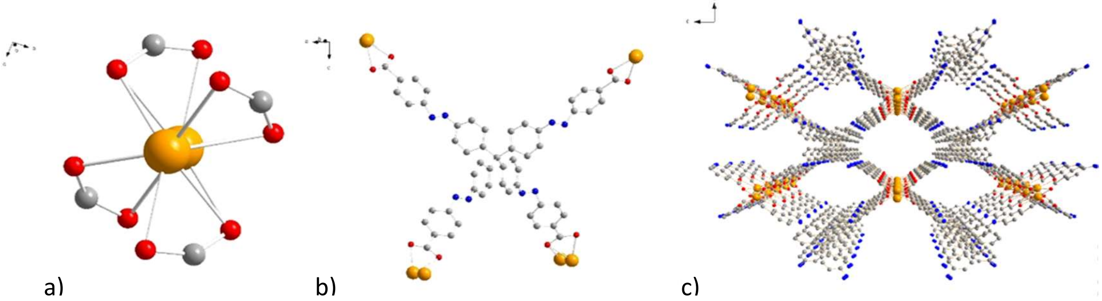

Figure 1 a) *Chelate-anti* coordination modes of MTA^{4-} linker. b) A view of the tetragonal pores propagating along the *c* crystallographic axis. c) The coordination environment.

The presence of accessible voids prompted an investigation of the CO_2 sorption behaviour of the LnMTA frameworks. CO_2 adsorption measurements performed at 1 bar and temperatures of 0 °C and 20 °C revealed a pronounced affinity toward CO_2 for all materials, confirming the accessibility of the porous structure. Among the studied compounds, TbMTA exhibited the highest low-pressure adsorption capacity, reaching 3.7 $mmol{\cdot}g^{-1}$ at 0 °C and 1 bar. The adsorption behaviour of PrMTA and GdMTA was further examined under high-pressure conditions up to 40 bar at 0 °C, 10 °C, and 25 °C. The highest adsorption capacities were observed at 0 °C and 21 bar, with PrMTA and GdMTA adsorbing 3.31 $mmol{\cdot}g^{-1}$ and 4.38 $mmol{\cdot}g^{-1}$ of CO_2, respectively. Isosteric heats of CO_2 adsorption (Q_{st}), derived from high-pressure isotherms measured at different temperatures, reached 31.6 $kJ{\cdot}mol^{-1}$ for PrMTA and 27.5 $kJ{\cdot}mol^{-1}$ for GdMTA. These values indicate moderately strong host–guest interactions and highlight the potential of LnMTA materials for efficient CO_2 capture.

The magnetic properties of the LnMTA frameworks were investigated by dc magnetization and magnetic susceptibility measurements. The NdMTA and SmMTA compounds exhibit ideal paramagnetic behaviour, with field-dependent magnetization well described by the Brillouin function down to 2 K, indicating negligible magnetic exchange interactions. In contrast, EuMTA shows only a weak magnetic response due to the nonmagnetic ground state of the Eu^{3+} ion ($J = 0$). Deviations from Curie–Weiss behaviour observed in the temperature-dependent susceptibility, particularly for SmMTA and EuMTA, are attributed to Van Vleck paramagnetism associated with low-lying excited electronic states.

In summary, a series of lanthanide-based coordination polymers derived from the tetratopic azo-carboxylate ligand H_4MTA was successfully synthesized and characterized. The isostructural porous frameworks exhibit accessible channels, enabling efficient CO_2 adsorption with moderate host–guest interactions. Magnetic studies reveal predominantly paramagnetic behaviour governed by the electronic configuration of the lanthanide ions, with negligible magnetic exchange interactions. These results demonstrate that LnMTA materials represent versatile multifunctional systems combining sorption and magnetic properties.

Acknowledgements

This work was supported by VEGA 1/0058/25, 1/0442/25 and Funded by the EU NextGenerationEU through the Recovery and Resilience Plan for Slovakia under the project No. 09I03-03-V05-00008 (VVGS-ESGV-2923).

References

[1] W. Lu., Z. Wei., Z. - Y. Gu, T. - F Liu et al. Chem. Soc. Rev. **43** (2014) 5561–5593.
[2] S. Su, W. Chen, Ch. Qin, S. Song, Z. Guo et al. Cryst. Growth Des. **12** (2012) 1808.
[3] M. Almáši, N. Király, V. Zeleňák, M. Vilková, S. Bourrelly, RSC Adv. **11** (2021) 20137.

Advanced Characterization of Porous Materials for Sustainable Applications

R. Landl[a]*

[a]Anton Paar Slovakia, Hattalova 12 831 03 Bratislava, Slovakia

*richard.landl@anton-paar.com

Porous materials such as zeolites, metal–organic frameworks (MOFs), advanced ceramics, and functional adsorbents play a crucial role in environmental applications including gas separation, pollutant adsorption, catalysis, and water treatment. The performance of these materials is governed by a complex interplay of particle size, surface charge, pore structure, phase composition, and processability. Comprehensive and reliable characterization is therefore essential throughout material development and application.

Anton Paar offers an integrated portfolio of analytical instruments designed to support the complete characterization workflow of porous materials. **Dynamic Light Scattering (DLS)** and **laser diffraction** enable accurate determination of particle size and size distribution across a wide particle size range, while **zeta potential measurements** using the **Litesizer™** provide critical insight into surface charge and dispersion stability. **X-ray diffraction (XRD)** delivers phase identification and crystallinity analysis essential for structural understanding of zeolites, MOFs, and ceramic materials. In addition, **gas and vapor adsorption analyzers** allow precise determination of surface area, pore size distribution, and adsorption capacity, directly linking structure to environmental performance. Complementary **rheological measurements** support optimization of suspensions, slurries, and pastes relevant to processing, shaping, and scale-up.

By combining particle characterization, structural analysis, adsorption measurements, and rheology, Anton Paar enables a holistic, application-driven understanding of porous materials, supporting efficient development of sustainable environmental technologies.

Figure 1 Instruments for material characterization A) Autosorb – adsorption analyzer and B) XRDynamic 500 – X-ray diffractometer.

Figure 2 Litesizer DIF – Laser diffractometer for particle size analysis.

Porous Materials for Environmental Applications 2026

Book of Abstracts

Edited by: Dr. Nikolas Király & Assoc. Prof. Miroslav Almáši

Publisher: Pavol Jozef Šafárik University in Košice, Publishing ŠafárikPress

Year: 2026

Pages: 140

Author's sheets: 8.28

Edition: First

Publication date: March 2026

ISBN 978-80-574-0507-8 (e-publication)
DOI: https://doi.org/10.33542/PMEA-0507-8